INSTITUTO DE TECNOLOGÍA QUÍMICA

APPLICATION OF SOLID STATE NMR IN HETEROGENEOUS CATALYSIS

Teresa Blasco

UNIVERSITAT POLITÈCNICA DE VALÈNCIA

Outline

- Fundaments of NMR spectroscopy
  - Solid state NMR
- Aplication on heterogeneous catalysis: Zeolites:
  - Structural characterization
  - Chemical Physical properties
  - Reaction Mechanisms

Outline

- **Fundaments of NMR spectroscopy**
  - Solid state NMR
- Aplication on heterogeneous catalysis: Zeolites:
  - Structural characterization
  - Chemical Physical properties
  - Reaction Mechanisms

Nuclear spin I= 1/2

Zeeman Nuclear

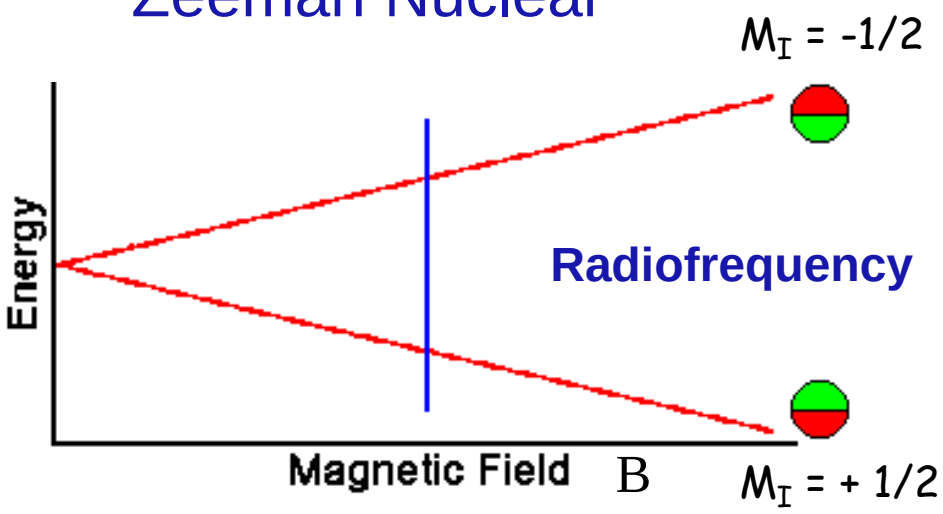

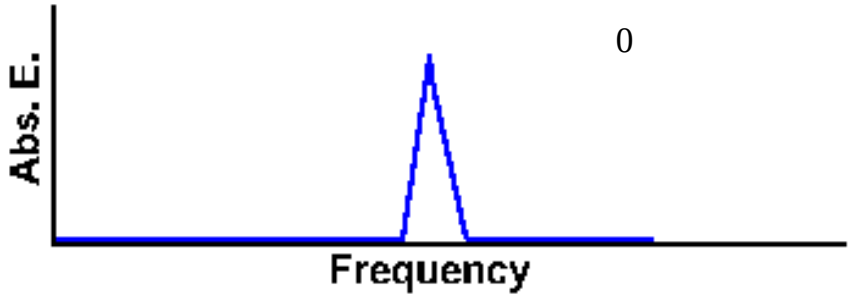

$$\omega_L = \gamma B_0$$

Larmor Frequency

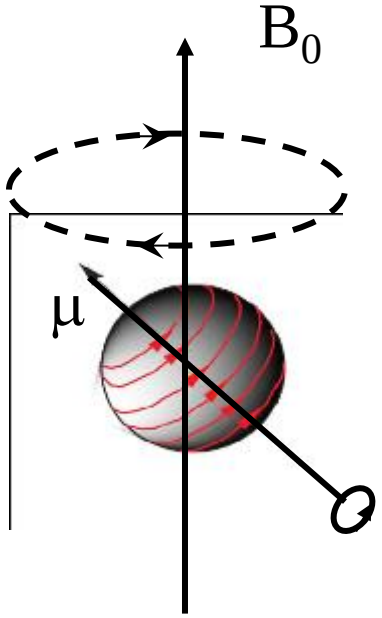

γ: giromagnetic ratio

γ and ω_L are characteristic of nuclei

Nuclear spin I= 1/2

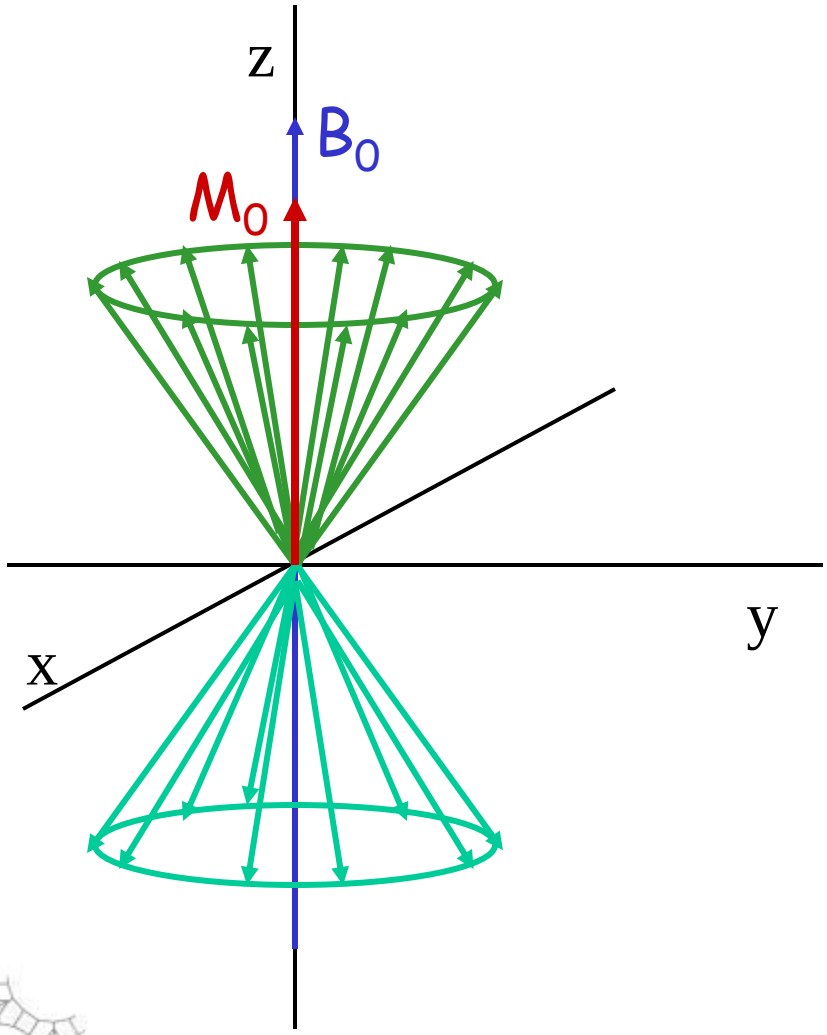

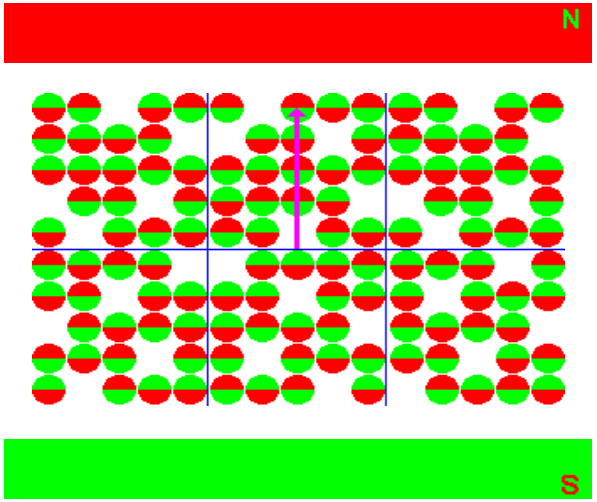

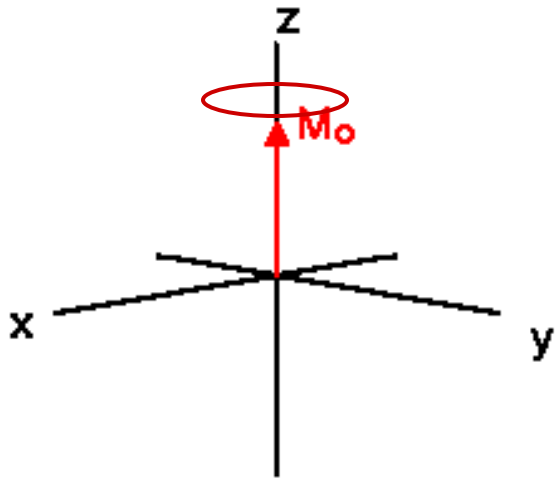

Isotope		Spin	Nat. Abund. (%)	Receptivity		Larmor Frequencies (MHz) vs. Bruker Field Strengths (Tesla) Freq. to 3 decimals are experimental for IUPAC Standards; freq. to 2 dec. are calculated from magn. moments										
				Natural rel. ^{13}C	Molar rel. ^{1}H	7.04925	9.39798	11.7467	14.0954	16.4442	17.6185	18.7929	19.9673	21.1416	22.3160	23.4904
1	H	1/2	99.9885	5.87E+03	**1.00E+00**	**300.130**	**400.130**	**500.130**	**600.130**	**700.130**	**750.130**	**800.130**	**850.130**	**900.130**	**950.130**	**1000.130**
2	H	1	0.0115	6.52E−03	9.65E−03	46.072	61.422	76.773	92.124	107.474	115.150	122.825	130.500	138.175	145.851	153.526
3	H	1/2		-	1.21E+00	320.131	426.795	533.459	640.123	746.786	800.118	853.450	906.782	960.114	1013.446	1066.778
3	He	1/2	1.34E-04	3.48E−03	4.42E−01	228.636	304.815	380.994	457.173	533.352	571.441	609.531	647.620	685.710	723.799	761.889
6	Li	1	7.59	3.79E+00	8.50E−03	44.167	58.883	73.600	88.316	103.032	110.390	117.748	125.106	132.464	139.822	147.180
7	Li	3/2	92.41	1.59E+03	2.94E−01	116.642	155.506	194.370	233.233	272.097	291.529	310.961	330.393	349.825	369.257	388.688
9	Be	3/2	100.0	8.15E+01	1.39E−02	42.174	56.226	70.277	84.329	98.381	105.407	112.433	119.459	126.485	133.510	140.536
10	B	3	19.9	2.32E+01	1.99E−02	32.245	42.989	53.732	64.476	75.220	80.591	85.963	91.335	96.707	102.079	107.451
11	B	3/2	80.1	7.77E+02	1.65E−01	96.294	128.378	160.462	192.546	224.630	240.672	256.714	272.755	288.797	304.839	320.881
13	C	1/2	1.07	**1.00E+00**	1.59E−02	75.468	100.613	125.758	150.903	176.048	188.620	201.193	213.765	226.338	238.910	251.483
14	N	1	99.636	5.90E+00	1.01E−03	21.688	28.915	36.141	43.367	50.594	54.207	57.820	61.433	65.046	68.659	72.273
15	N	1/2	0.364	2.23E−02	1.04E−03	30.423	40.560	50.697	60.834	70.971	76.039	81.107	86.176	91.244	96.312	101.381
17	O	5/2	0.038	6.50E−02	2.91E−02	40.687	54.243	67.800	81.356	94.913	101.691	108.469	115.248	122.026	128.804	135.582
19	F	1/2	100.0	4.89E+03	8.32E−01	282.404	376.498	470.592	564.686	658.780	705.827	752.874	799.921	846.968	894.015	941.062
21	Ne	3/2	0.27	3.91E−02	2.46E−03	23.693	31.587	39.482	47.376	55.270	59.217	63.165	67.112	71.059	75.006	78.953
23	Na	3/2	100.0	5.45E+02	9.27E−02	79.390	105.842	132.294	158.746	185.198	198.424	211.650	224.876	238.101	251.327	264.553
25	Mg	5/2	10.00	1.58E+00	2.68E−03	18.373	24.494	30.616	36.738	42.859	45.920	48.981	52.042	55.103	58.163	61.224
27	Al	5/2	100.0	1.22E+03	2.07E−01	78.204	104.261	130.318	156.375	182.432	195.460	208.489	221.517	234.546	247.574	260.602
29	Si	1/2	4.685	2.16E+00	7.86E−03	59.627	79.495	99.362	119.229	139.096	149.030	158.963	168.897	178.831	188.764	198.698
31	P	1/2	100.0	3.91E+02	6.65E−02	121.495	161.976	202.457	242.938	283.419	303.659	323.900	344.140	364.380	384.621	404.861
33	S	3/2	0.75	1.00E−01	2.27E−03	23.038	30.714	38.390	46.066	53.742	57.580	61.418	65.256	69.094	72.932	76.770
35	Cl	3/2	75.76	2.10E+01	4.72E−03	29.406	39.204	49.002	58.800	68.598	73.497	78.396	83.295	88.194	93.093	97.992
37	Cl	3/2	24.24	3.88E+00	2.72E−03	24.478	32.634	40.789	48.945	57.101	61.179	65.256	69.334	73.412	77.490	81.568
39	K	3/2	93.258	2.79E+00	5.10E−04	14.005	18.672	23.338	28.004	32.671	35.004	37.337	39.670	42.003	44.337	46.670
41	K	3/2	6.730	3.34E−02	8.44E−05	7.687	10.249	12.810	15.371	17.932	19.213	20.494	21.774	23.055	24.336	25.616
43	Ca	7/2	0.135	5.10E−02	6.43E−03	20.199	26.929	33.659	40.389	47.119	50.484	53.849	57.214	60.579	63.944	67.309
45	Sc	7/2	100.0	1.78E+03	3.02E−01	72.907	97.199	121.490	145.782	170.074	182.220	194.366	206.511	218.657	230.803	242.949
47	Ti	5/2	7.44	9.18E−01	2.10E−03	16.920	22.557	28.195	33.833	39.470	42.289	45.108	47.926	50.745	53.564	56.383
49	Ti	7/2	5.41	1.20E+00	3.78E−03	16.924	22.563	28.203	33.842	39.481	42.300	45.120	47.939	50.759	53.578	56.398
50	V	6	0.250	8.18E−01	5.57E−02	29.924	39.894	49.865	59.835	69.805	74.790	79.775	84.761	89.746	94.731	99.716
51	V	7/2	99.750	2.25E+03	3.84E−01	78.943	105.246	131.549	157.852	184.155	197.306	210.458	223.609	236.761	249.912	263.064
53	Cr	3/2	9.501	5.07E−01	9.08E−04	16.965	22.617	28.270	33.922	39.575	42.401	45.227	48.054	50.880	53.706	56.532
55	Mn	5/2	100.0	1.05E+03	1.79E−01	74.400	99.189	123.978	148.768	173.557	185.951	198.346	210.741	223.135	235.530	247.924
57	Fe	1/2	2.119	4.25E−03	3.42E−05	9.718	12.955	16.193	19.431	22.669	24.288	25.906	27.525	29.144	30.763	32.382
59	Co	7/2	100.0	1.64E+03	2.78E−01	71.212	94.939	118.666	142.393	166.120	177.984	189.847	201.711	213.575	225.438	237.302
61	Ni	3/2	1.1399	2.40E−01	3.59E−03	26.820	35.756	44.692	53.628	62.564	67.032	71.500	75.968	80.436	84.904	89.372
63	Cu	3/2	69.15	3.82E+02	9.39E−02	79.581	106.096	132.612	159.127	185.643	198.901	212.158	225.416	238.674	251.931	265.189
65	Cu	3/2	30.85	2.08E+02	1.15E−01	85.248	113.652	142.055	170.459	198.863	213.065	227.266	241.468	255.670	269.872	284.074
67	Zn	5/2	4.102	6.92E−01	2.87E−03	18.779	25.035	31.292	37.549	43.806	46.934	50.063	53.191	56.319	59.448	62.576
69	Ga	3/2	60.108	2.46E+02	6.97E−02	72.035	96.037	120.038	144.039	168.041	180.041	192.042	204.043	216.043	228.044	240.045
71	Ga	3/2	39.892	3.35E+02	1.43E−01	91.530	122.026	152.523	183.020	213.517	228.765	244.013	259.262	274.510	289.758	305.007

NMR Frequencies vs. Bruker Field Strengths – sorted by increasing atomic number

Isotope	Spin	Abundance (%)	NMR Frequency (MHz) at field (T)				
			5.8717	7.0460	9.3947	11.7434	14.0921
^{1}H	1/2	99.98	250.000	300.000	400.000	500.000	600.000
^{2}H	1	$1.5x10^{-2}$	38.376	46.051		76.753	
^{3}H	1/2	0	266.658	319.990		533.317	
^{3}He	1/2	$1.3x10^{-4}$	190.444	228.533		380.888	
^{6}Li	1	7.42	36.789	44.146		73.578	
^{7}Li	3/2	92.58	97.158	116.590		194.317	
^{9}Be	3/2	100	35.133	42.160		70.267	
^{10}B	3	19.58	26.866	32.239		53.732	
^{11}B	3/2	80.42	80.209	96.251		160.419	
^{13}C	1/2	1.108	62.860	75.432		125.721	
^{14}N	1	99.63	18.059	21.671		36.118	
^{15}N	1/2	0.37	25.332	30.398		50.664	
^{17}O	5/2	$3.7x10^{-2}$	33.892	40.670		67.784	
^{19}F	1/2	100	235.192	282.231		470.385	
^{21}Ne	3/2	0.257	19.736	23.683		39.472	
^{23}Na	3/2	100	66.128	79.353		132.256	

NMR spectrometer

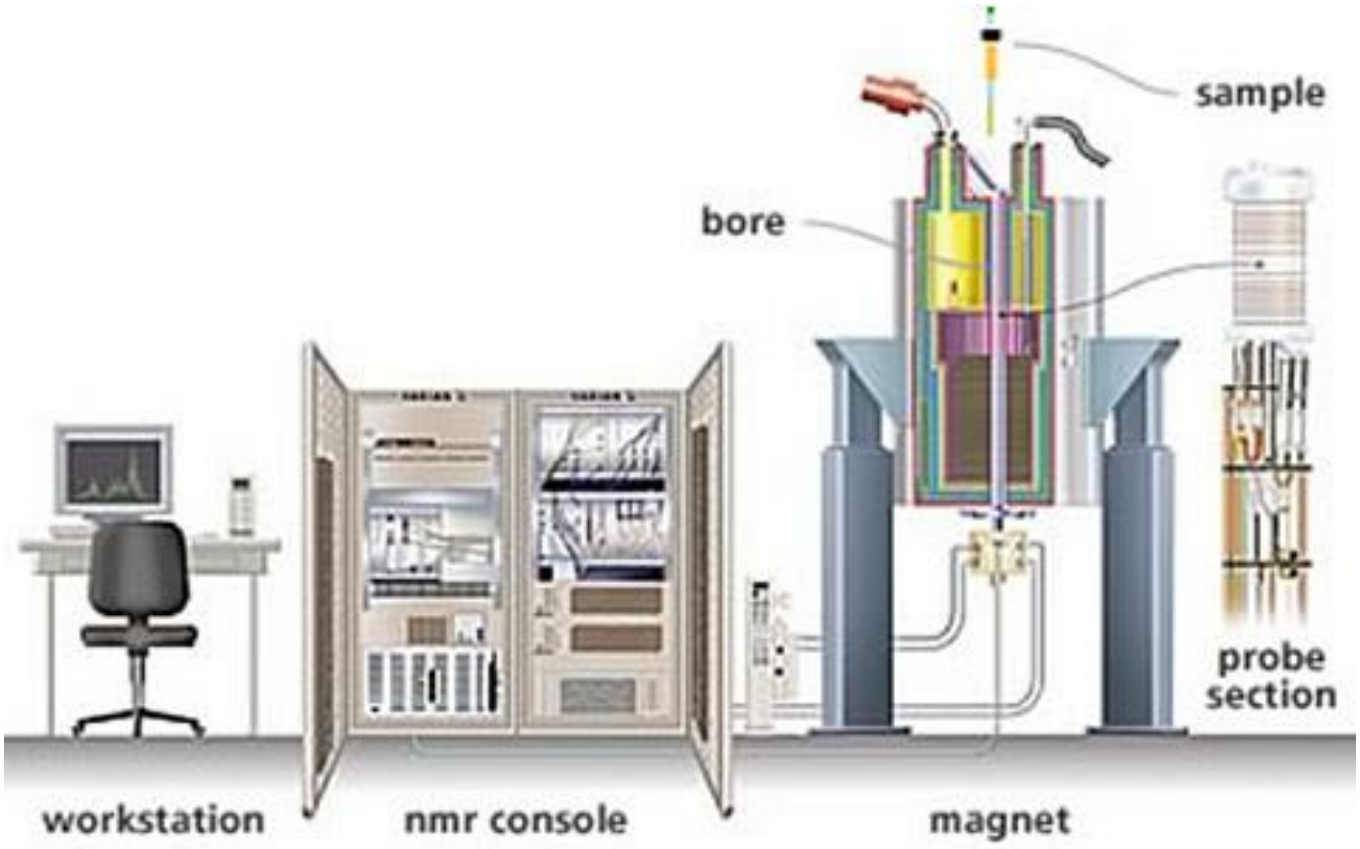

http://www.agilent.com/labs/images/mnmr.jpg

Superconducting magnet

Superconducting permanent magnet

NMR probe

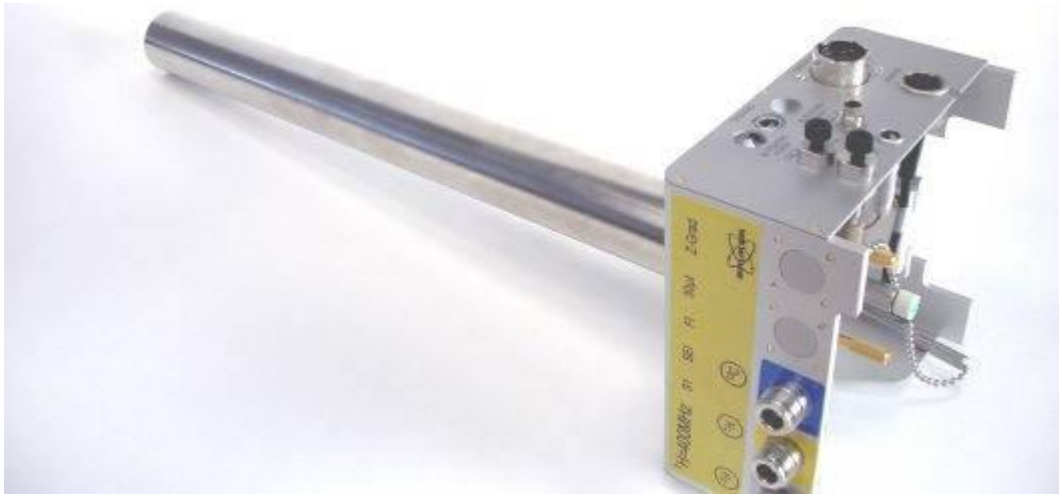

Simple probes have conections for 1H/19F and X nuclei

Single pulse experiment

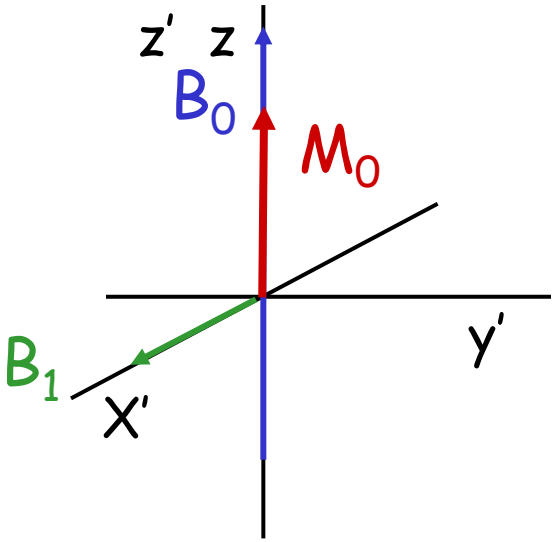

$\theta = \gamma B_1 t_p$

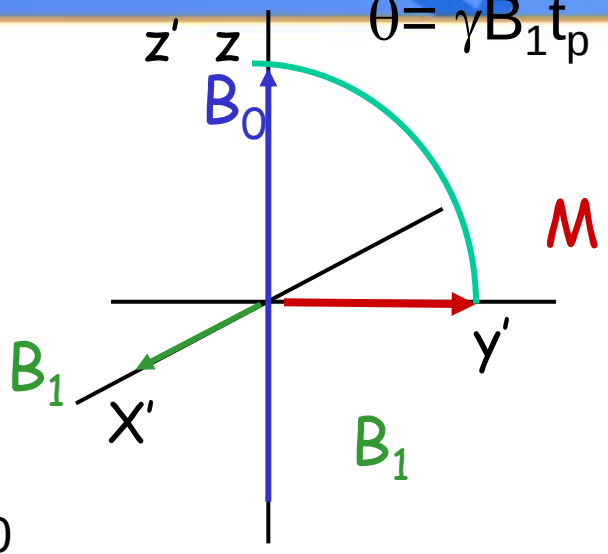

$\omega_L = \gamma B_0$

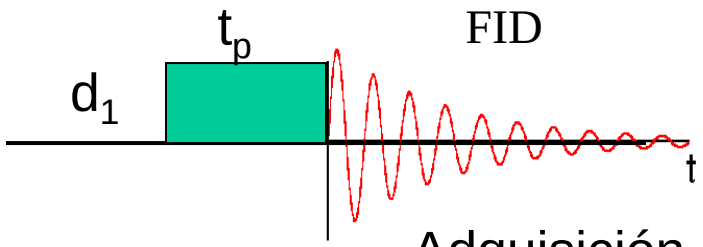

Adquisición at

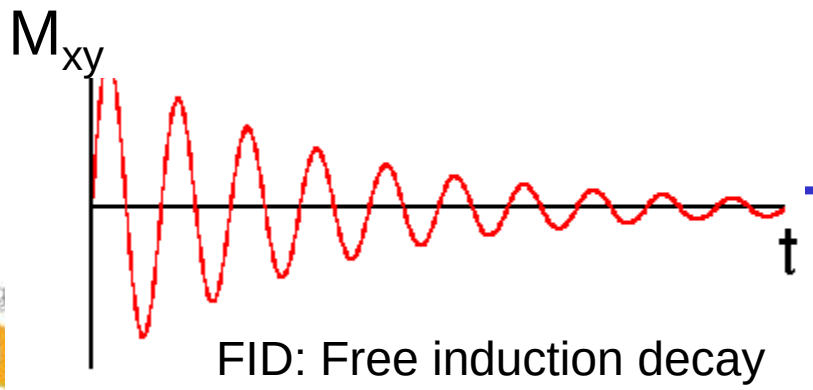

FT

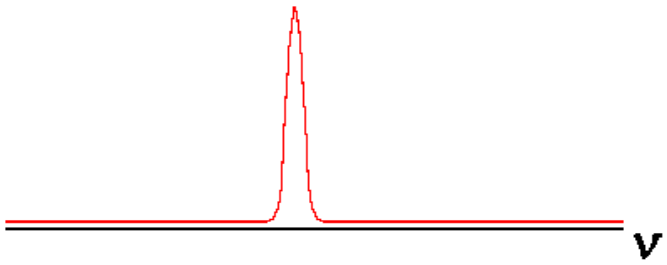

FID: Free induction decay

Shielding: Chemical shift ppm

The electrons around the nucleus generates a local fiedl opposite to B_0 $B = Bo\ (1-\sigma)$

The resonance frequency of a nuclus depends on its environment

$$\nu = \gamma/2\pi Bo\ (1-\sigma)$$

$$\delta\ (ppm) = (\nu - \nu_{ref})\ x10^6 / \nu_{ref} \approx (\sigma_{ref} - \sigma)\ 10^6$$

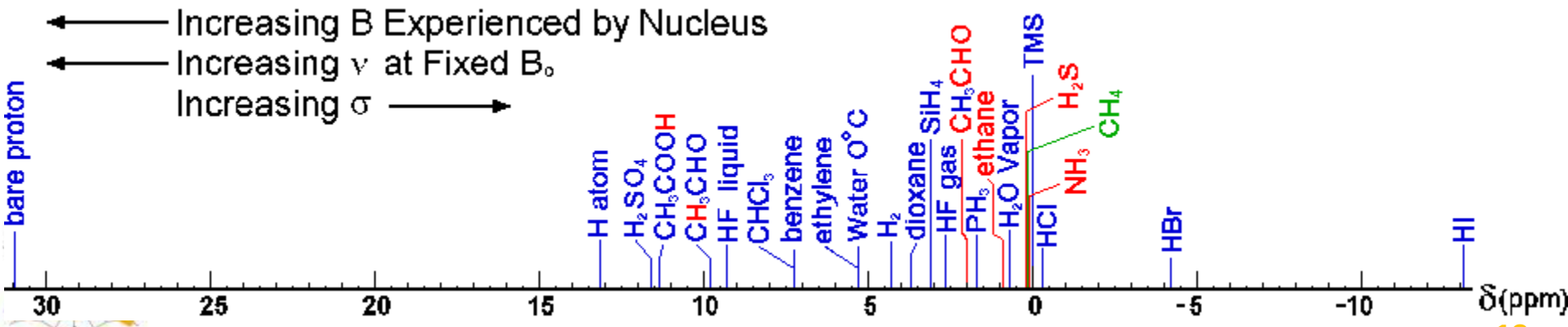

Relaxation

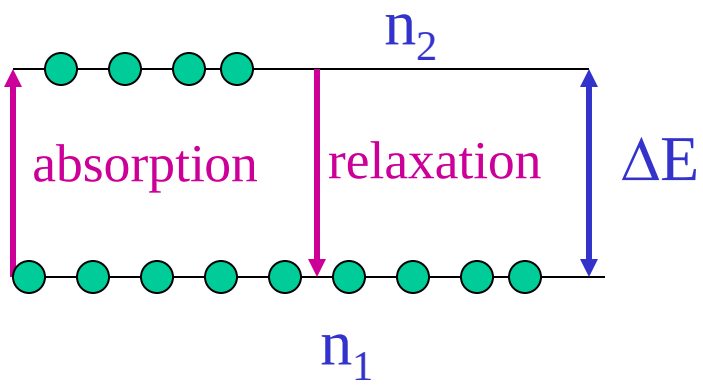

The population of states is given by de Boltzman distribuition:

The probability of transition is given by the difference of population

T_1: longitudinal relaxation time restores the equilibrium distribution

T_2: Spin-spinl relaxation time. Different type of interactions which provokes magnetization losses in the x-y plane.

^{13}C NMR

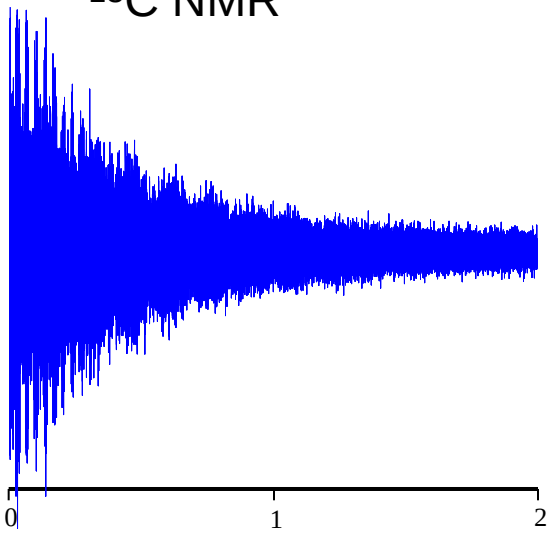

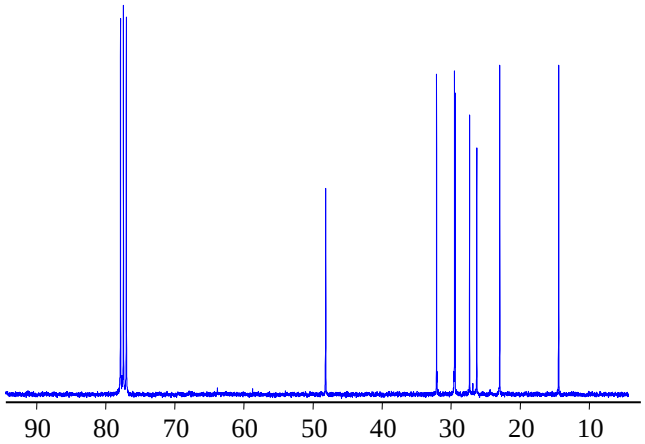

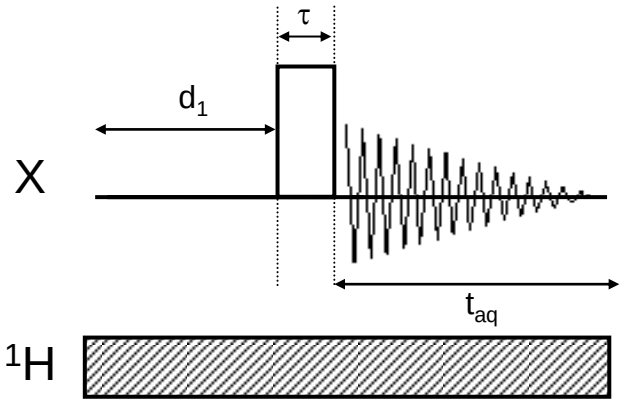

^{13}C MAS NMR

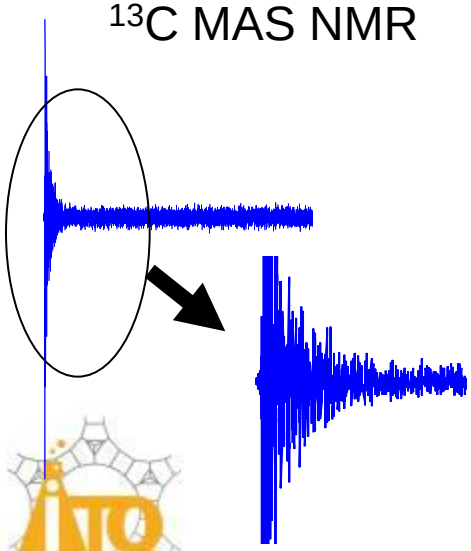

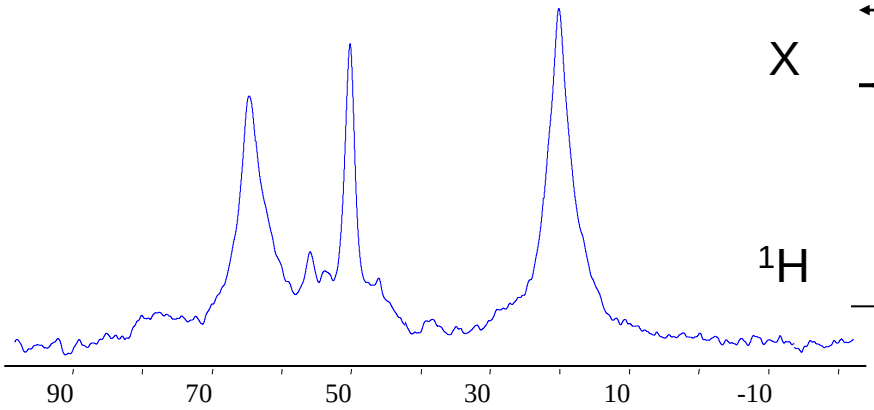

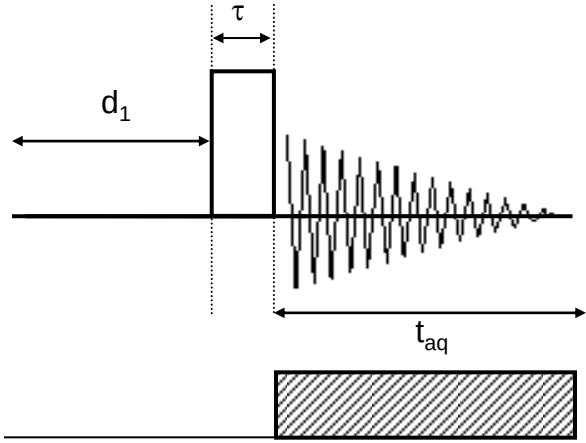

2D NMR Spectroscopy

a)

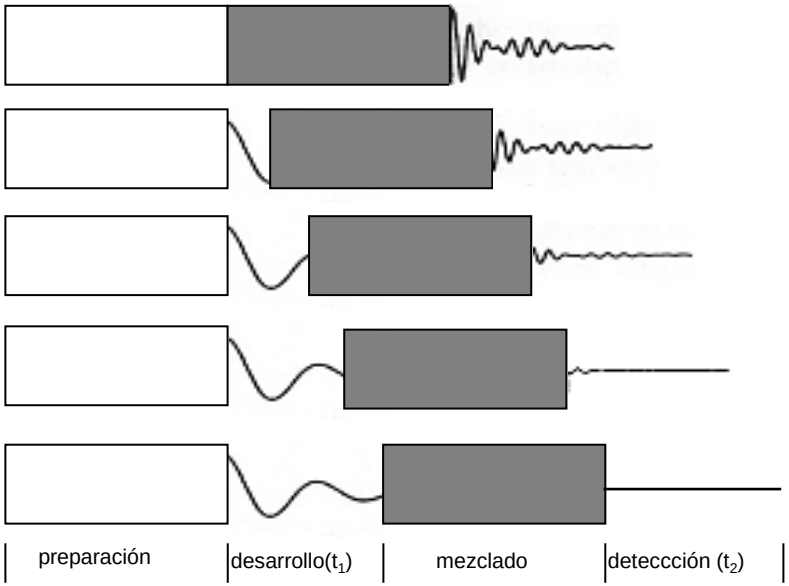

b)

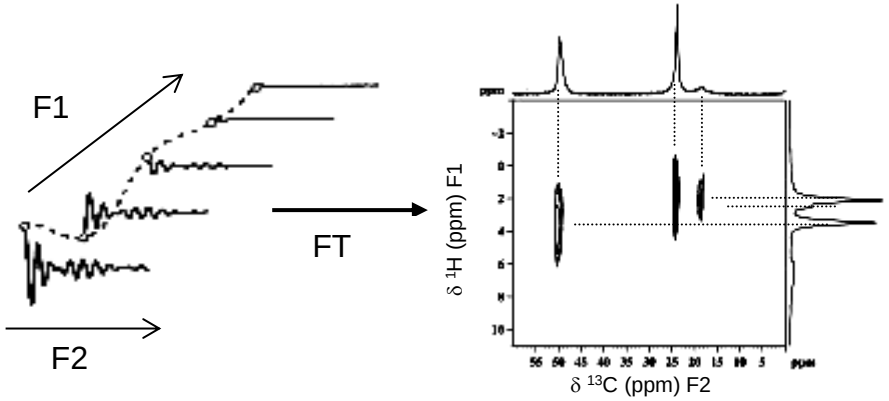

Pulse sequences

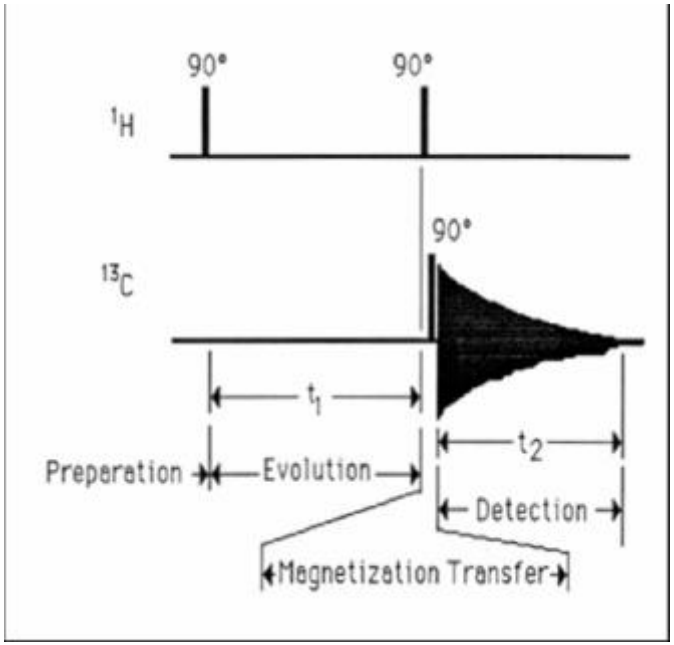

HETCOR

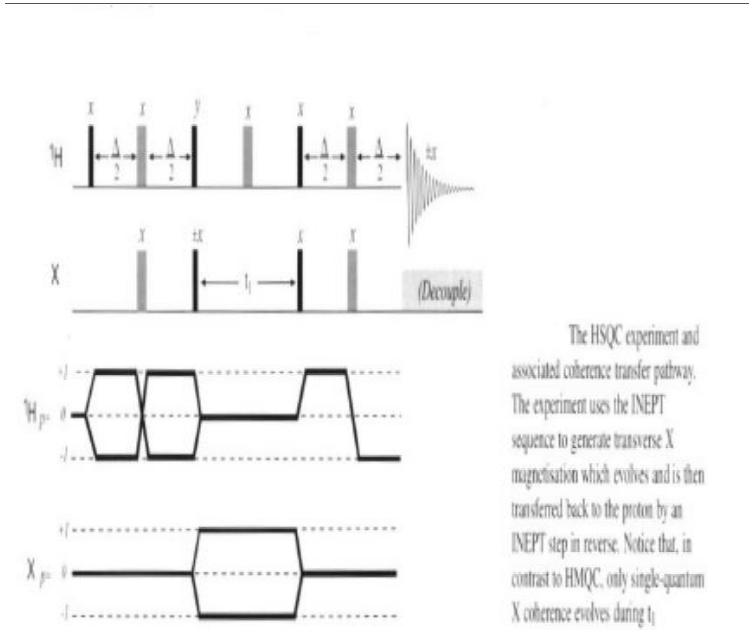

HSQC
***H*eteronuclear Single *Q*uantum *C*orrelation**

Thera are many pulse sequences providing different information

NMR spectroscopy

- Element specific:

- Gives information on the environment of the nucleus: functional groups, chemical environment, ….

NMR spectroscopy: Nobel prizes

Bloch

1952: Física

"Desarrollo de Nuevos métodos de Medida de propiedades magnéticas y nucleares y descubrimientos relacionados"

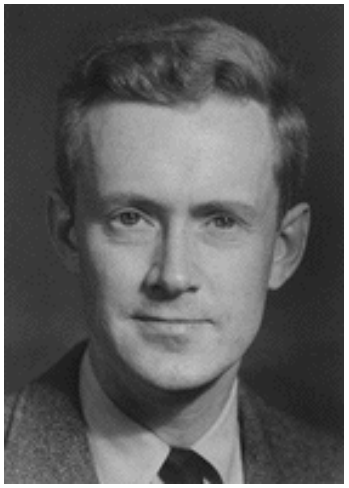

Purcell

Richard Ernst

1991: Química

"Por sus contribuciones al desarrollo de la metodología de la espectroscopia de RMN de alta resolución"

NMR spectroscopy: Nobel prizes

Kurt Wüthrich

2002: Química

"por sus desarrollos en espectroscopia de RMN para la determinación de estructura tridimensional de macromoléculas biológicas en disolución"

Paul Lauterbur

2003: Medicina

"por sus descubrimientos relativos a la resonancia magnética de imagen"

Sir Peter Mansfield

Outline

- **Fundaments of NMR spectroscopy**
  - **Solid state NMR**
- Aplication on heterogeneous catalysis: Zeolites:
  - Structural characterization
  - Chemical Physical properties
  - Reaction Mechanisms

Solid State NMR

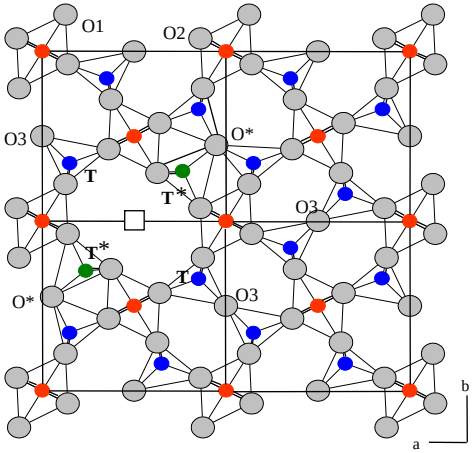

Solids: low mobility

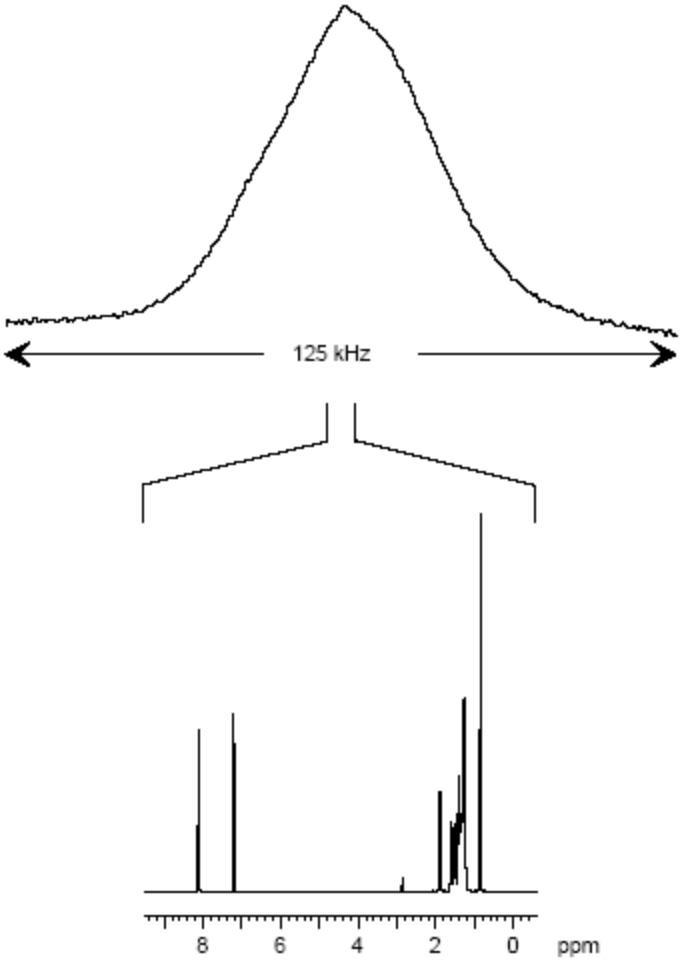

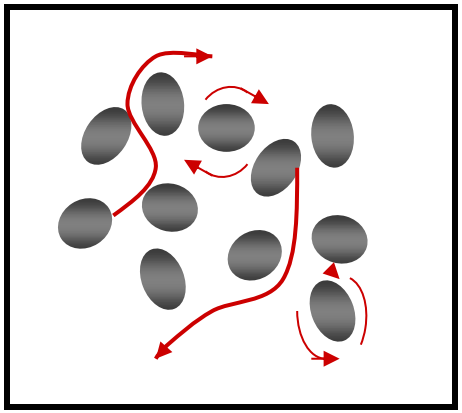

Liquids: high mobility

Solid State NMR: Anisotropy

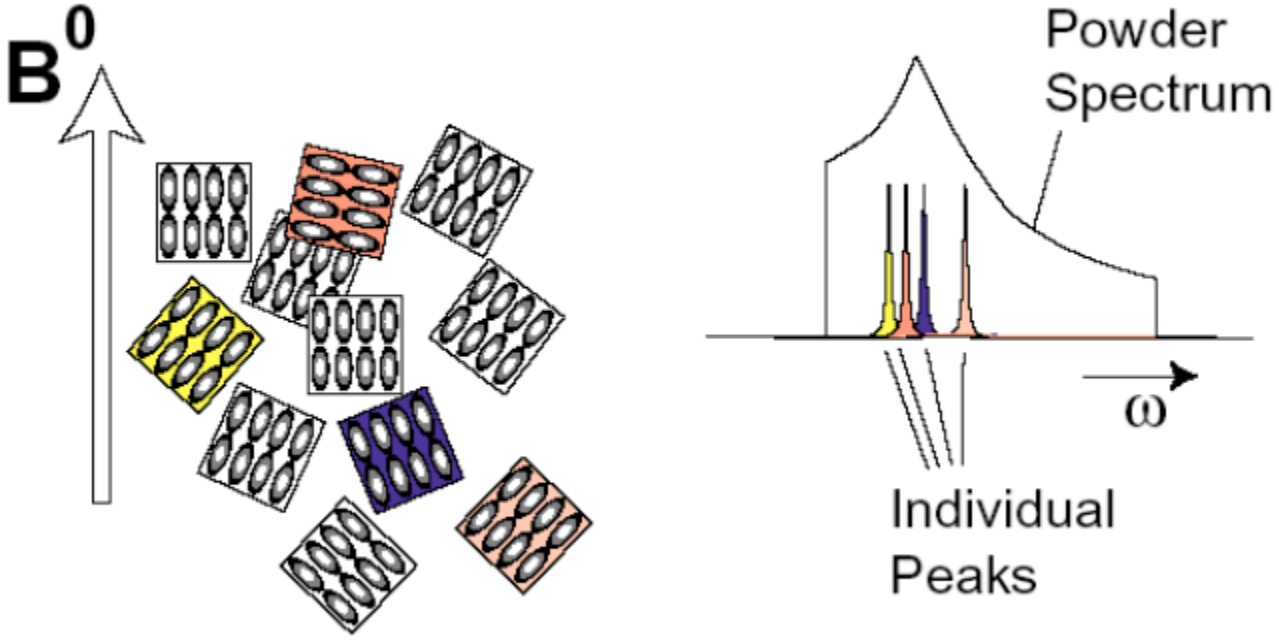

Anisotropic interactions in solids

1: Chemical Shift Anisotropy CSA:

δ orientaion of the molecule or the crystal respect B0

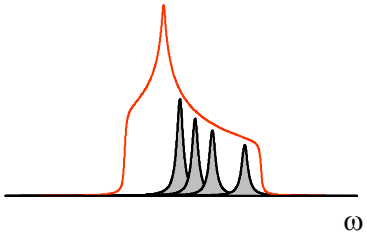

2: Dipolar coupling:

Through space interaction of two close nuclei I≠0.

- ***Heteronuclear***
- *Homonuclear*

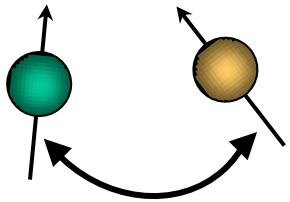

3: Quadrupolar interactions I>1/2.

Interaction of the quadrupolar moment with the electric field gradient generated by the charges around it.

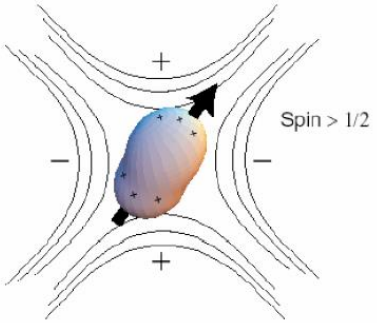

1: Chemical shift anisotropy: CSA

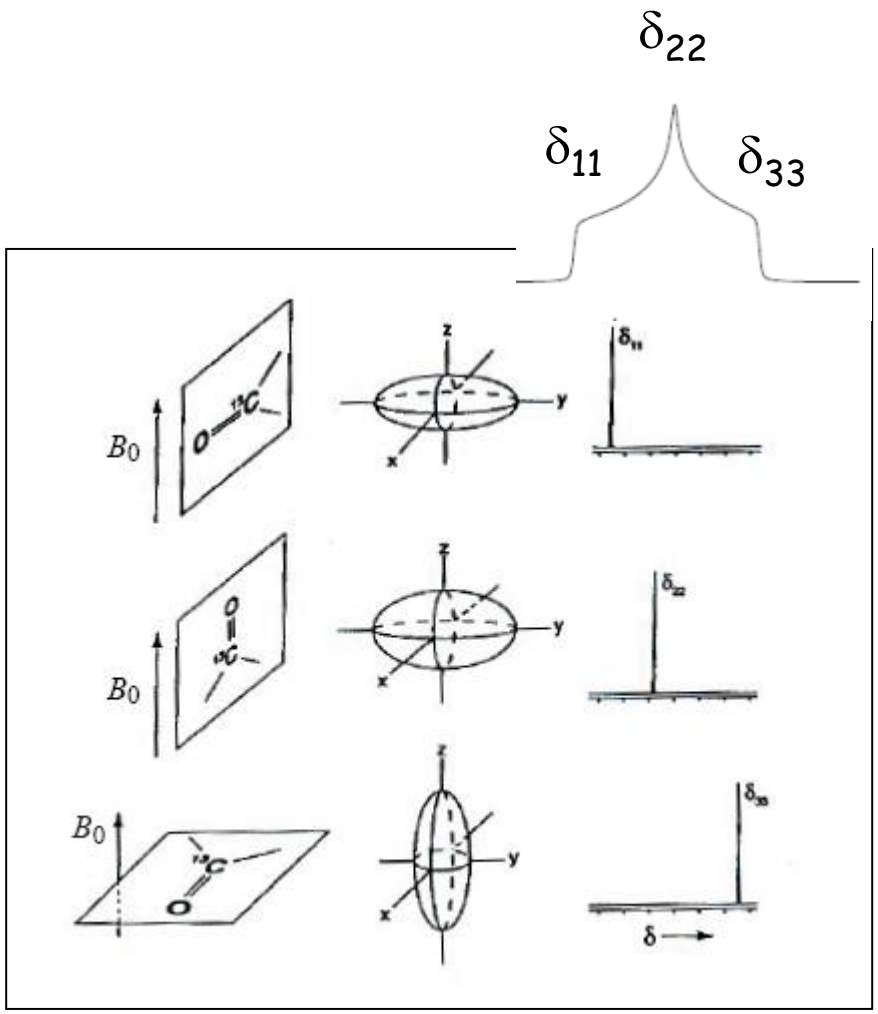

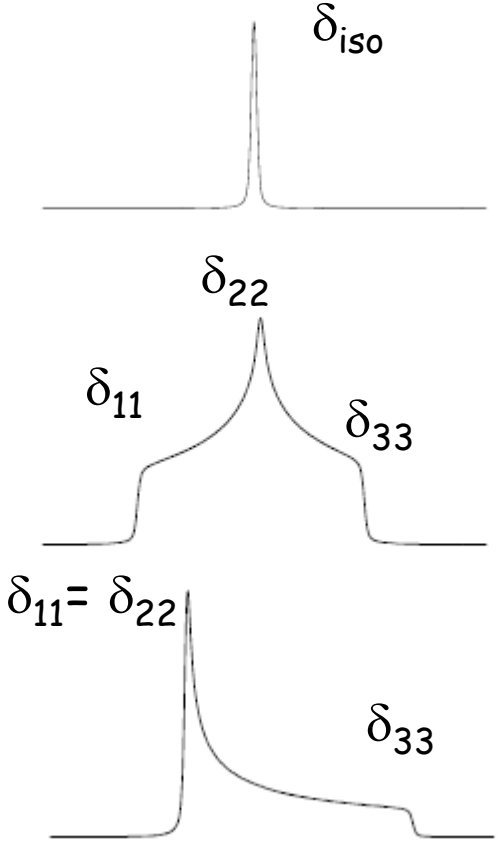

The resinance frequency of $^{13}C{=}O$ dependes on the orientation respect B_0.

2: Dipolar interacions

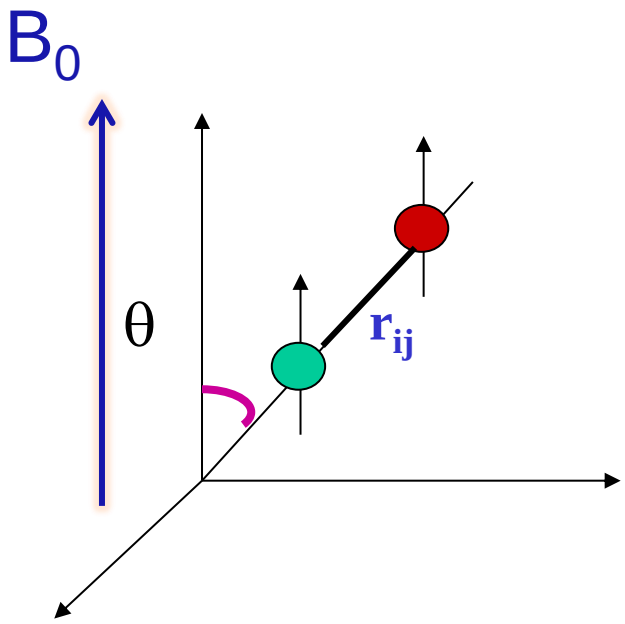

- Depends on the orientation of the dipolar vector respec B_0
- Through space interaction, it does not need chemical bonding
- Decreases sharply with distances
- The magnitud is propotional to γ_I and γ_S

2: Dipolar interaction

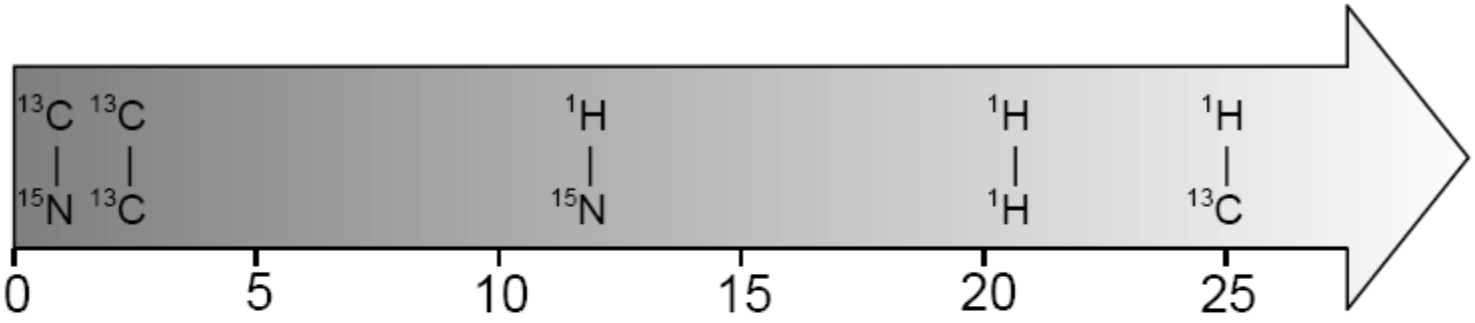

$|b_{12}| / 2\pi$ [kHz]

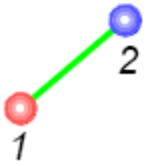

Nuclear Pair	Internuclear Distance	R^{DD} (Hz)
^{1}H, ^{1}H	10 Å	120 kHz
^{1}H, ^{13}C	1 Å	30 kHz
^{1}H, ^{13}C	2 Å	3.8 kHz

1: MAS: Magic angle spinning

CSA
Dipolar interactions

$$P_2(\cos\theta) = \frac{1}{2}(3\cos^2\theta - 1)$$

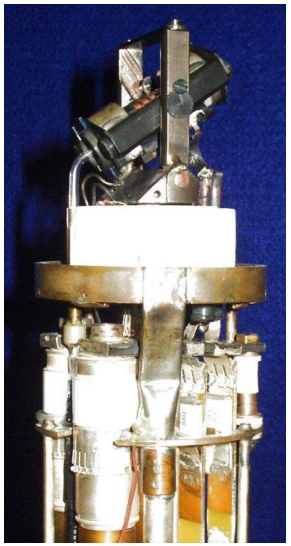

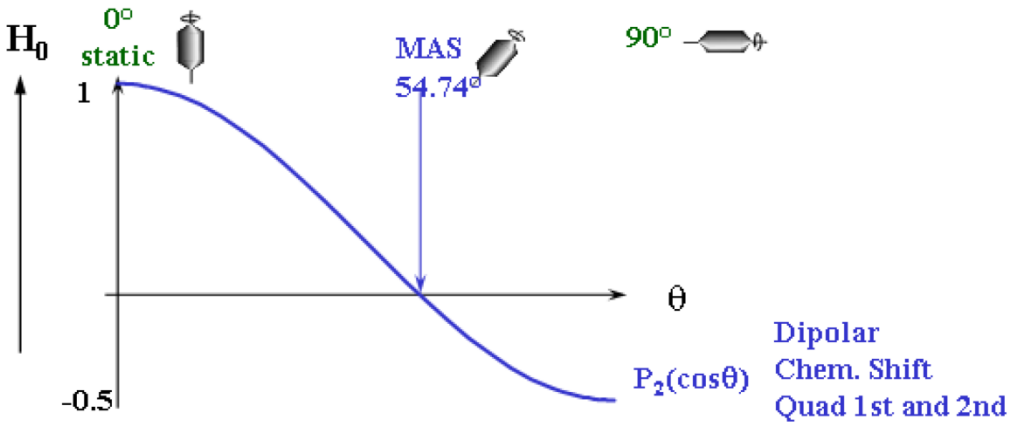

The interaction is averaged spinning the sample at the MA at rate 3 or 4 times higher than the interaction

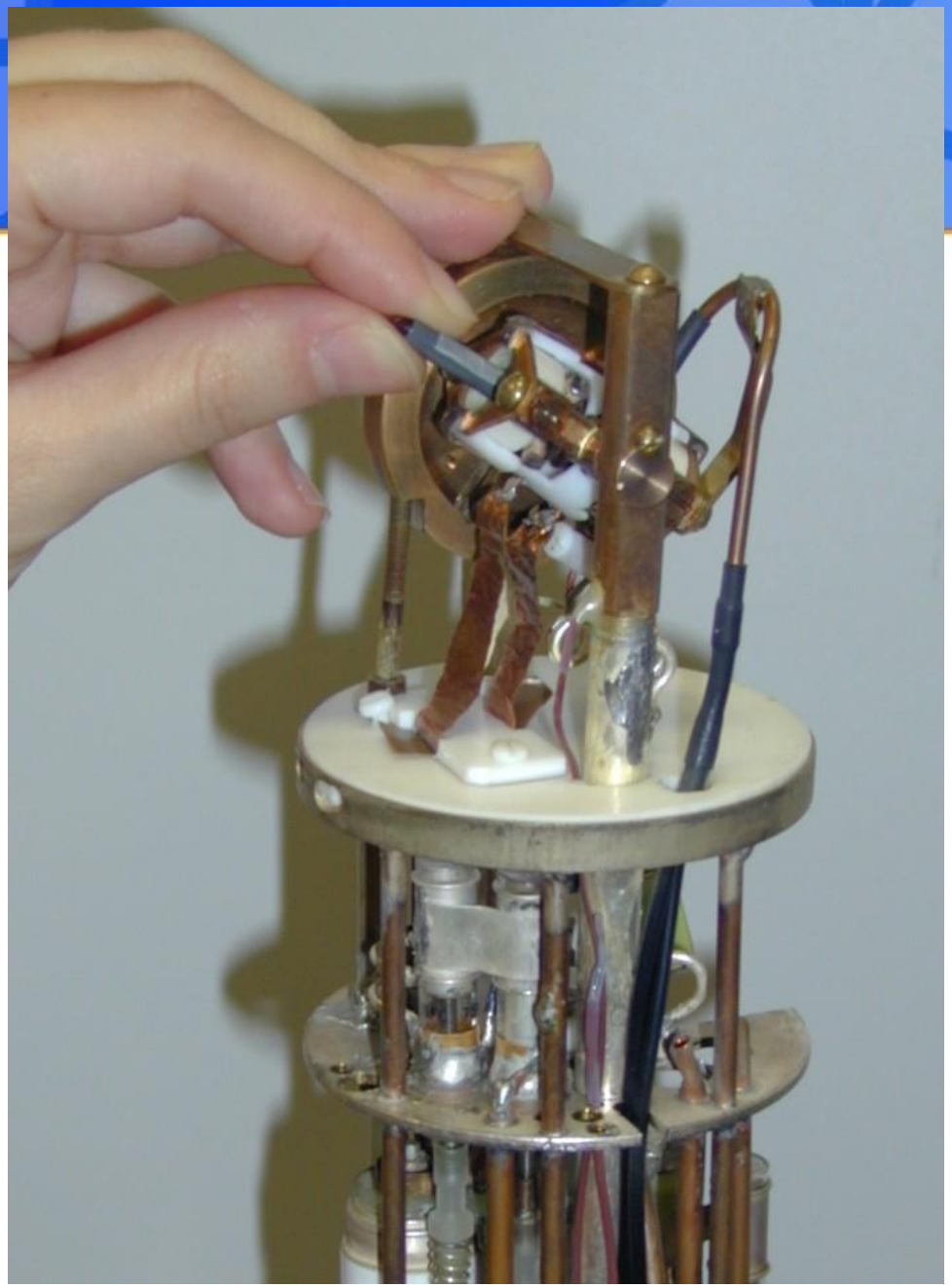

Rotor caps

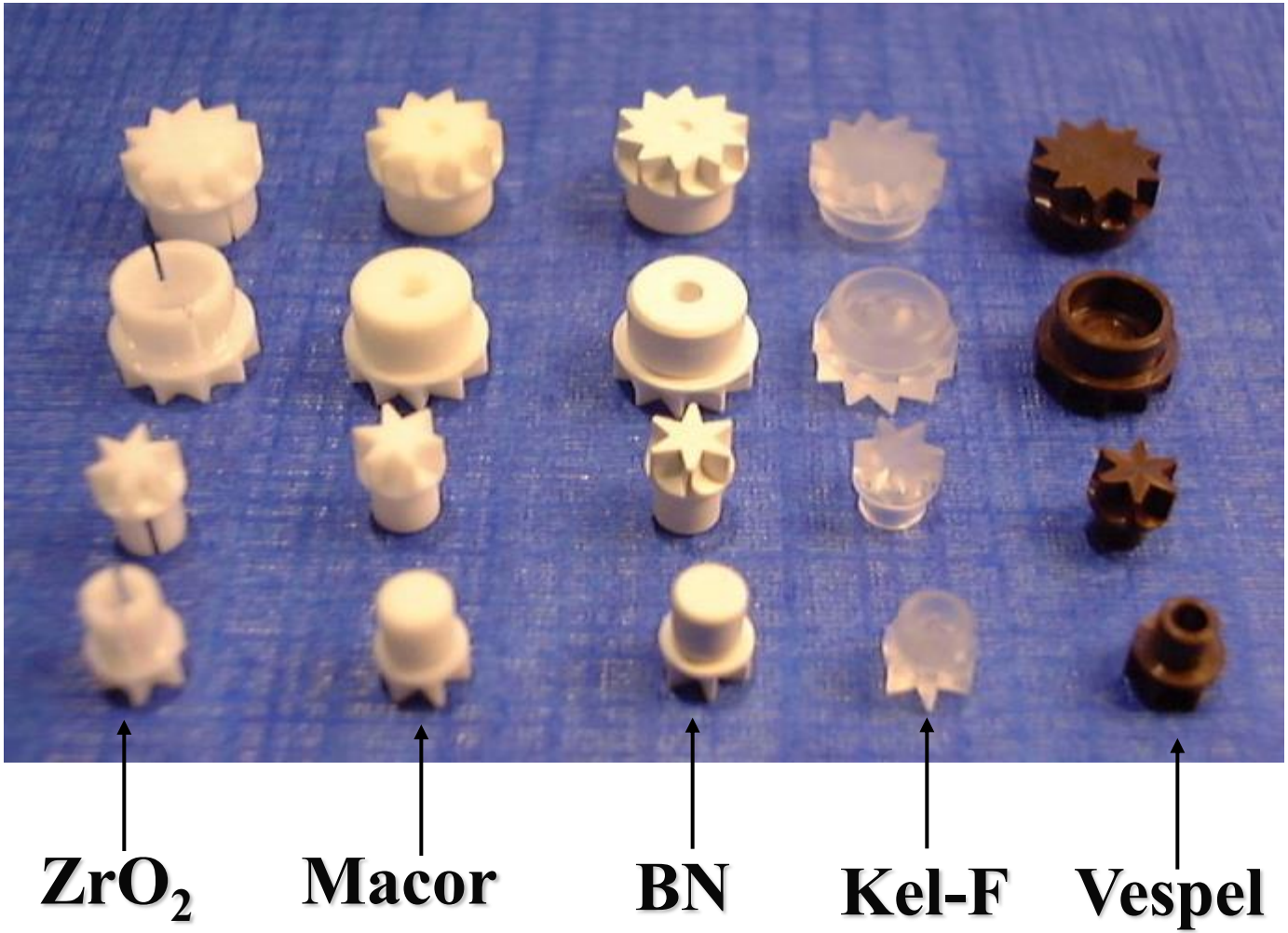

CSA: Spinning side bands

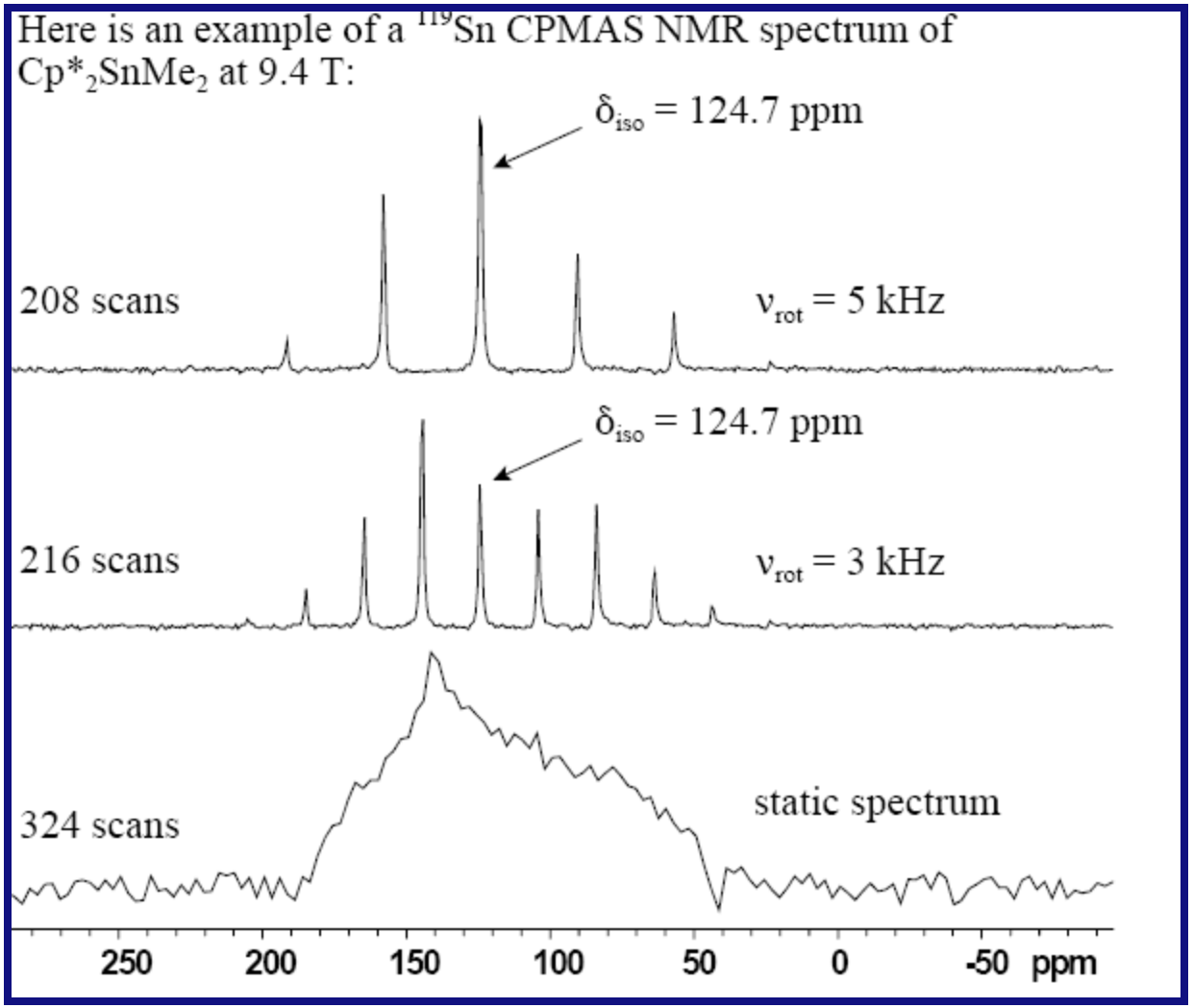

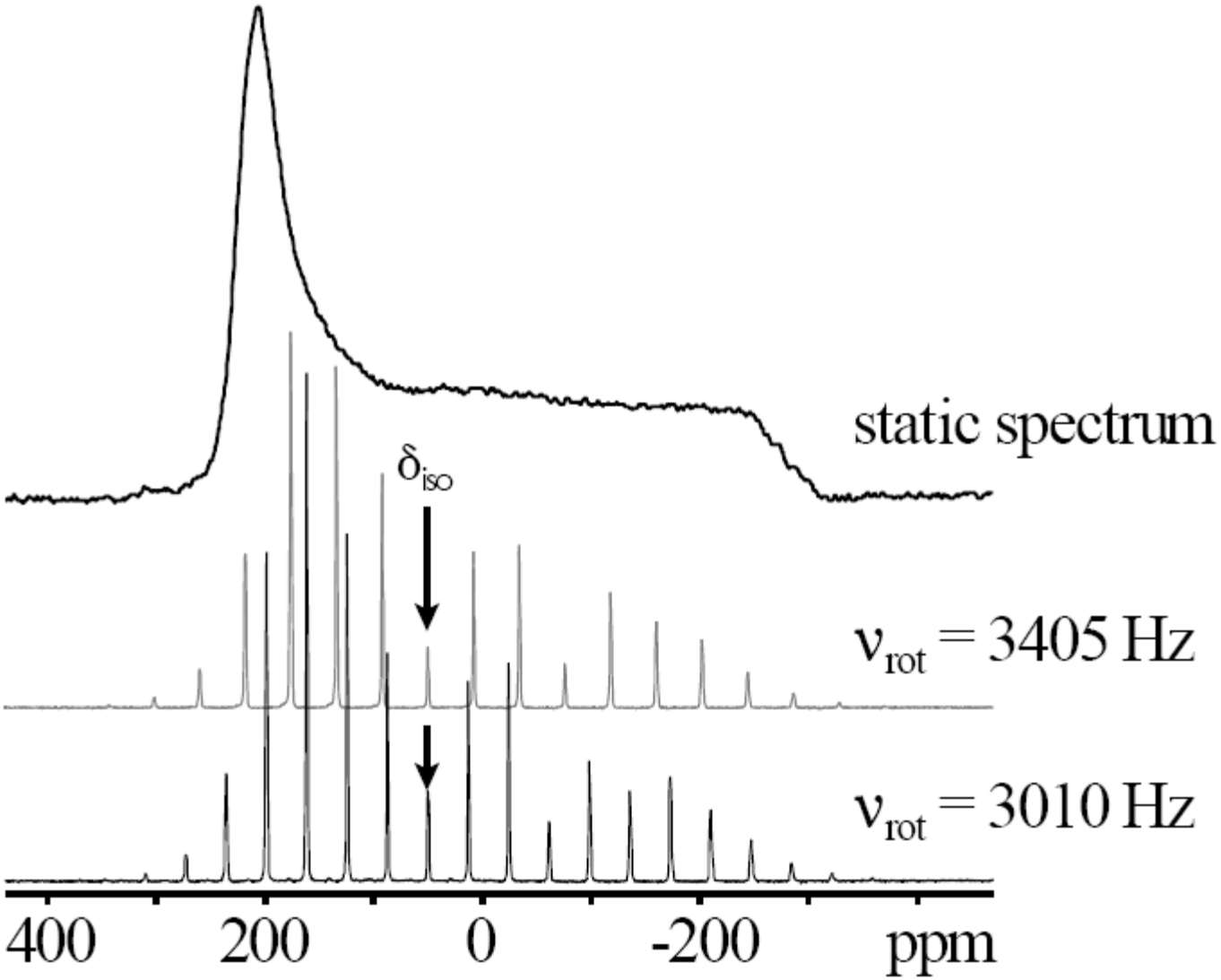

Ω= 500 ppm, 40000 Hz (^{31}P a 4.7 T)

2: Dipolar interactions: Cross polarization

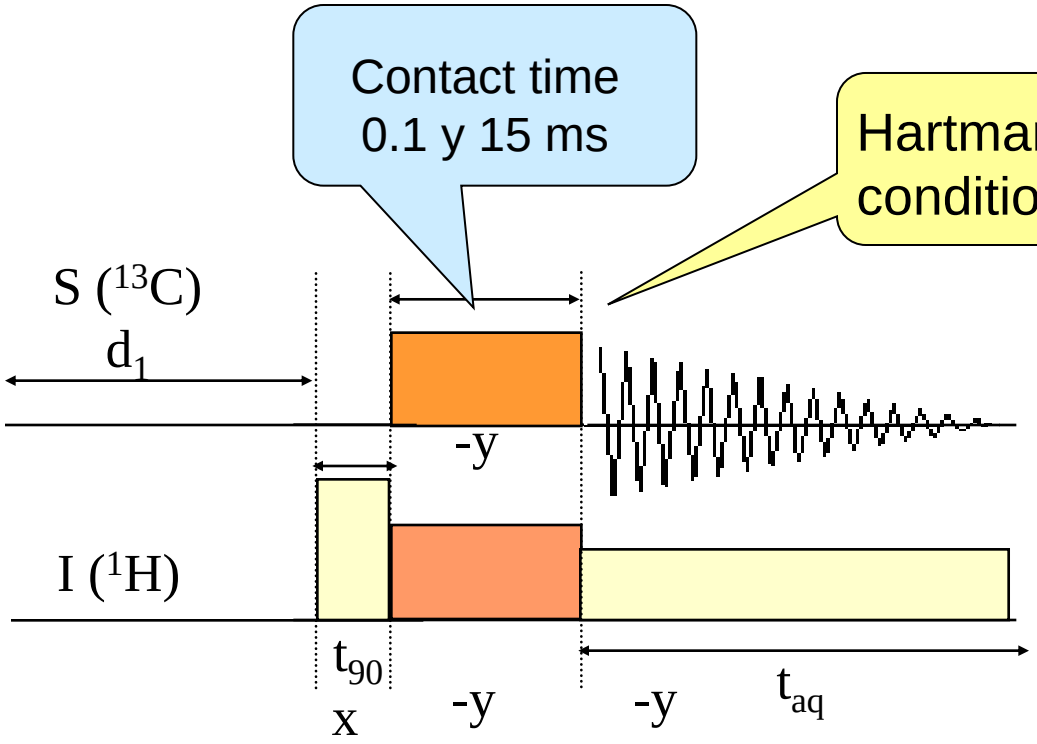

$\gamma_I B_1(I) = \gamma_I B_1(S)$

Dipolar interactions: Cross polarization experiment

Magnetization transfer from highly to low polarized nuclei

- Increases de intensity of low γ nuclei (^{13}C); potencialmente en un factor γ_I/γ_S
- It can be used to obtain chemical information
- he efficiency of the magnetization transfer decreases with the spinning rate.

3: Quadrupolar interactions

I=1/2 spheric

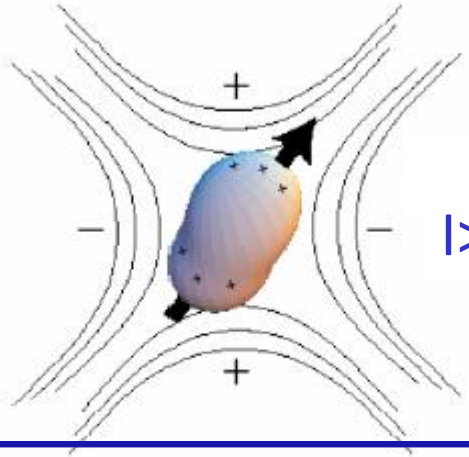

I>1/2, non- spheric

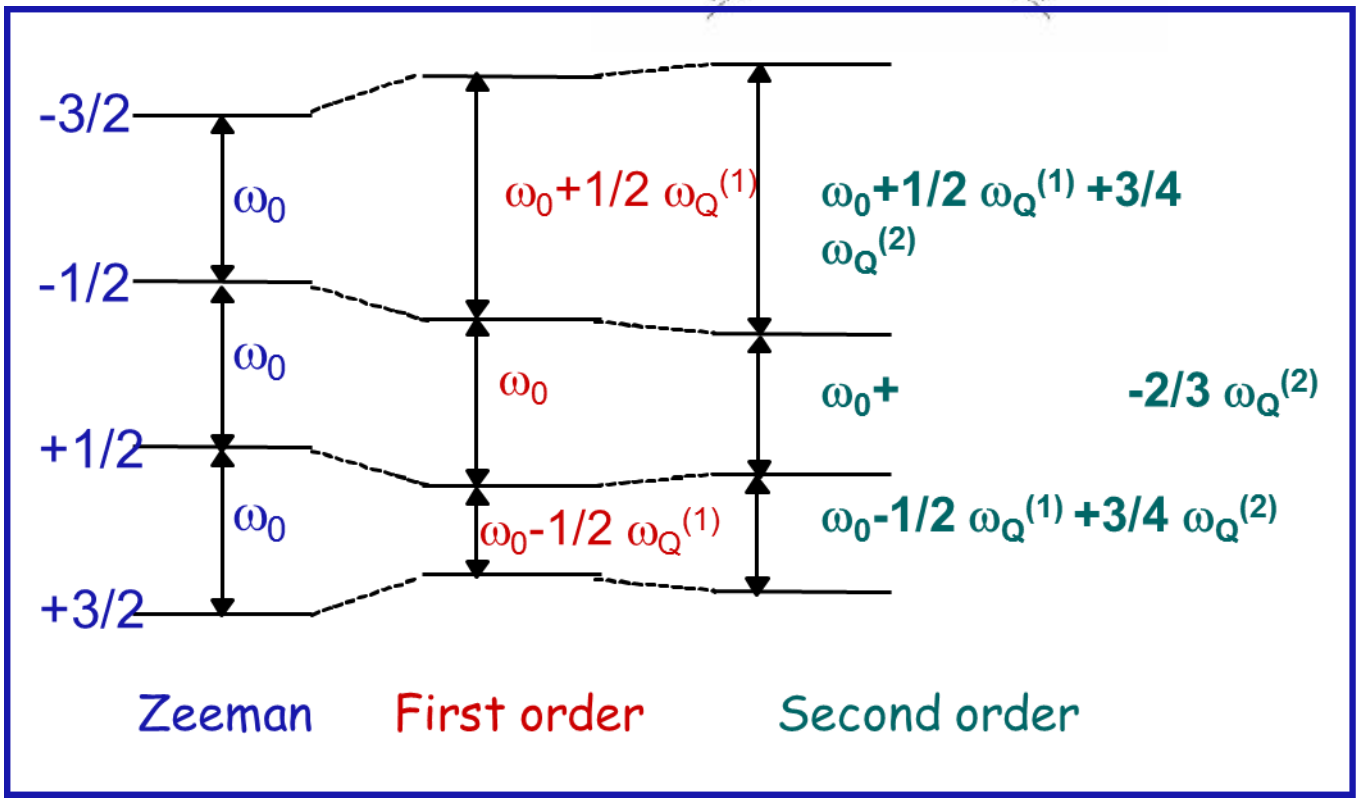

3: Interacciones cuadrupolares

First order quadrupolar interaction are averaged spinning at MAS

Second order quadrupolar interaction are not averaged spinning MAS

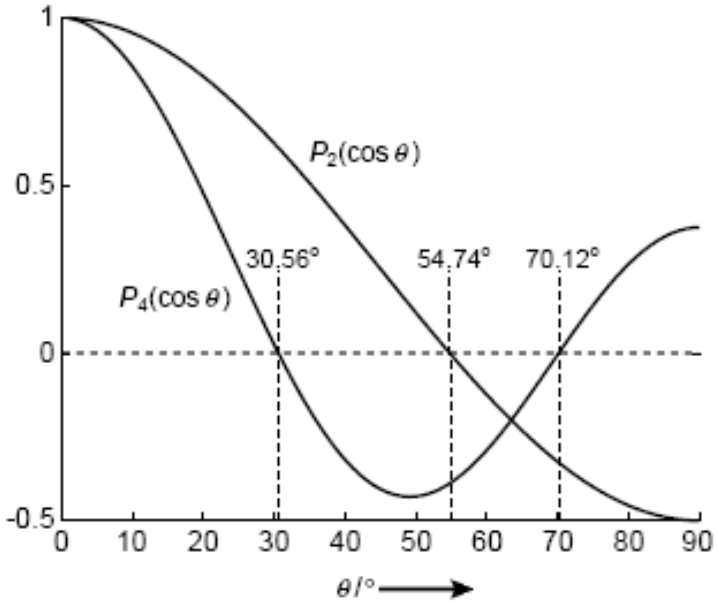

Figure 47. Plot of the second- and fourth-order Legendre polynomials $P_2(\cos\theta)$ and $P_4(\cos\theta)$, respectively, as a function of θ. $P_2(\cos\theta) = 0$ at the magic angle of 54.74°; $P_4(\cos\theta) = 0$ at angles of 30.56° and 70.12°.

3: Interacciones cuadrupolares

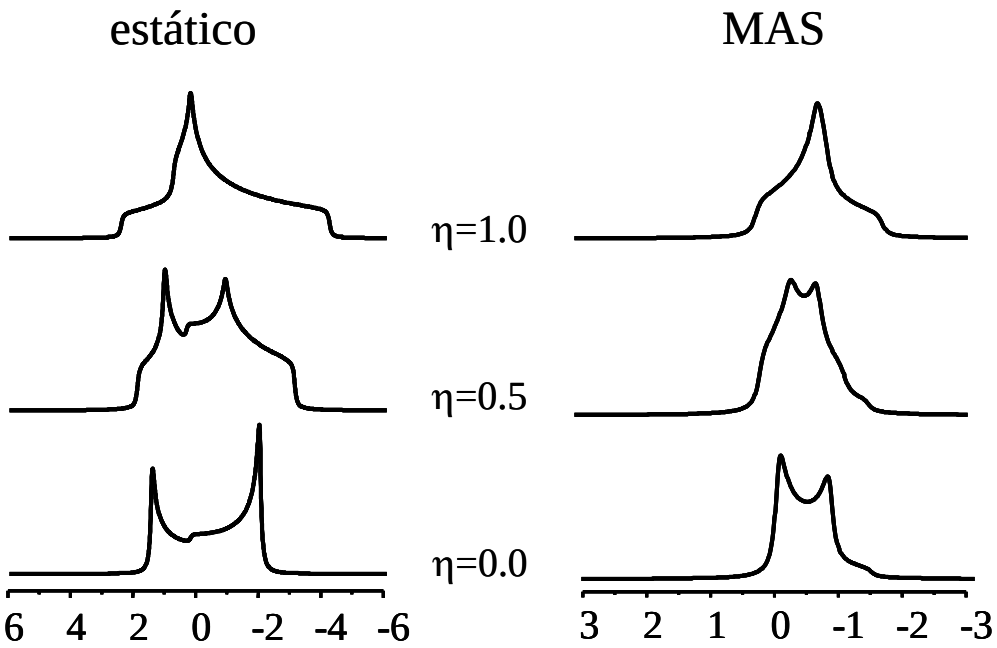

Forma de la transición central de un núcleo cuadrupolar I>1/2: izquierda: en estático, derecha: girando al ángulo mágico. (QCC=4 MHz).

3: Interacciones cuadrupolares

27Al NMR

I=5/2

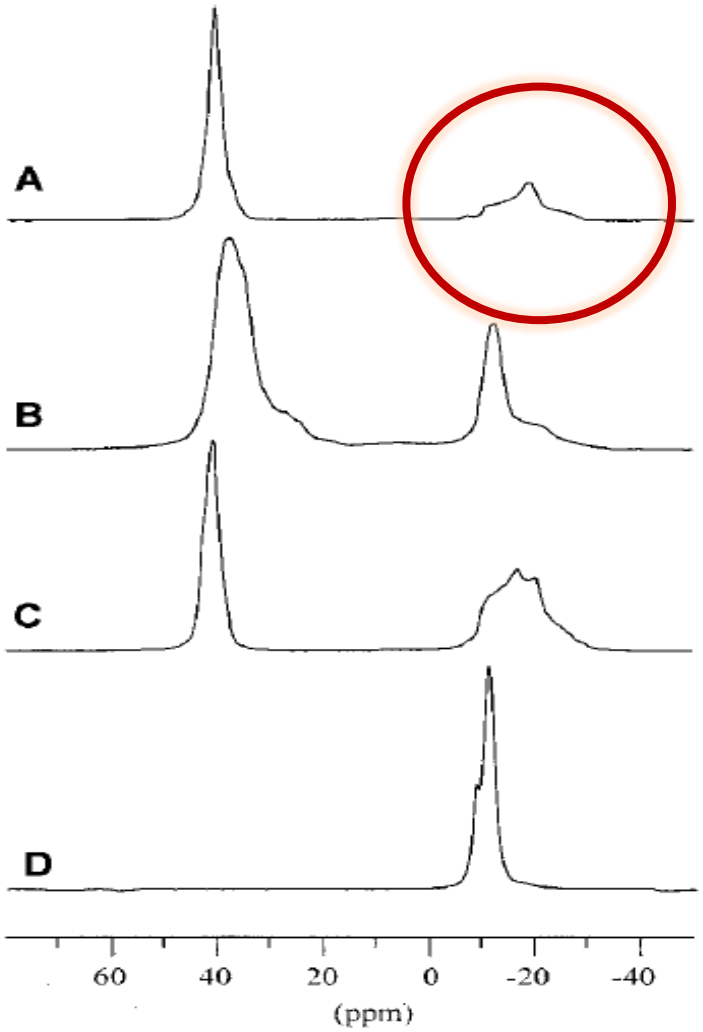

Figure 4. ^{27}Al MAS NMR spectra of VPI-5(a), $AlPO_4$-8(b), $AlPO_4$—H3(c) and metavariscite(d).

3: Quadrupolar interactions

- Decreases when B_0 increases

- Second orden quadrupolar interctions are **NOT** averaged by MAS.

  – Signal is high field shifted

  – Signals are broadened

3: Interacciones cuadrupolares: ·MQ MAS

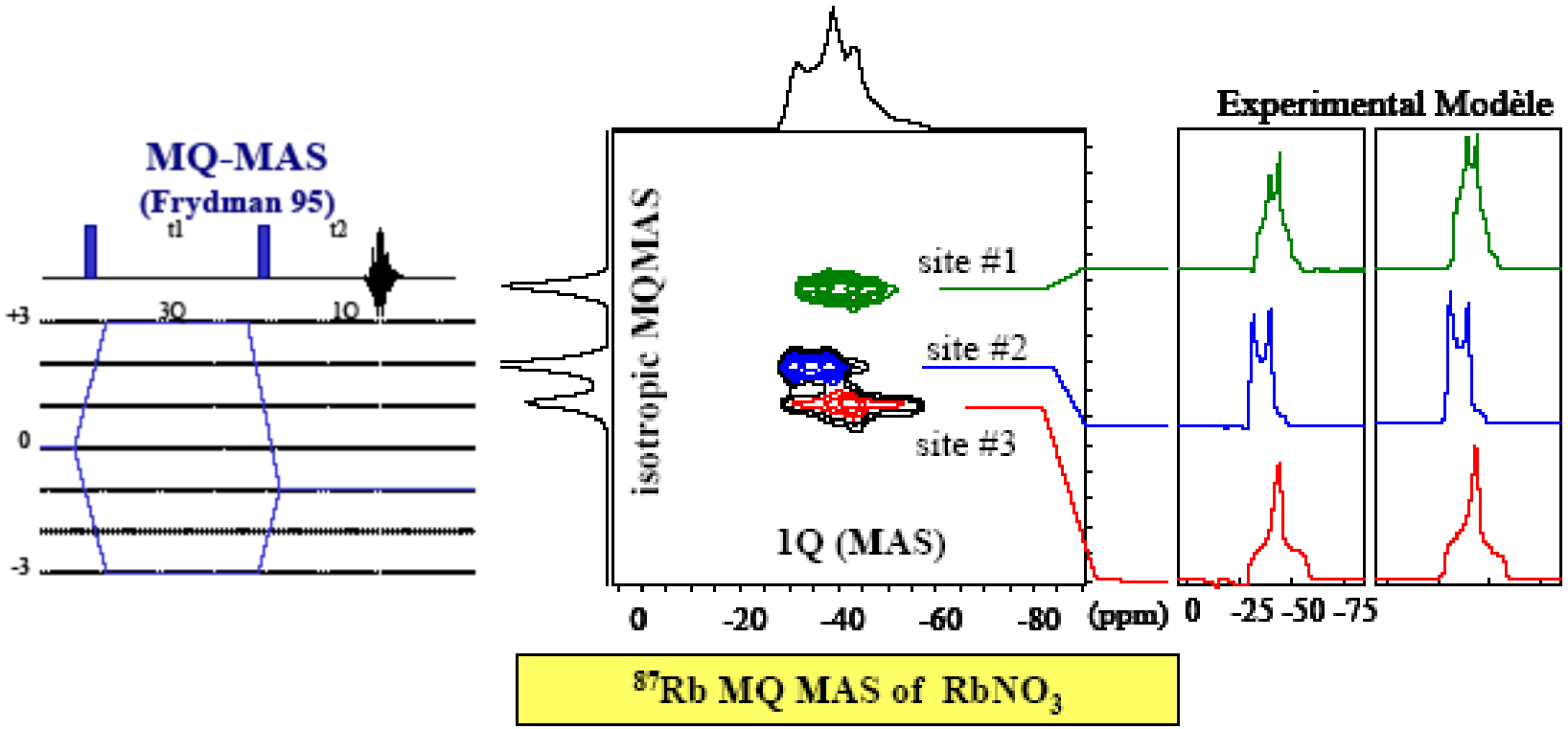

Lucio Frydman 1995

δ_{iso}, Parámetros cuadrupolares

3: Quadrupolar interactions

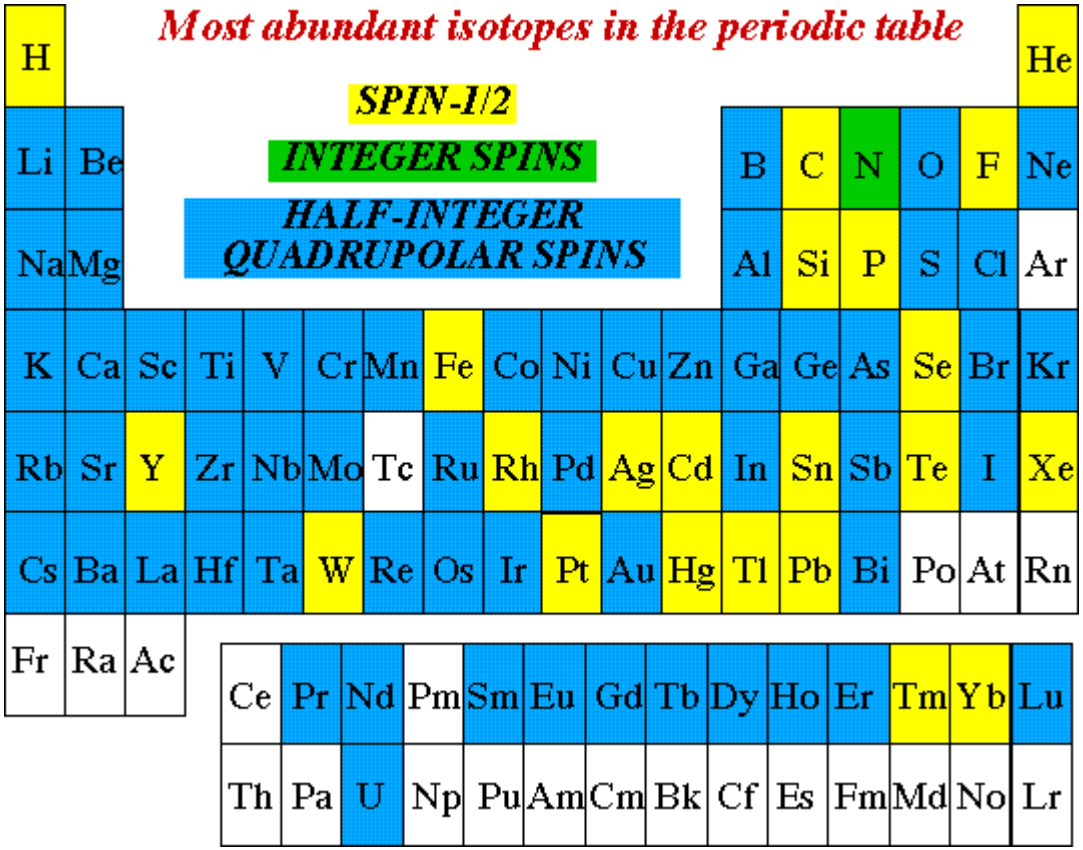

Outline

- Fundements of NMR spectroscopy
  - Solid state NMR
- **Aplication on heterogeneous catalysis: Zeolites:**
  - Structural characterization
  - Chemical Physical properties
  - Reaction Mechanisms

Heterogeneous Catalysis

- Zeolites are the most used heterogeneous catalysts in industry.

  - Oil refining
  - Petrochemical industry
  - Fine chemistry

ZEOLITES

Porous crystalline inorganic materials with a regular distribution of pores and / or cavities of molecular dimensions.

- **Typically, aluminosilicates**
- Silicates
- Aluminophosphates
- Silico-germanates
- Germanates
- Berilosilicates
- Galophosphates
- etc

ZEOLITES

Large variety of structures

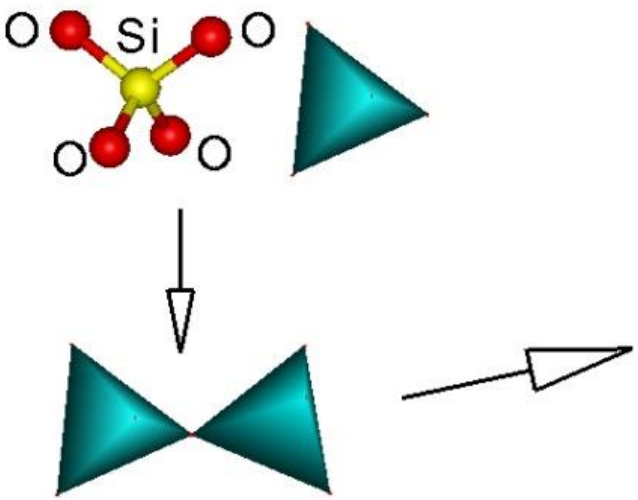

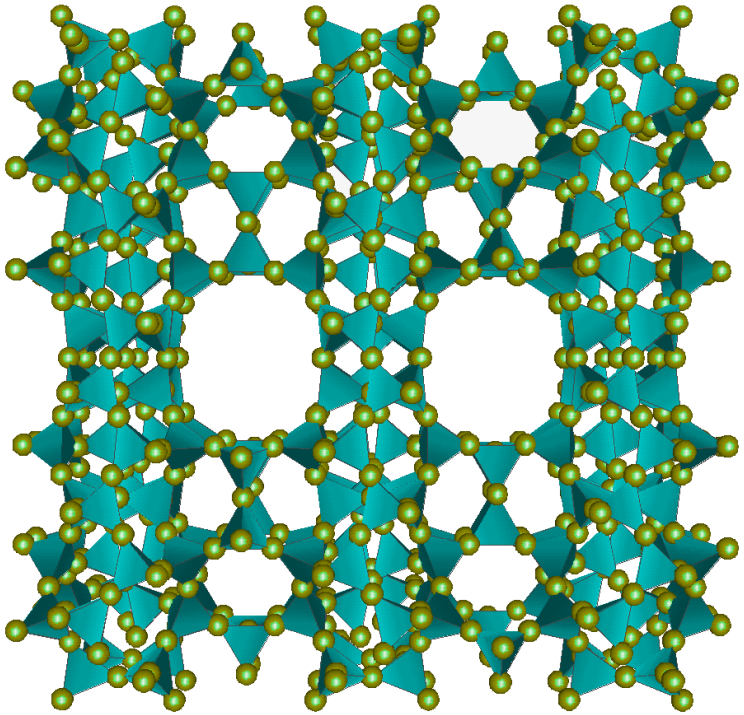

ZEOLITES

(a)

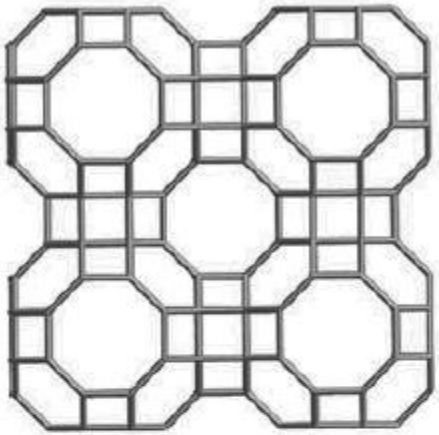

(b)

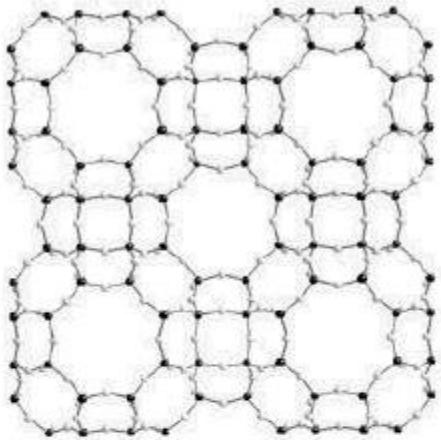

(c)

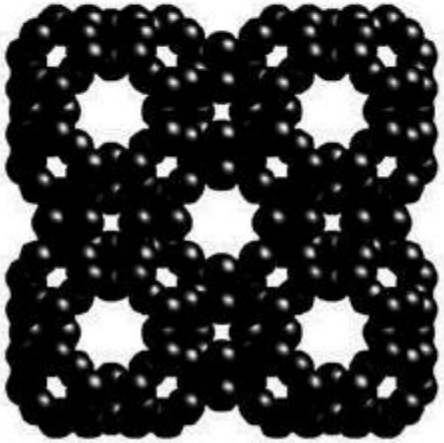

(d)

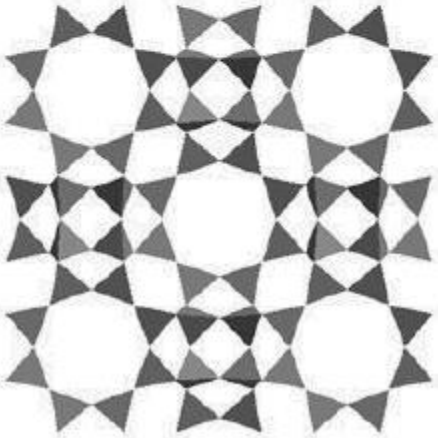

Zeolites: Pores and cavities of molecular dimmensions

Small pore

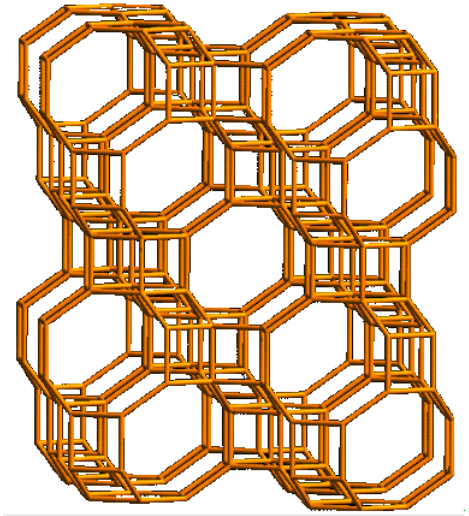

Chabazita
8 TO_2
3.8 x 3.8 Å

Medium pore

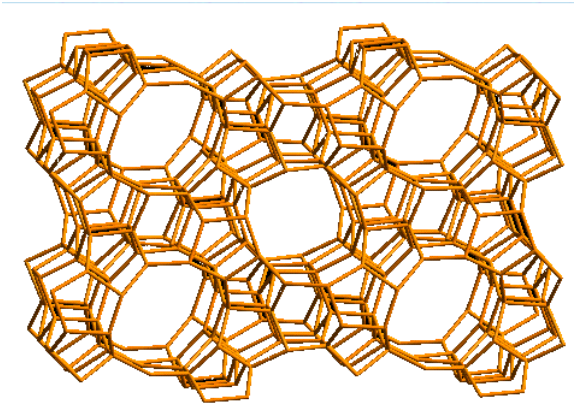

ZSM-5
10 TO_2
5.5 x 5.1 Å

Large pore

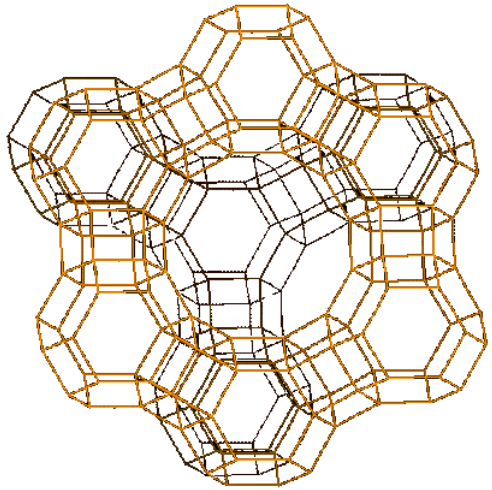

Faujasita
12 TO_2
7.4 x 7.4 Å

Zeolites: Extra-large pores zeolites

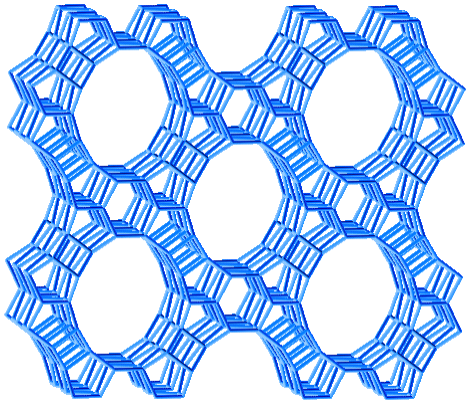

UTD-1
14 TO_2
8.2 x 8.1 Å

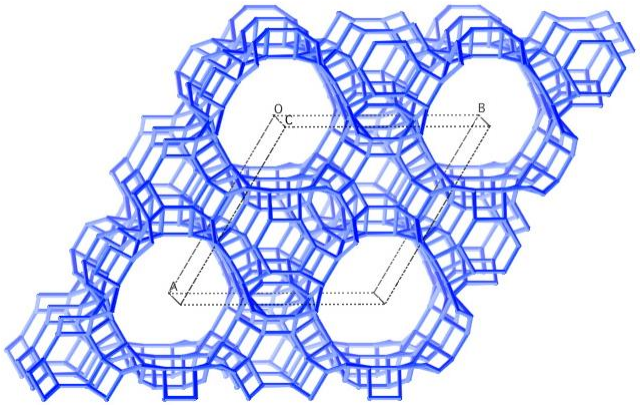

ECR-34
18 TO_2
10.1 x 10.1 Å

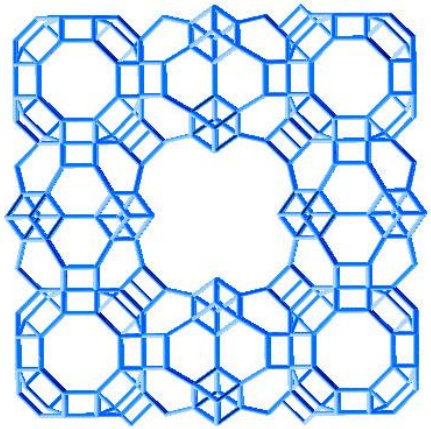

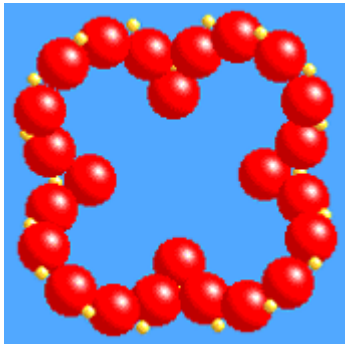

Cloverita
20 TO_2
13.2 x 6.0 x 3.5 Å

ZEOLITES

Chemical reactions take place within the internal cavities and pores

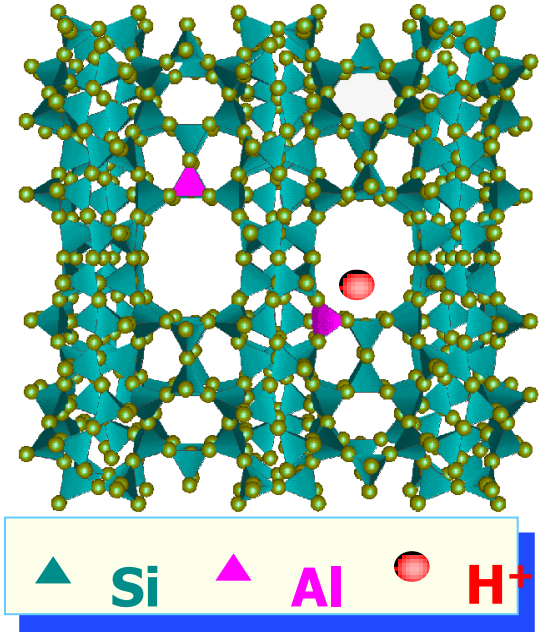

Acid catalysts

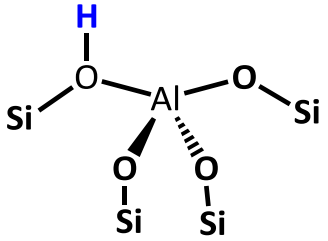

Lowenstein Rule:

- **No Al-O-Al linkage:Al (4 Si)**
- **The maximum Al content corresponds to a Si/Al = 1**

Brønsted acid site

ZEOLITES

Chemical reactions take place within the internal cavities and pores

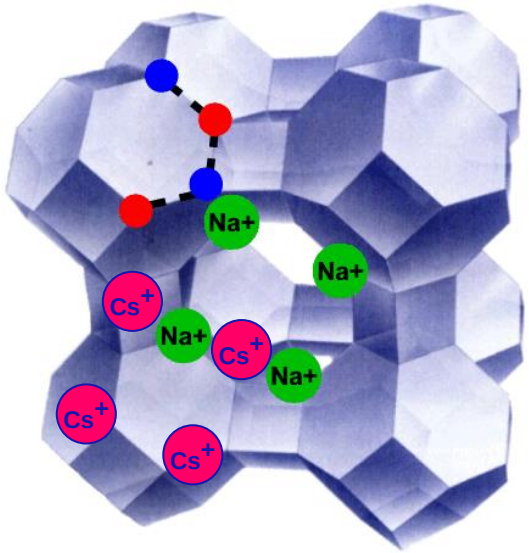

Basic catalysts

TMI: redox catalysts

ZEOLITES AS CATALYSTS: Shape selectivity

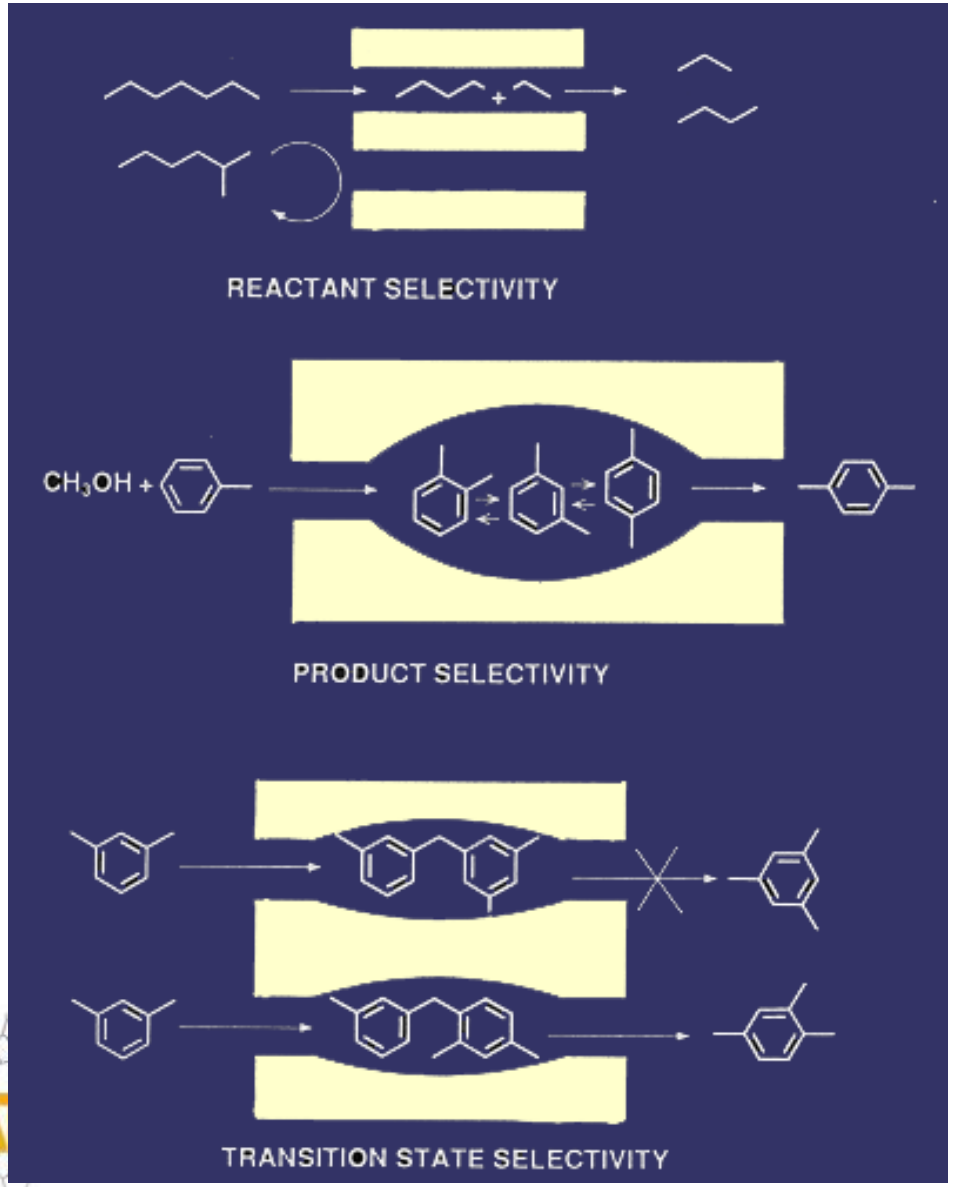

Reactant selectivity: clevage of hydrocarbons

Product selectivity: Methylation of toluene

Restricted transition state selectivity: disproportionation of m-xylene

SYNTHESIS OF ZEOLITES

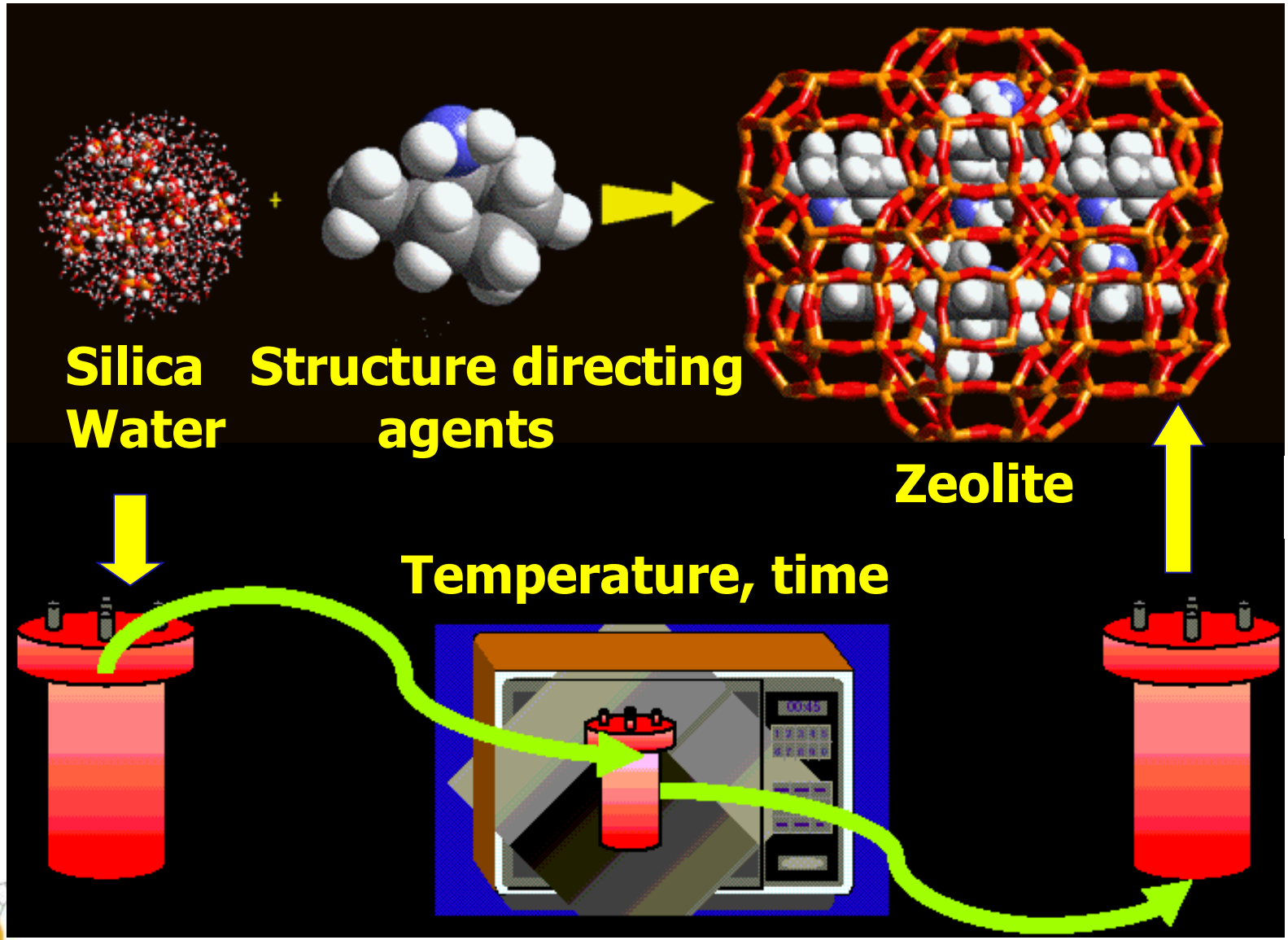

Zeolites Activation

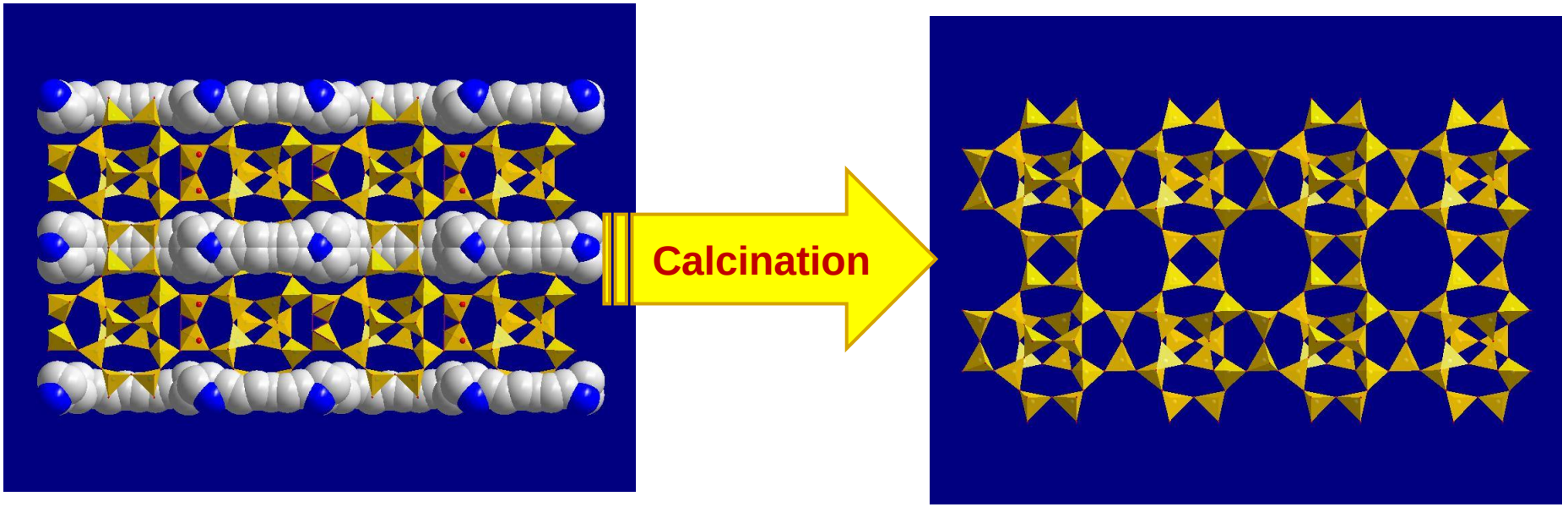

Number of zeolite structures

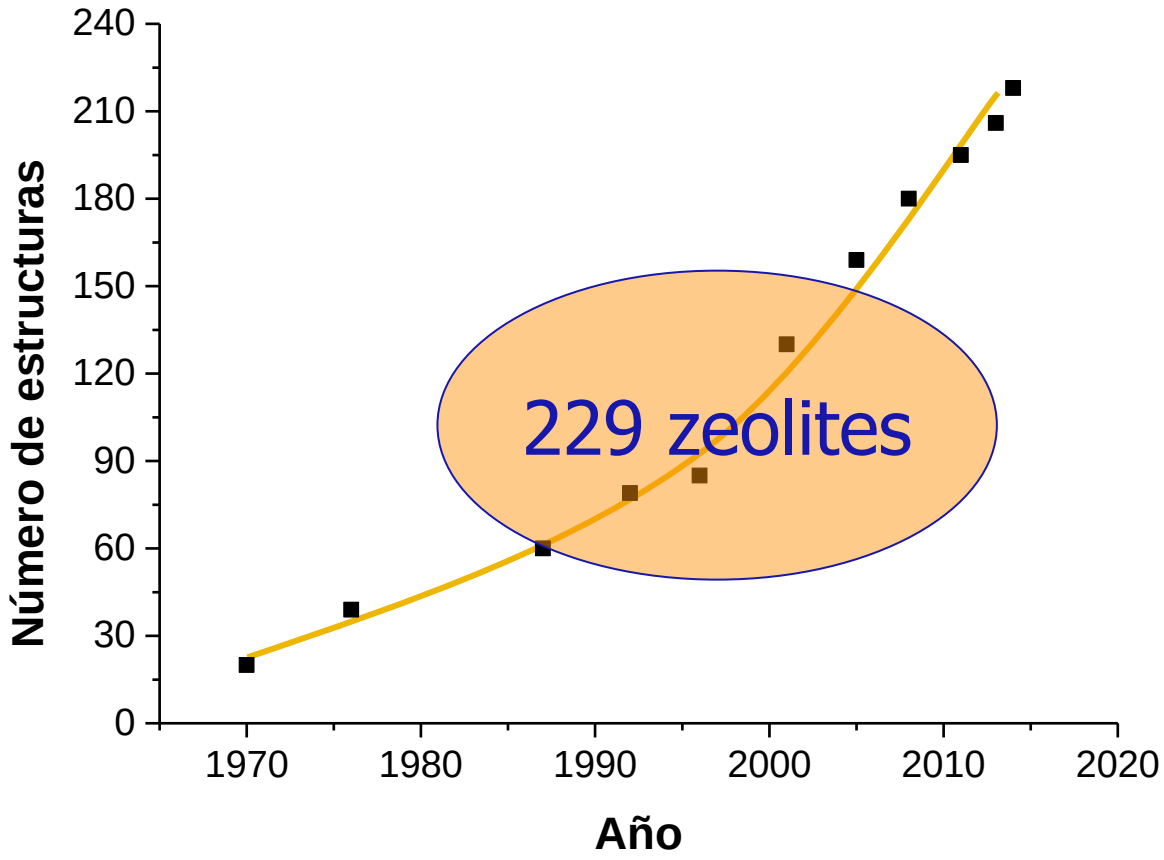

Characteristics of zeolites

- Large number of structures with varying pore dimmensions (shape selectivity)
- Large range of chemical composition (Varying physical chemical and catalytic properties

TAYLORING THE PROPERTIES OF ZEOLITES FOR A SPECIFIC CATALYTIC APPLICATION

Catalyst preparation

Chararacterization

- Structure
- Physical-chemical properties
- Textural

Active sites

Catalytic Reaction

- Reaction Mechanism

NMR Active nuclei

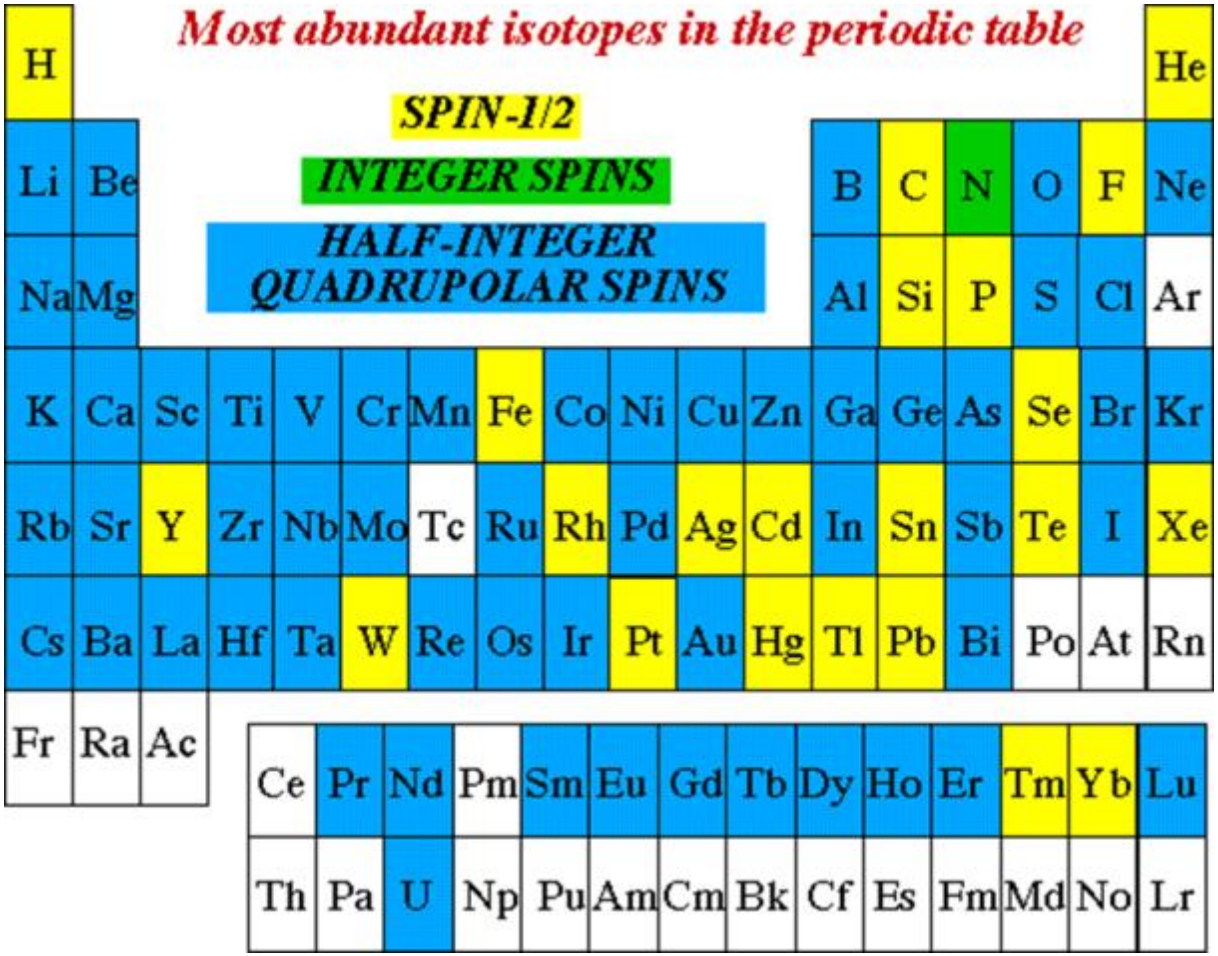

Outline

- Fundaments of NMR spectroscopy
  - Solid state NMR
- Aplication on heterogeneous catalysis: Zeolites**:**
  - **Structural characterization**
  - Chemical Physical properties
  - Reaction Mechanisms

Some usual elements in zeolites

Isótopo		Spin	Abund. Natural %	Sensibilidad		ν RMN al campo mag. (T)			
				Relativa	Absoluta	7.0463	9.3950	11.7440	14.0926
1	H	1/2	99.98	1.00	1.00	300	400	500	600
6	Li	1	7.42	8.50×10^{-3}	6.31×10^{-4}	44.146	58.862	73.578	88.292
7	Li	3/2	92.58	0.29	0.27	116.590	155.454	194.317	233.180
11	B	3/2	80.42	0.17	0.13	9.251	128.335	160.419	192.502
13	C	1/2	1.108	1.59×10^{-2}	1.76×10^{-4}	75.432	100.577	125.721	150.864
17	O	5/2	3.7×10^{-2}	2.91×10^{-2}	1.08×10^{-5}	40.670	54.227	67.784	81.340
19	F	1/2	100	0.83	0.83	282.231	376.308	470.385	564.462
23	Na	3/2	100	9.25×10^{-2}	9.25×10^{-2}	79.353	105.805	132.256	158.706
27	Al	5/2	100	0.21	0.21	18.172	104.229	130.287	156.344
29	Si	1/2	4.7	7.84×10^{-3}	3.69×10^{-4}	59.595	79.460	99.325	119.190
31	P	1/2	100	6.63×10^{-2}	6.63×10^{-2}	121.442	161.923	202.404	242.884
133	Cs	7/2	100	4.7×10^{-2}	4.7×10^{-2}	39.351	532.548	65.585	78.702

Structural characterization of zeolites:

- ^{29}Si NMR
- ^{27}Al NMR
- New zeolite structures

^{29}Si NMR of zeolites

- Chemical composition of the local environement

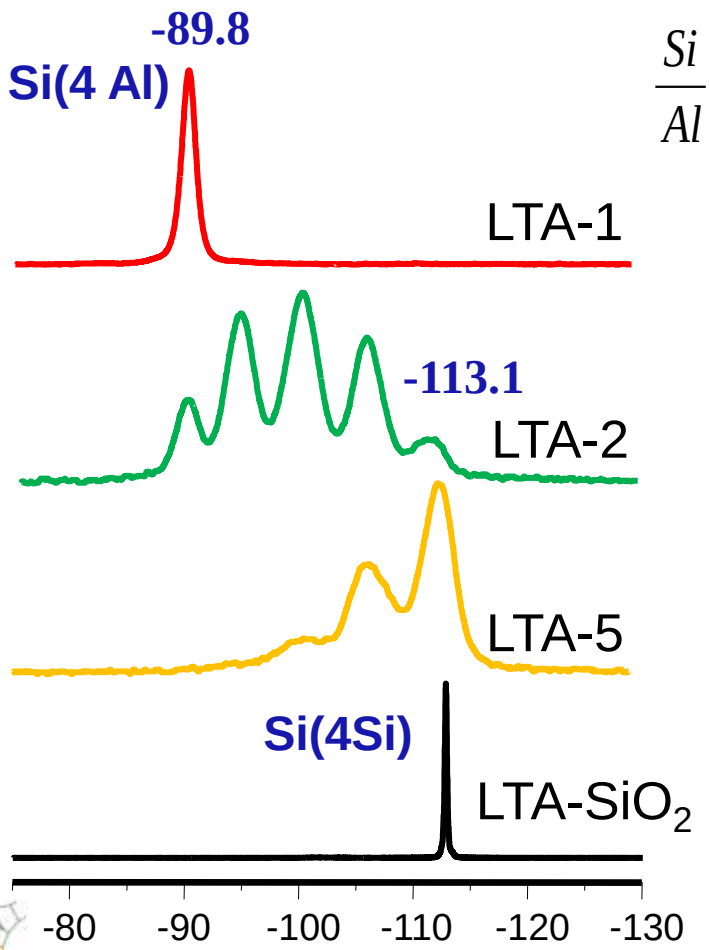

$$\frac{Si}{Al} = \frac{\sum_{n=0}^{n=4} I_{Si(nAl)}}{\sum_{n=0}^{n=4} \frac{n}{4} I_{Si(nAl)}}$$

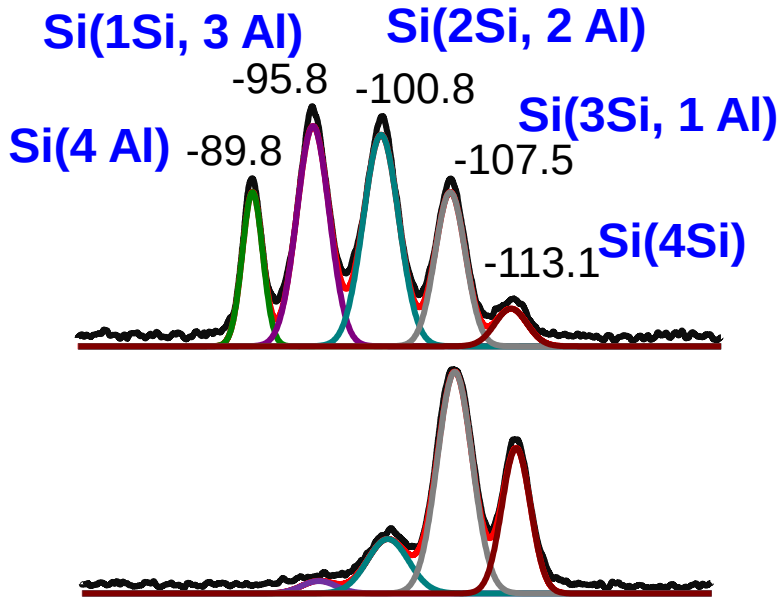

RMN de ^{29}Si en zeolitas

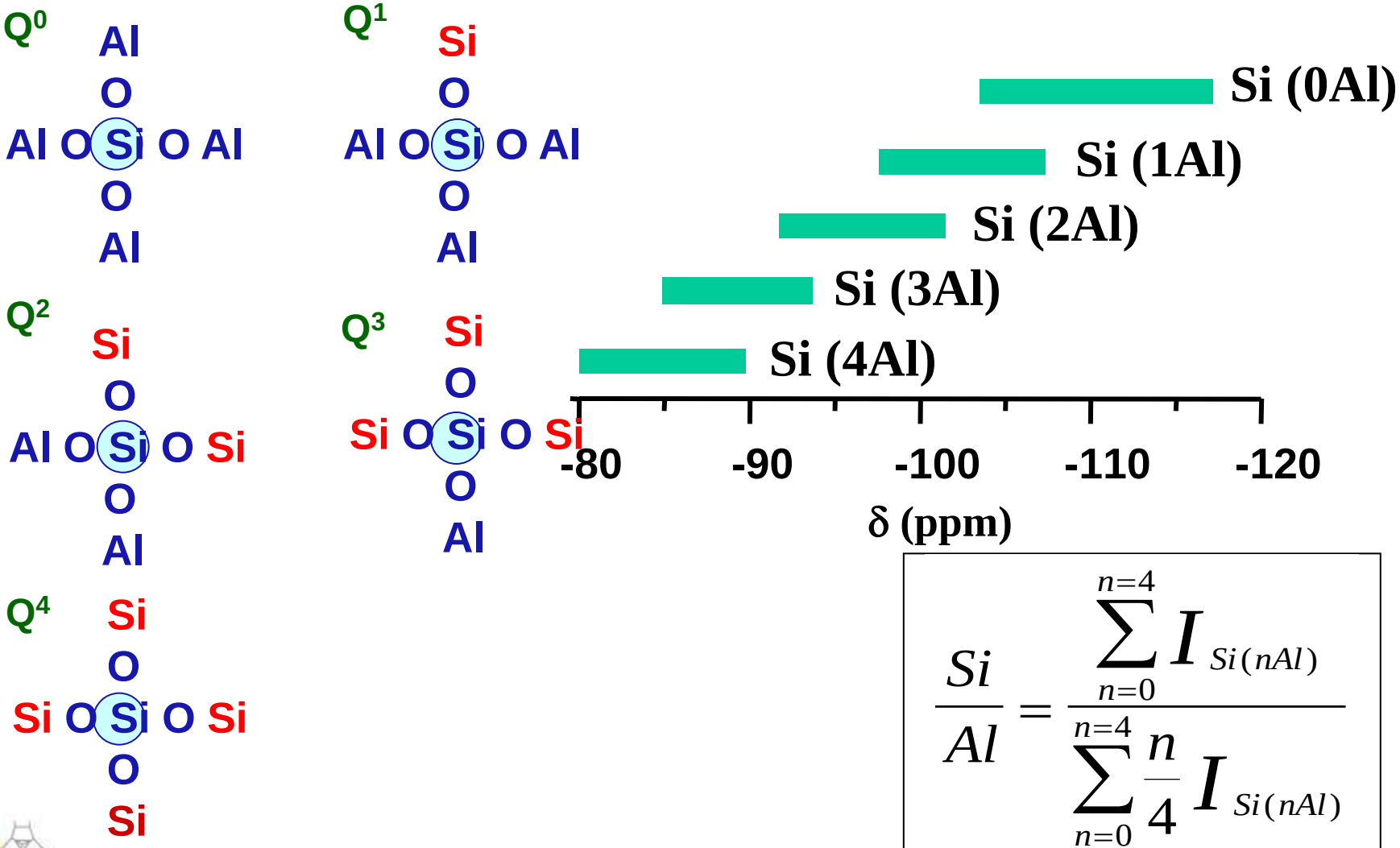

$$\frac{Si}{Al} = \frac{\sum_{n=0}^{n=4} I_{Si(nAl)}}{\sum_{n=0}^{n=4} \frac{n}{4} I_{Si(nAl)}}$$

ITQ Valencia

^{29}Si NMR of zeolites

- Non-equivalent crystallographic sites, connectivities and proximity of other atoms.

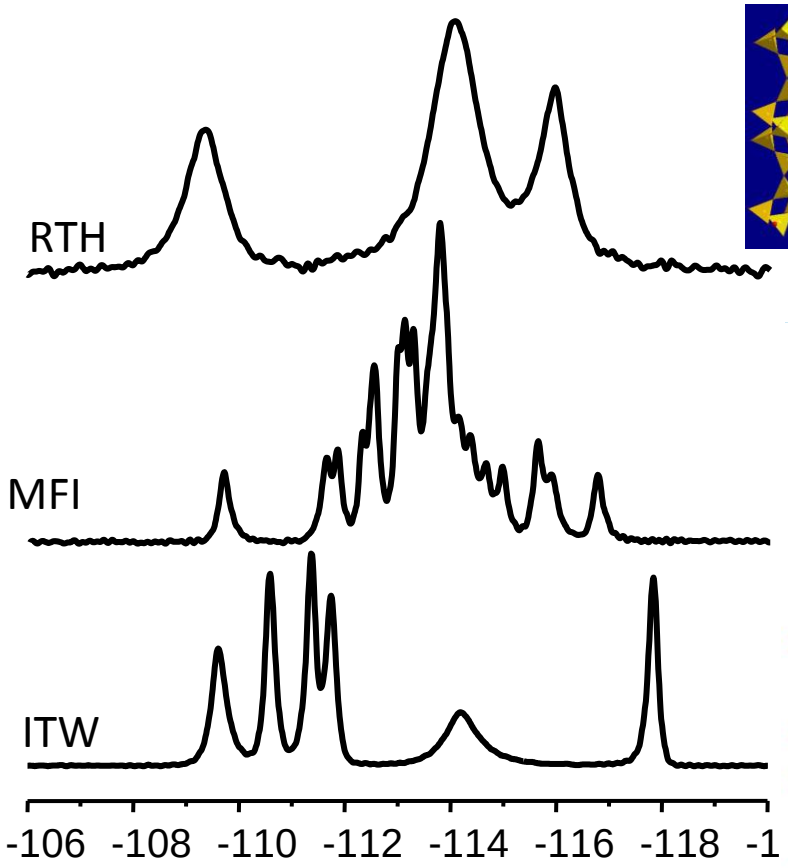

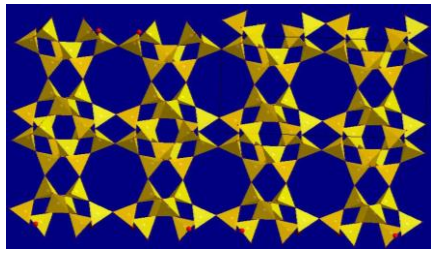

4 T
8 MR = 4.1 x 3.8 A
5.6 x 2.5.

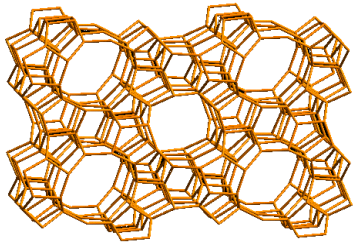

24 T
10 MR
5,5 A.

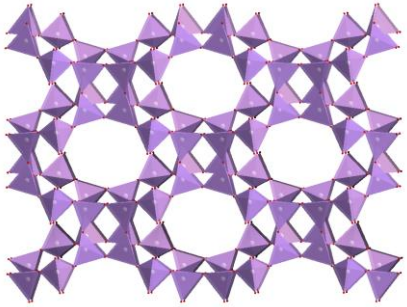

6 T
8 MR

^{29}Si NMR of zeolites

- Non-equivalent crystallographic sites, connectivities and proximity of other atoms.

Zeolita Sigma-2 **$SR26_4$ (Dipolares)** **INADEQUATE (J^2 ^{29}Si-^{29}Si)**

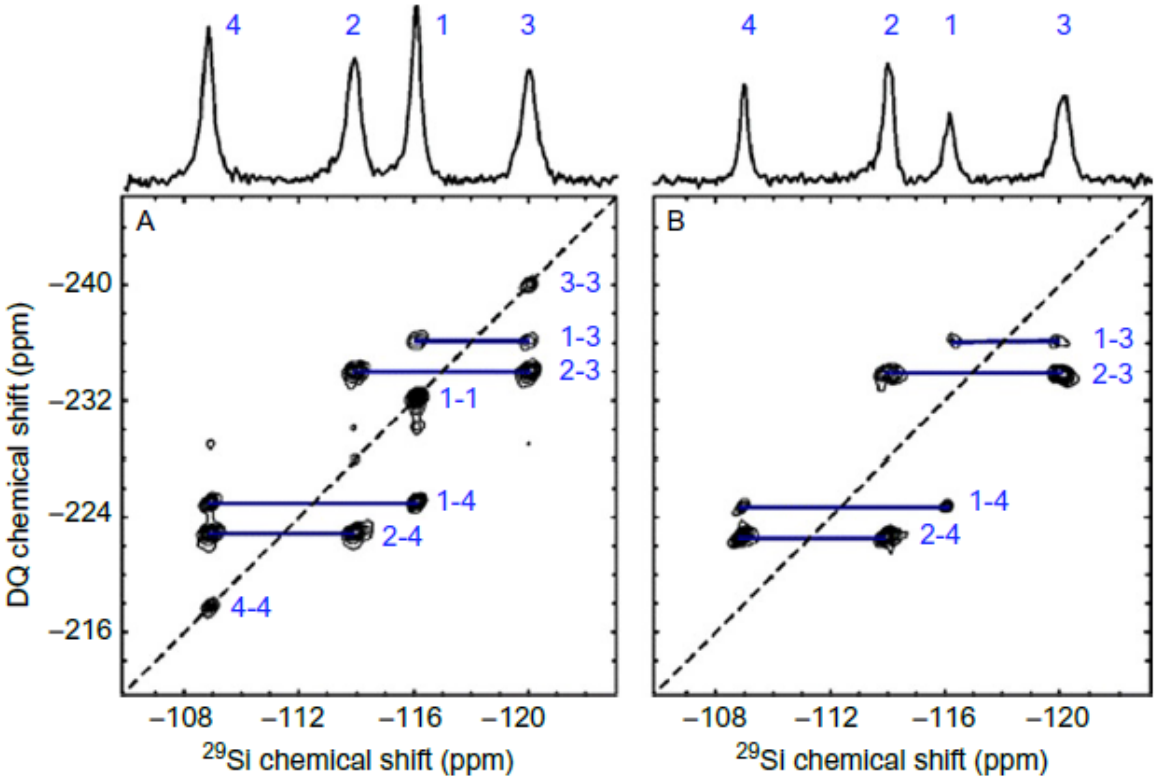

Figure 4.4 ^{29}Si QD correlation spectra of zeolite Sigma-2 obtained by using (A) the $SR26_4$[11] dipolar recoupling sequence and (B) the J-coupling based INADEQUATE. *Reprinted with permission from Ref. 47. Copyright (2005) American Chemical Society.*

Structural characterization of zeolites:

- ^{29}Si NMR
- ^{27}Al NMR
- New zeolite structures

^{22}Al NMR of zeolites

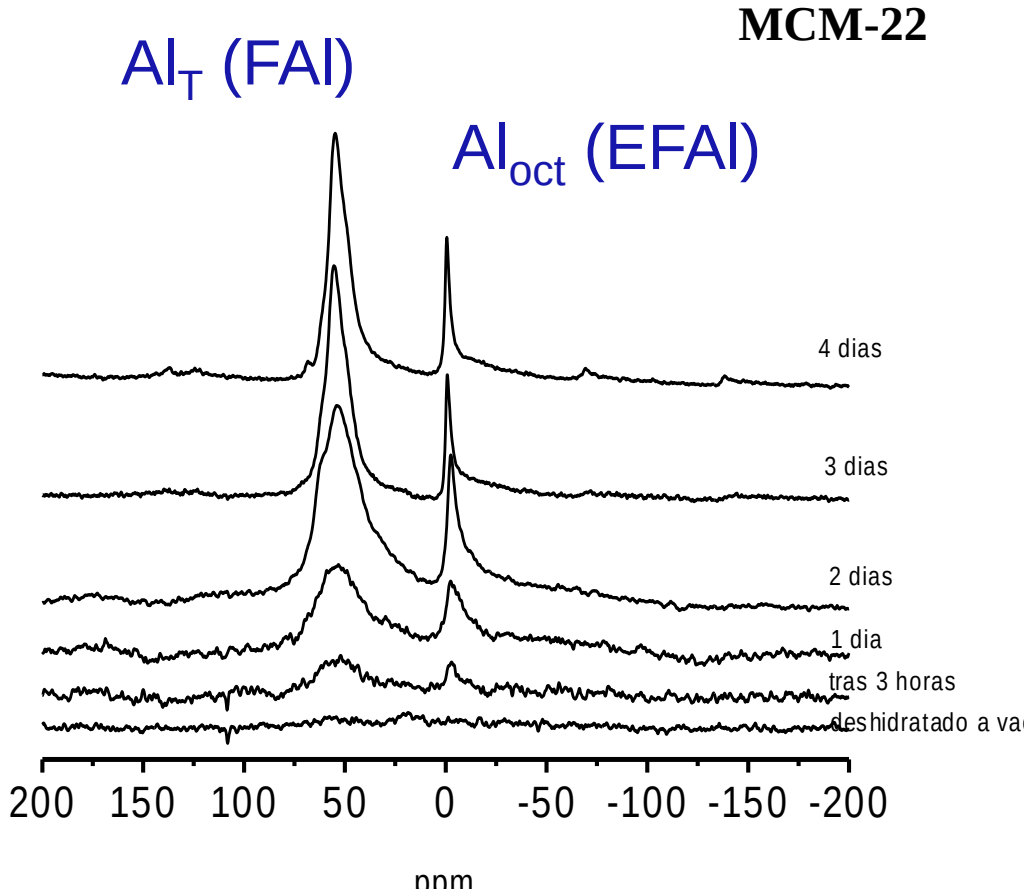

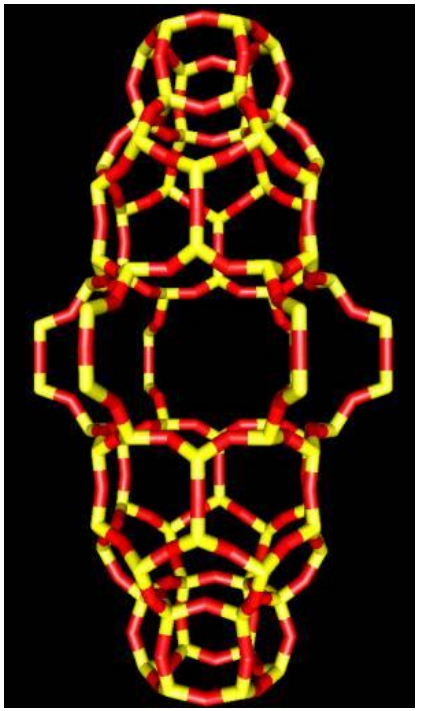

^{22}Al NMR of zeolites

Zeolita USY

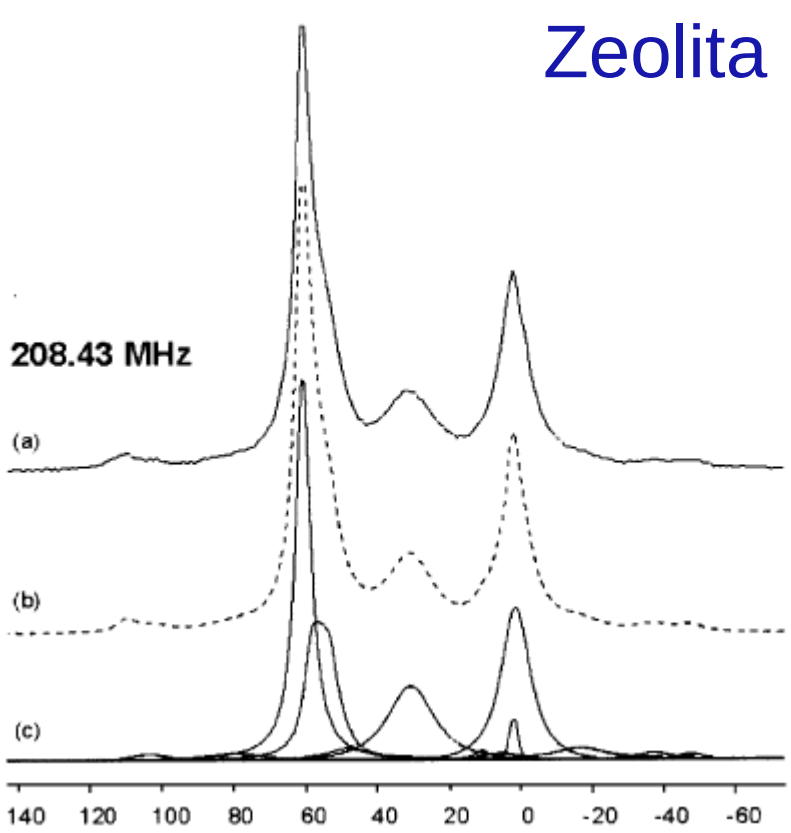

18.8 T

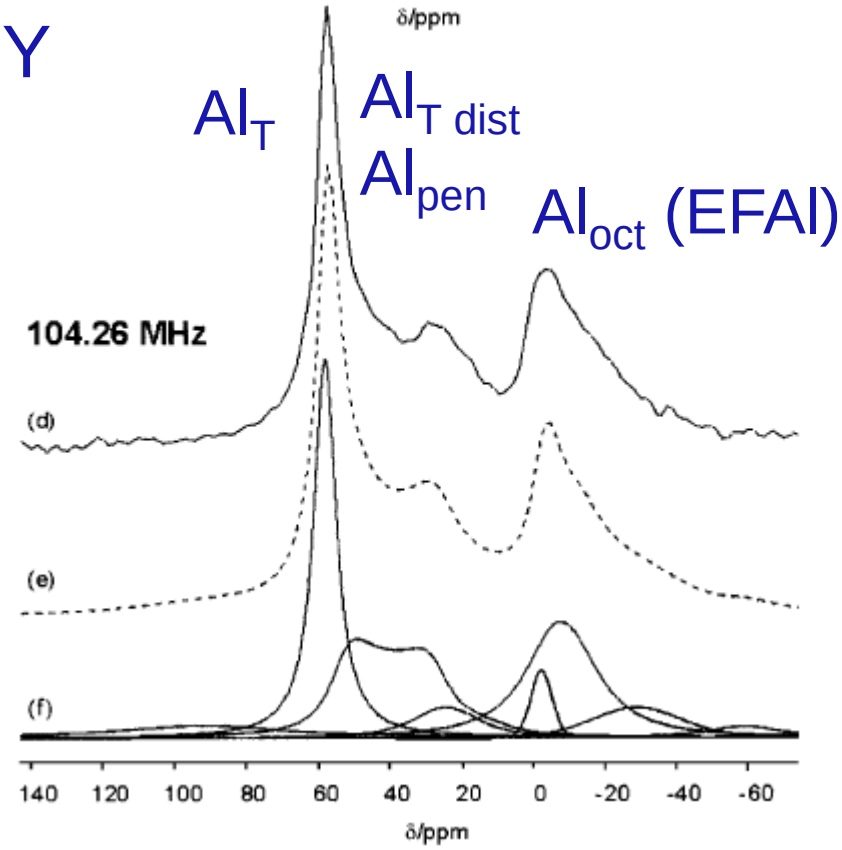

9.4 T

C, Fyfe et al. Chem. Commun. 2000, 1575

Structural characterization of zeolites:

- ^{29}Si NMR
- ^{27}Al NMR
- New zeolite structures

SYNTHESIS OF ZEOLITES

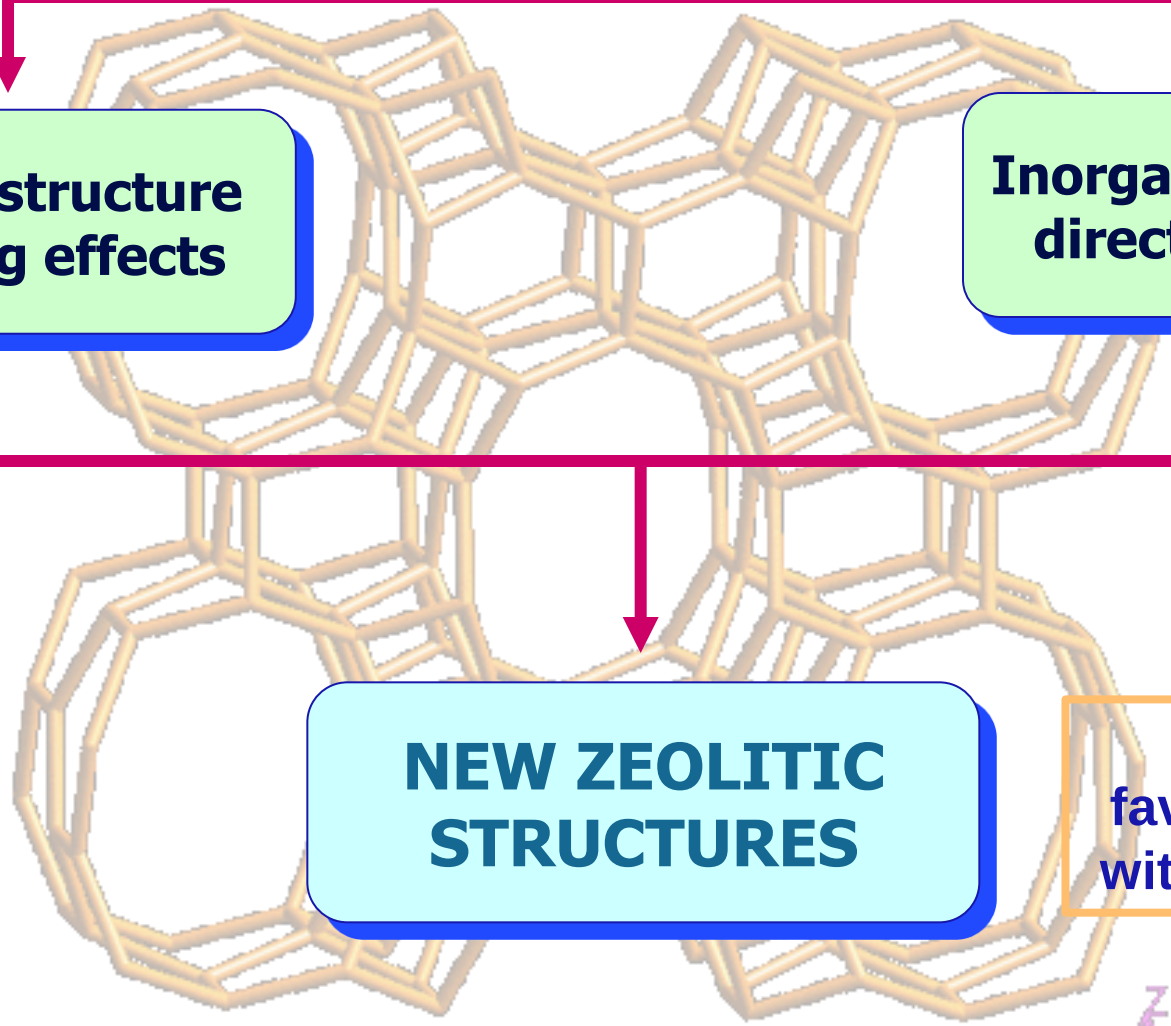

Organic structure directing effects

Inorganic structure directing effects

NEW ZEOLITIC STRUCTURES

F- and Ge favours zeolites with small cages

Si-Ge Zeolites: Structure directing effect o Ge

Mean T-O-T angle

Si-O-Si ≈135º

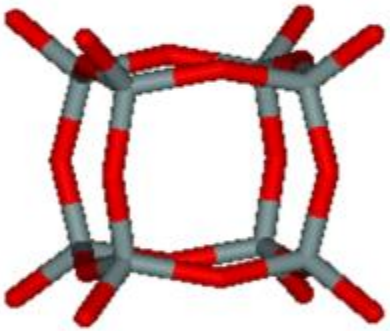

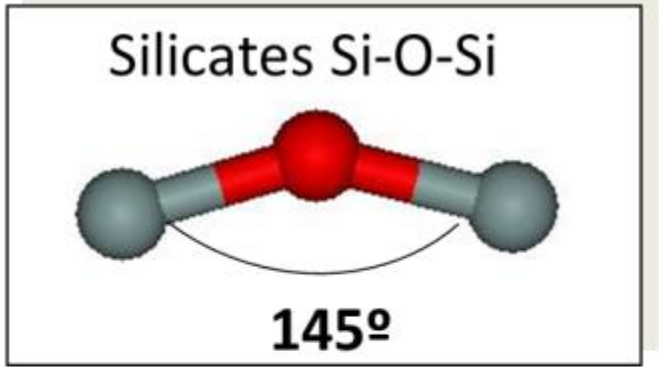

Theoretical calculations

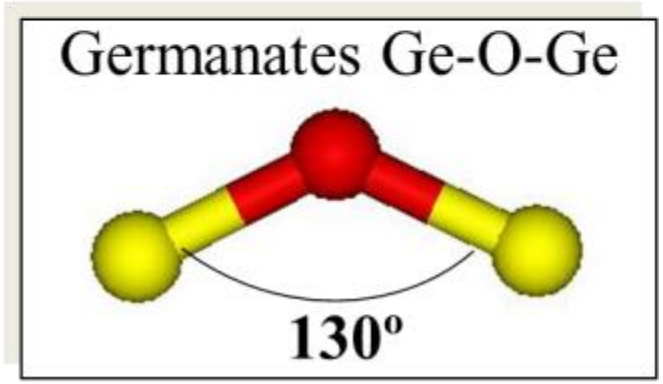

^{19}F NMR of silicate zeolites

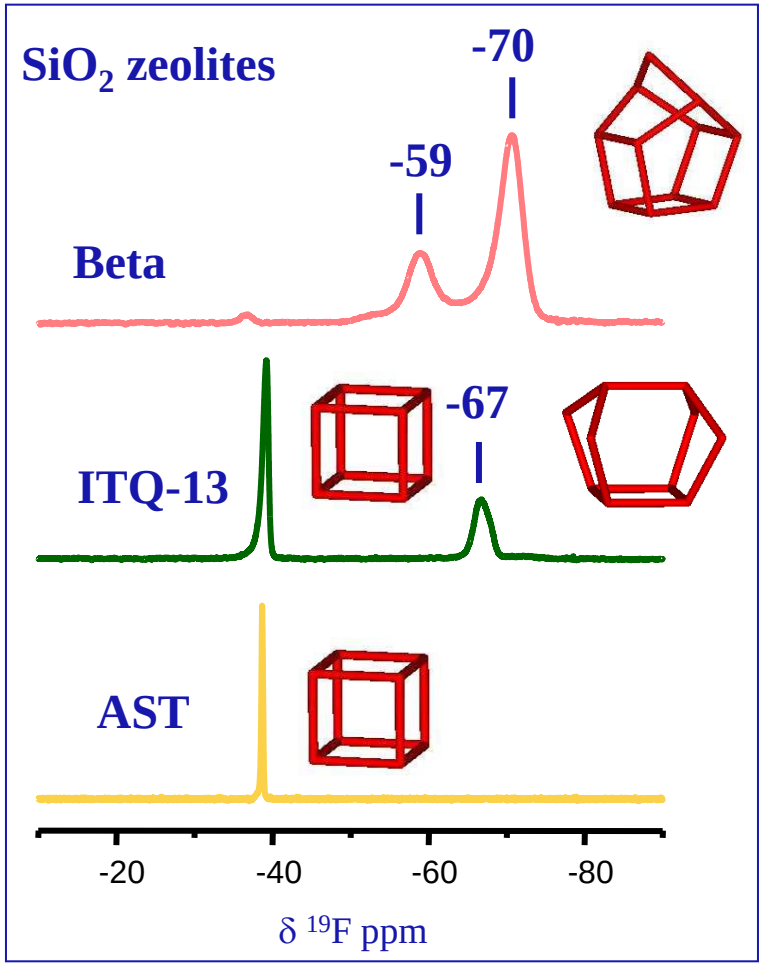

F^- is placed within the small zeolite cages

^{19}F MAS NMR: $\delta^{19}F$ depends on its location

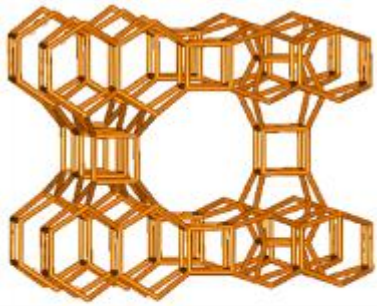

ITQ-7

Si, Ge Zeolites containing D4R synthesized with F^-

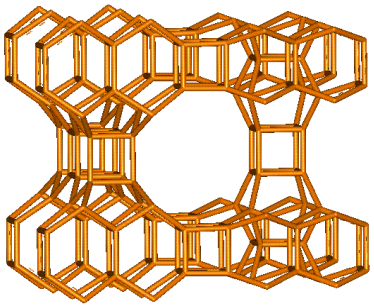

ITQ-7

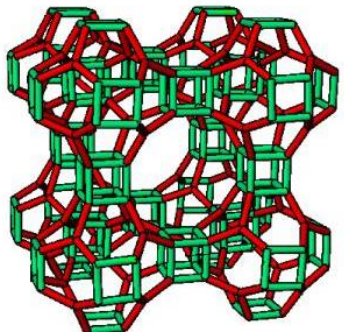

ITQ-21

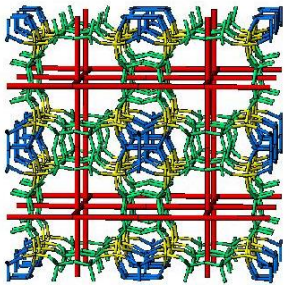

ITQ-17

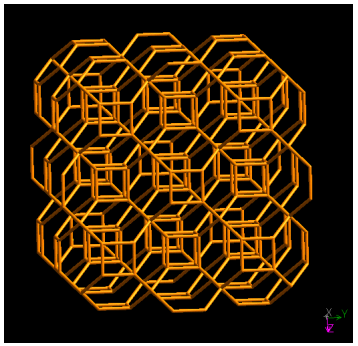

Octadecasil

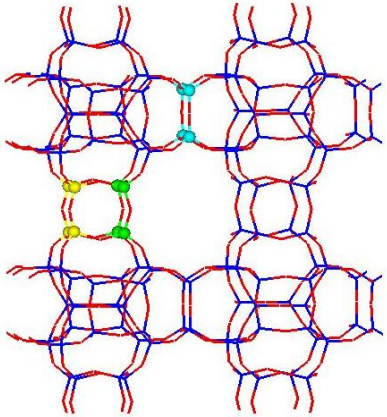

ITQ-13

^{29}Si of NMR pure silica zeolite ITQ-7

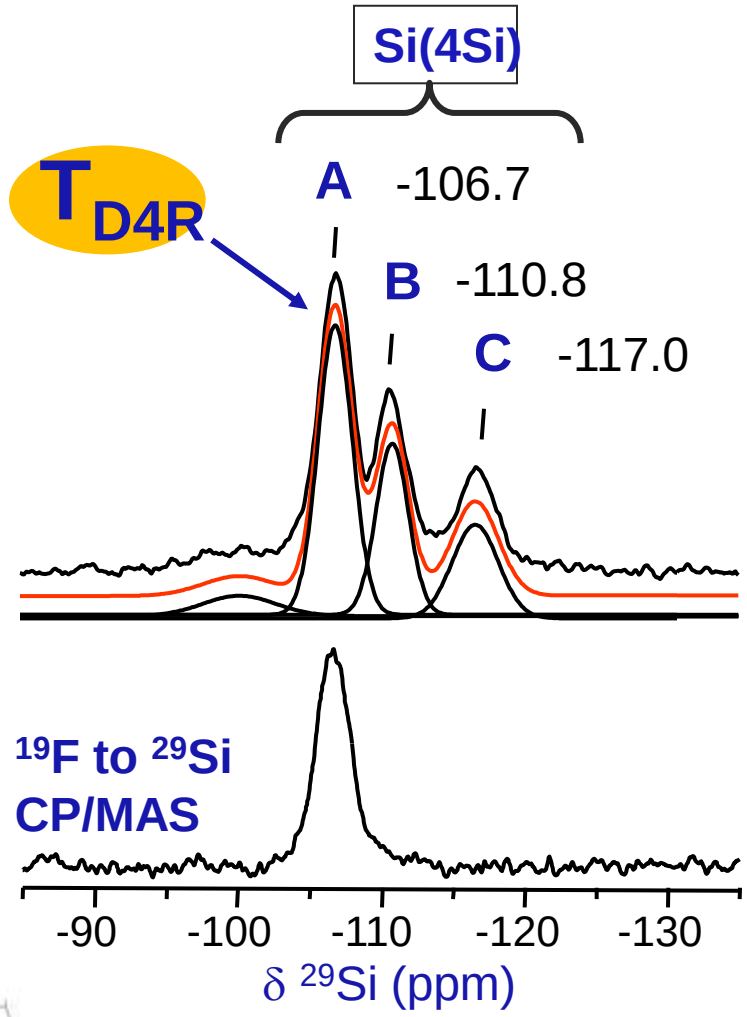

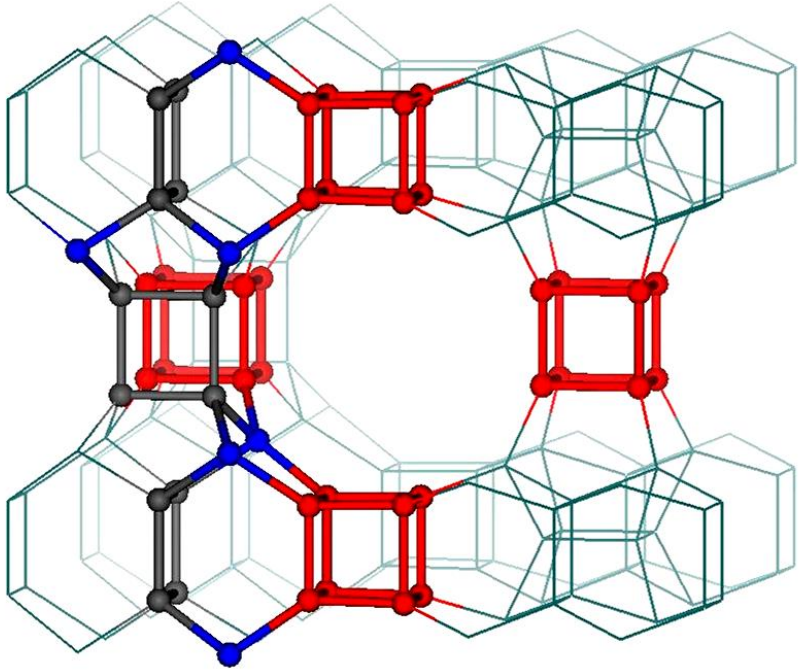

- T_{D4R} 50%
- T_n 25%
- T_{4R} 25%

J. Phys. Chem. B (2002), 106(10), 2634-2642.

^{29}Si NMR of Si,Ge-ITQ-7 zeolites

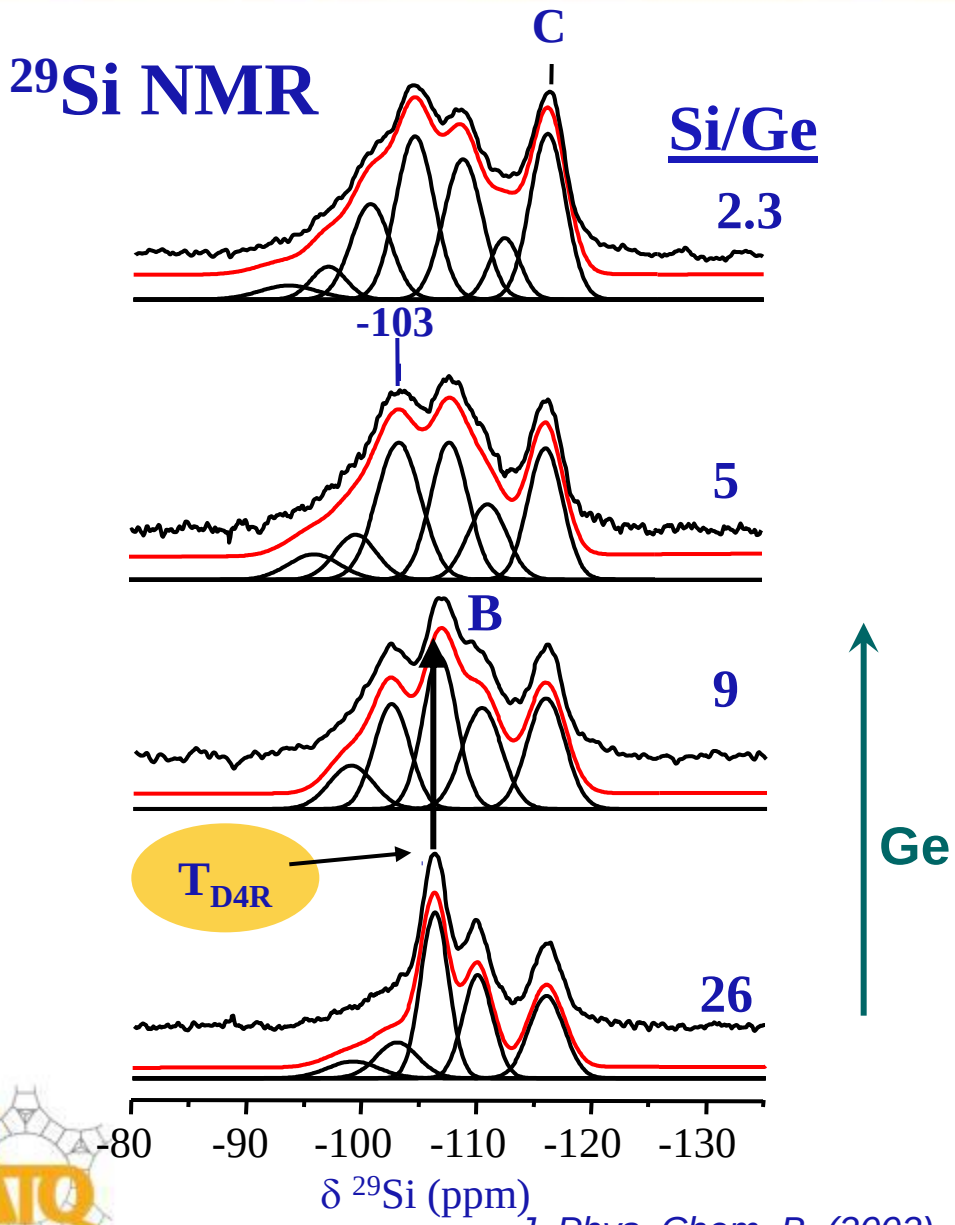

Si, Ge-Zeolites

The intensity of peak C changes only slightly with the incorporation of Ge

Selective incorporation of Ge to certain crystallographic sites

J. Phys. Chem. B (2002), 106(10), 2634-2642.

^{19}F NMR of Si,Ge-ITQ-7 zeolites

Assingment of the ^{19}F NMR signals from the analysis of the ^{29}Si and ^{19}F MAS NMR spectra

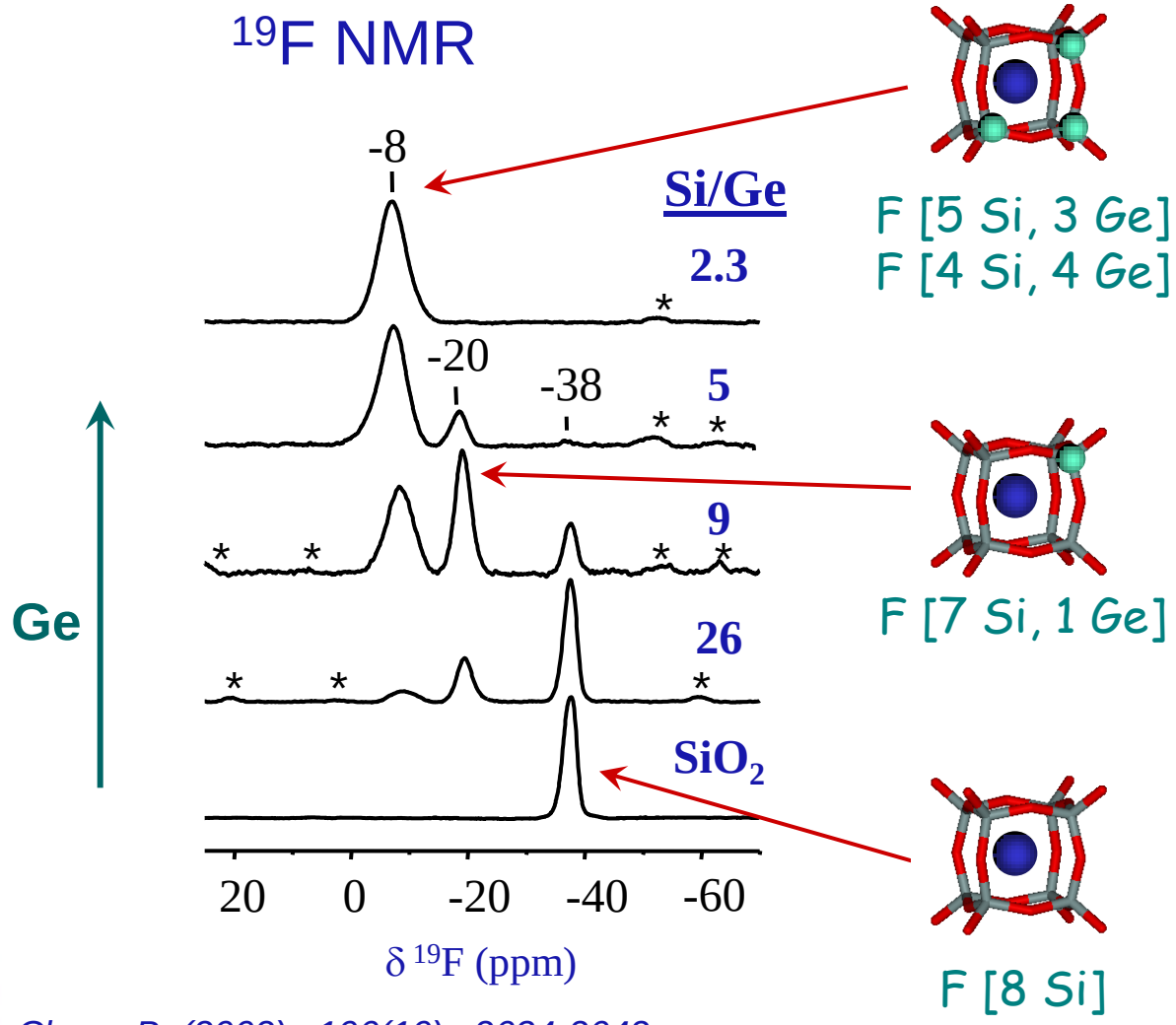

J. Phys. Chem. B (2002), 106(10), 2634-2642.

Si,Ge-ITQ-17

Good agreement in the mean site occupancy from XRD and ^{19}F NMR.

- T1 (D4R)
- T2
- T3 (4R)

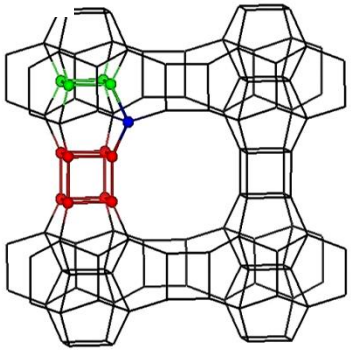

ITQ-17

% Ge atoms in D4R

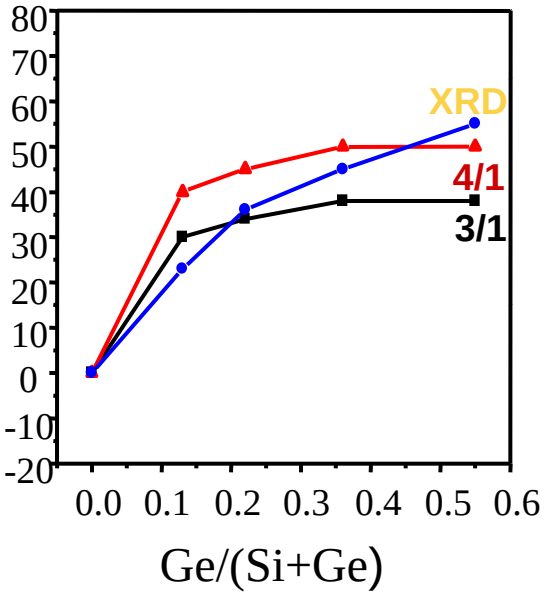

% Ge atoms in other T sites

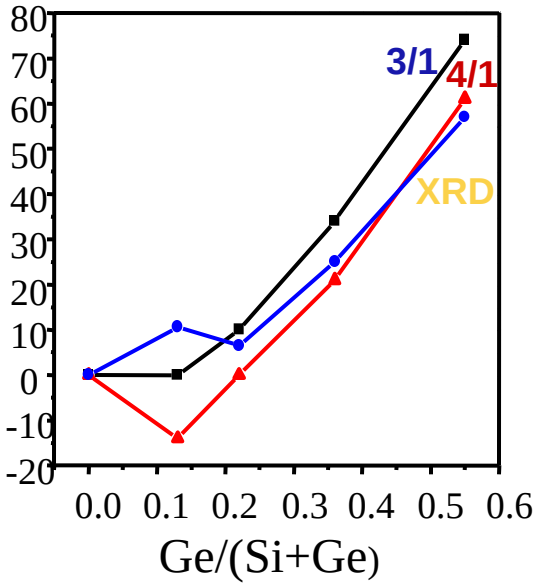

Angew. Chem., Int. Ed. (2002), 41(24), 4722-4726.

Synthesis of Zeolites

Structure directing effect of Germanium

Synthesis in Fluoride medium

ITQ-17 (BEC), ITQ-24 (IWR), ITQ-29 (LTA), AST, ITQ-12 (ITW), ITQ-13 (ITH), ITQ-7 (ISV), IM-10 (UOZ), ITQ-21, ITQ-26 (IWS), ITQ-27 (IWV), ITQ-40 (IRY), ITQ-44 (IRR), ITQ-37 (ITV), ITQ-38 (ITG)

Synthesis in basic (OH) medium

ITQ-22 (IWW), ITQ-17 (BEC) ITQ-24 (IWR), ITQ-21, ITQ-15 (UTL), ITQ-33, ITQ-13 (ITH)

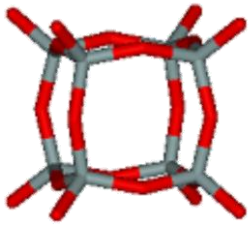

14 Novel Zeolite Structures

SYNTHESIS OF ZEOLITES

Organic Structure directing agents

Inorganic structure directing effects

NEW ZEOLITIC STRUCTURES

F- and Ge favours zeolites with small cages

P-CONTAINING STRUCTURE DIRECTING AGENTS

P-containing SDAs: Phosphonium phosphenes

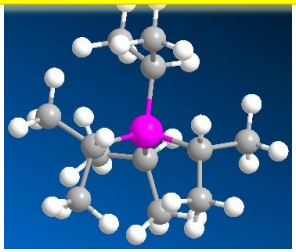

OSDA

- **Crystallization of novel zeolite structure types: ITQ-27, ITQ-26, ITQ-34, Boggsite**
- **Expand the chemical composition of known zeolites**

Calcination

P_2O_5

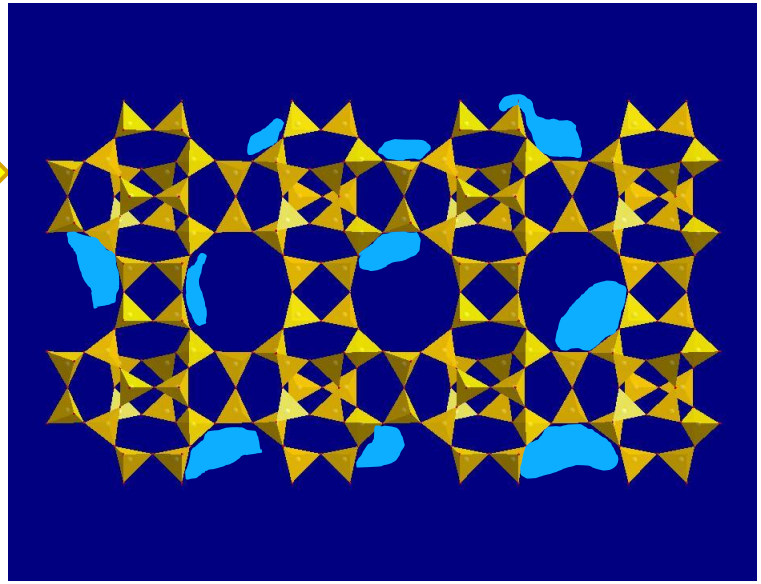

Estabilization of framework aluminium and then zeolite acidity

Synthesis of zeolite RUB 13

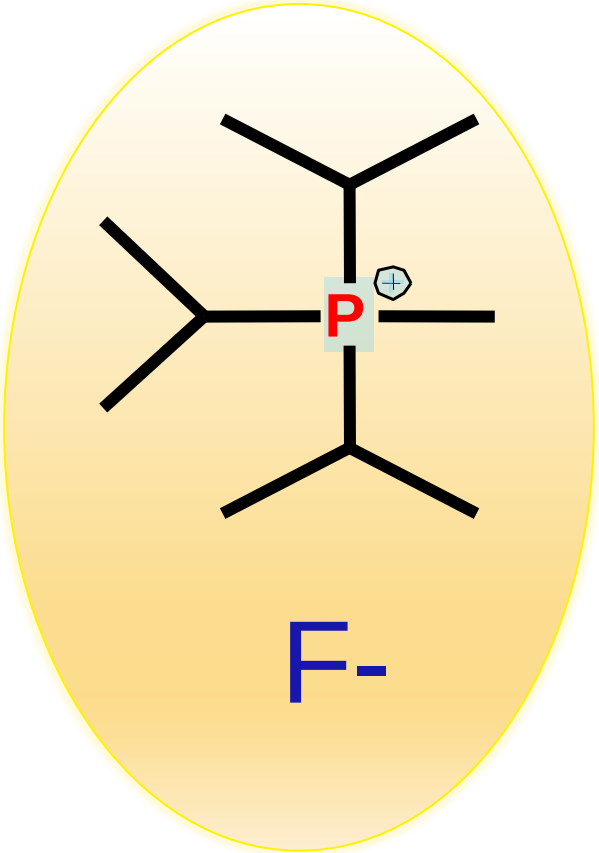

Zeolite RUB 13

As prepared

Si/Al=13

Calcined

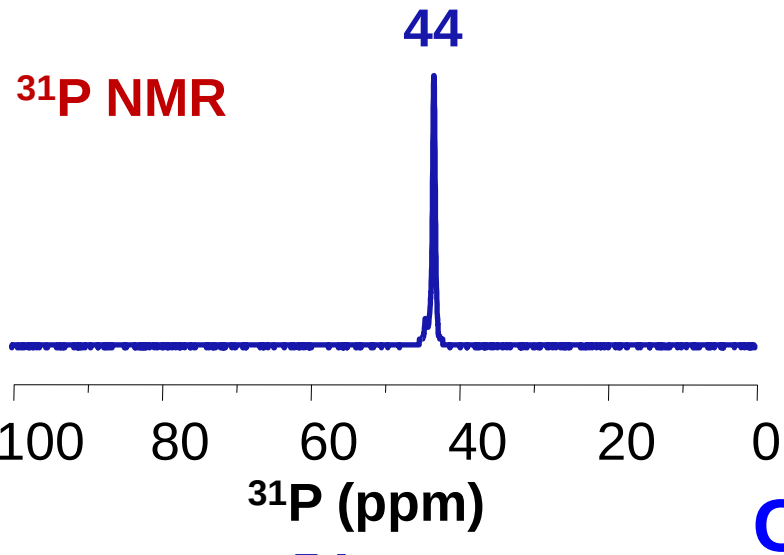

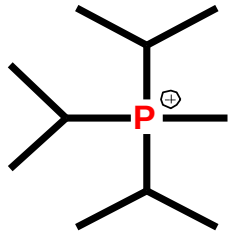

F-

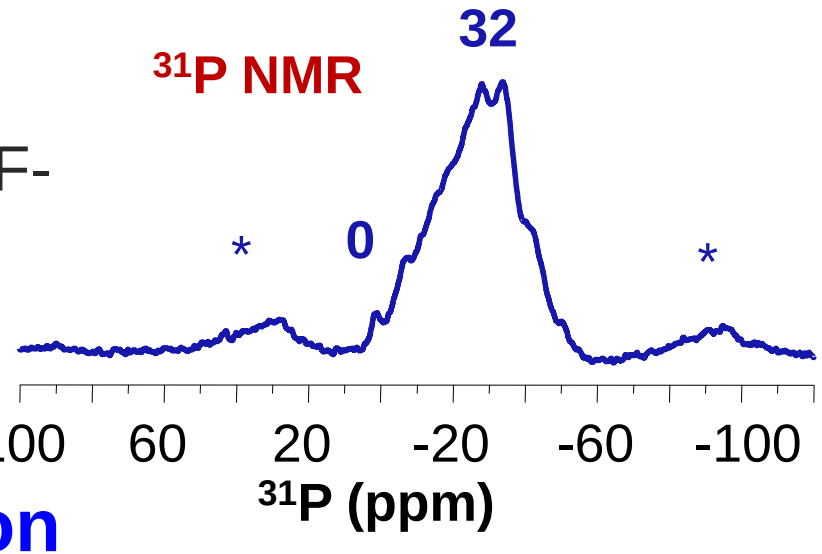

Calcination

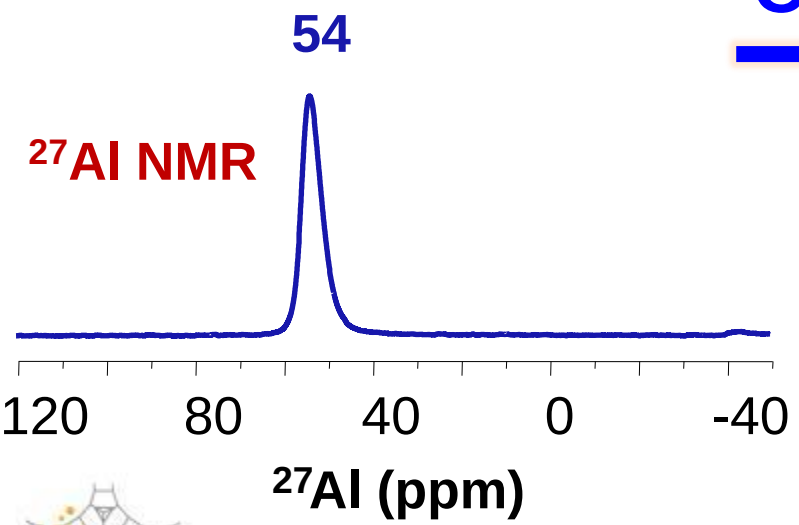

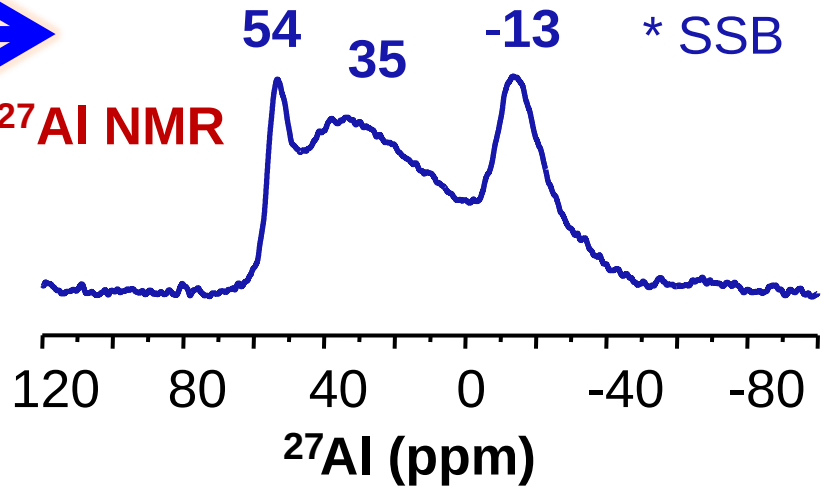

^{27}Al 3QMAS NMR of Zeolite RUB 13

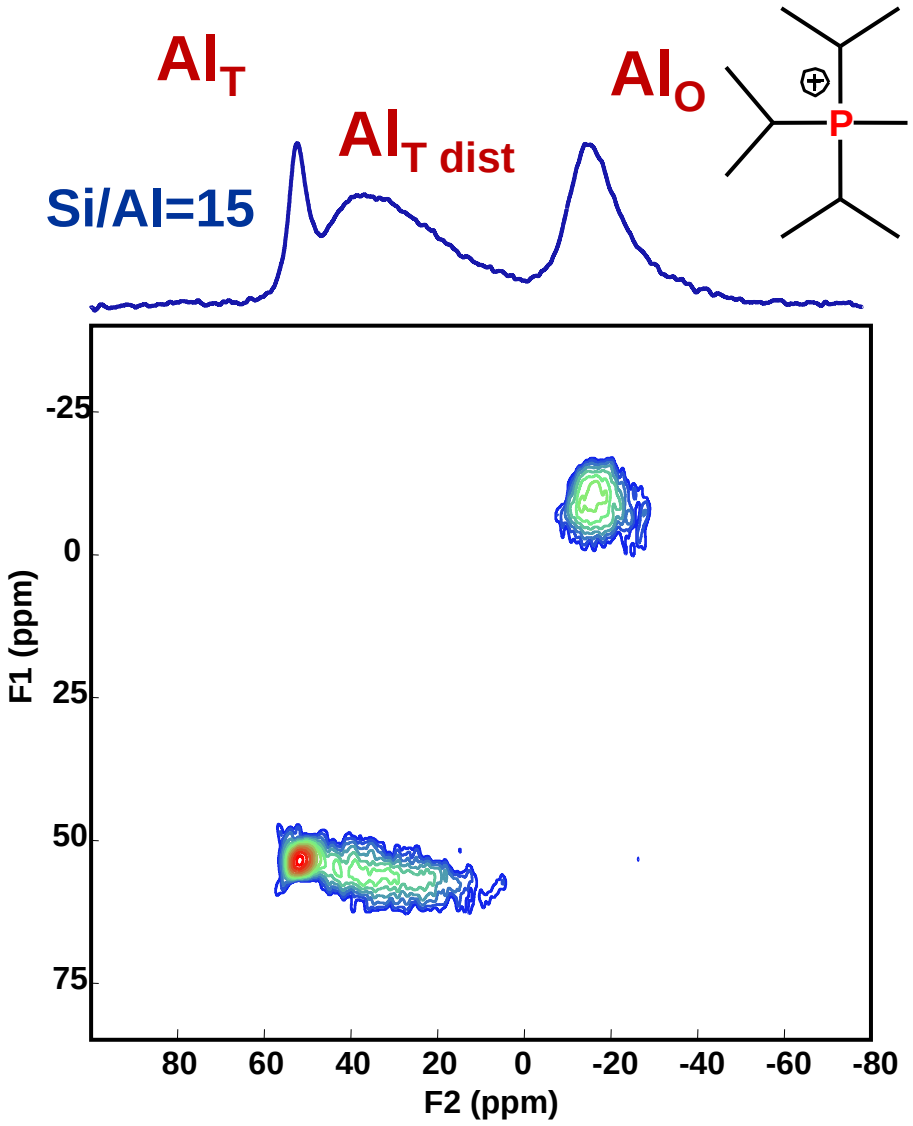

^{29}Si MAS NMR spectra of SiO_2-RUB-13

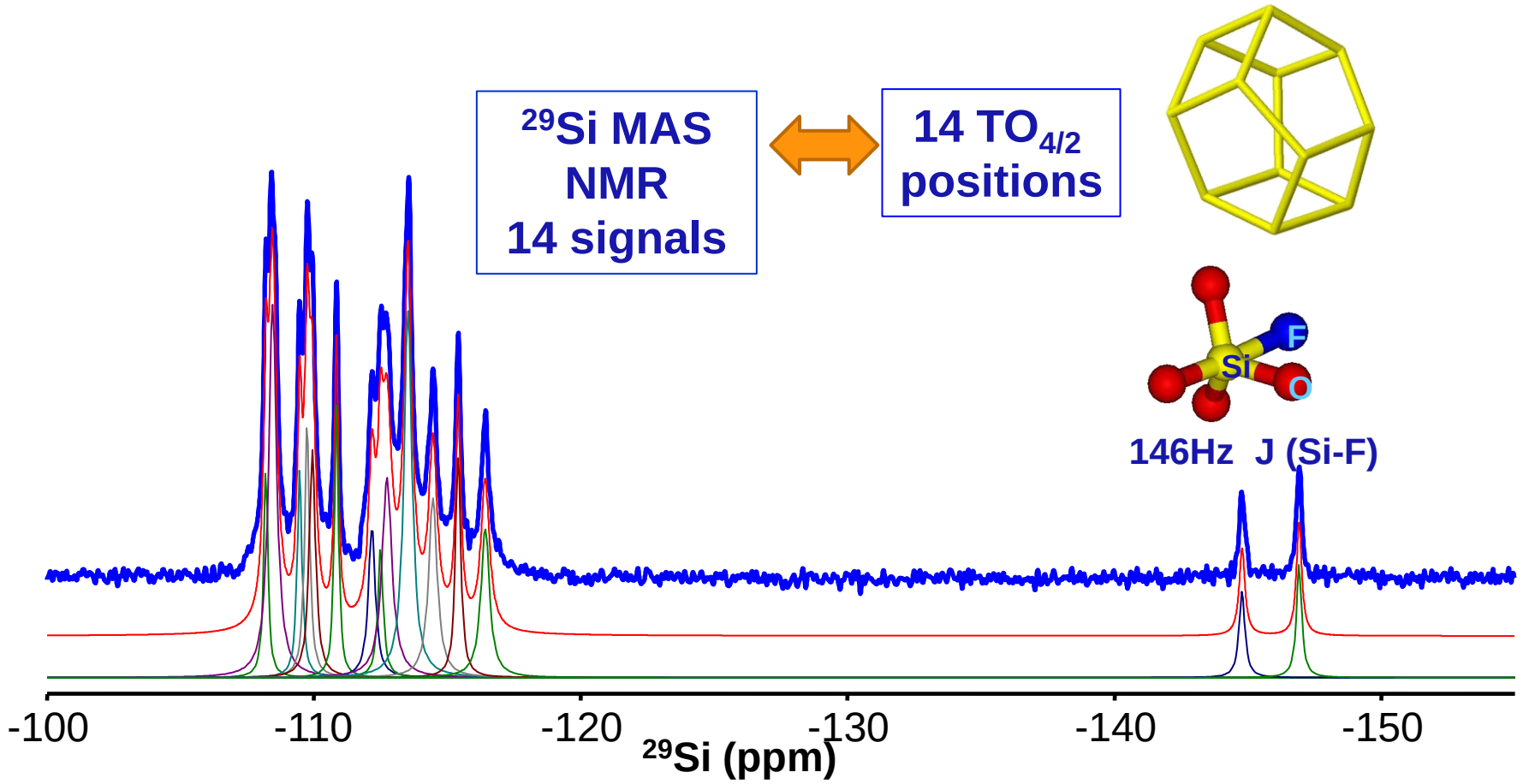

Outline

- Fundaments of NMR spectroscopy
  - Solid state NMR
- Aplication on heterogeneous catalysis: Zeolites**:**
  - Structural characterization
  - **Chemical Physical properties**
  - Reaction Mechanisms

Physical Chemical characterization

- Interaction between the framework and the molecules filling the zeolite pores.
- The use of probe molecules to study the zeolite properties.
- Mobility of atoms and molecules.
- …

Outline

- Fundaments of NMR spectroscopy
  - Solid state NMR
- Aplication on heterogeneous catalysis: Zeolites**:**
  - Structural characterization
  - Chemical Physical properties
  - **Reaction Mechanisms**

Heterogeneous catalysis

- Elucidation of reaction mechanisms can contribute to the development of improved catalyst

- In situ NMR spectroscopy is suitable to probe the structures of organic adsorbates (^{13}C), active and framework sites, cations. It usually requires the use of labelled (^{13}C, ^{15}N) compounds

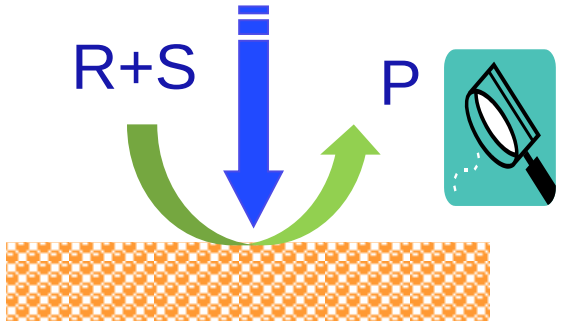

In situ NMR spectroscopy

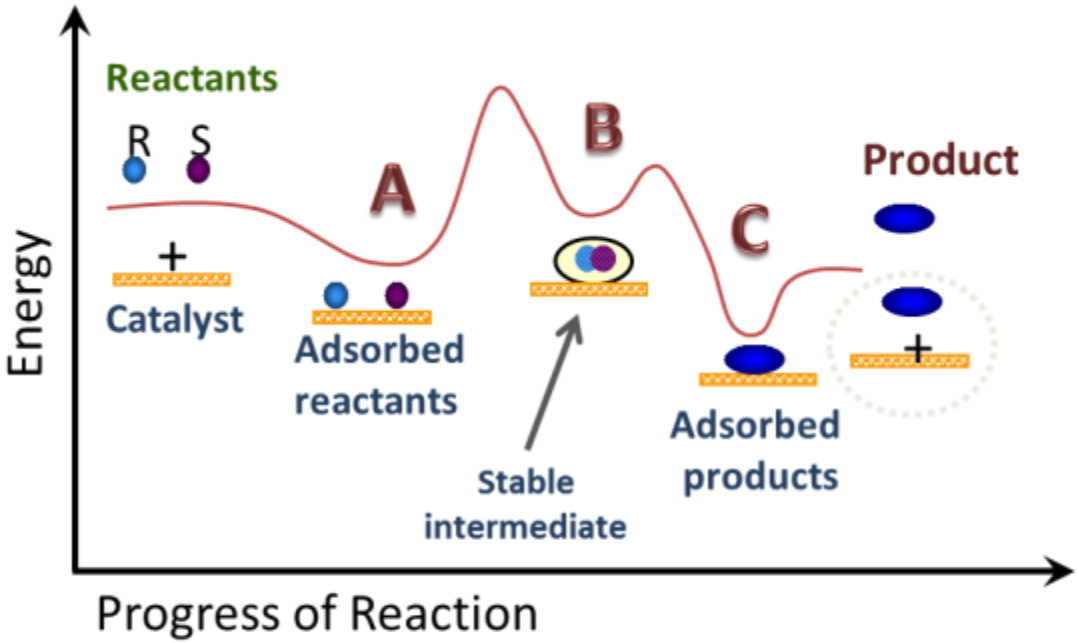

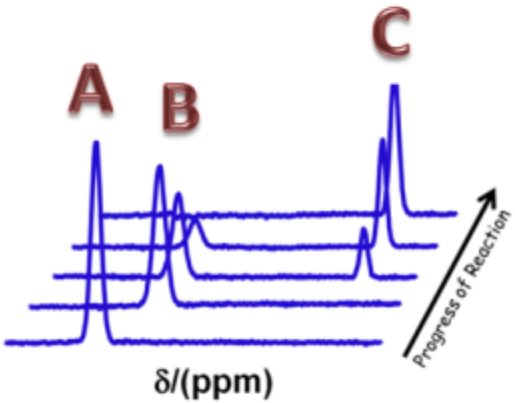

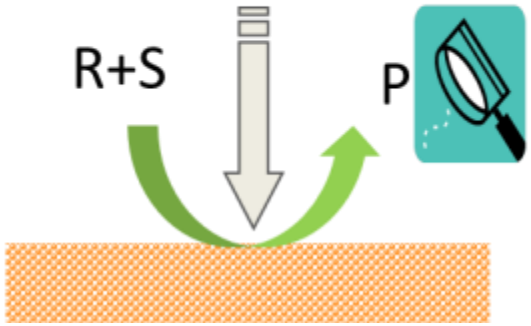

T. Blasco, Chem. Soc. Rev., 39 (2010) 4685
I. I. Ivanova, Y. G. Kolyagin, Chem. Soc. Rev., 39 (2010) 5018

Batch reaction: NMR Glass Inserts

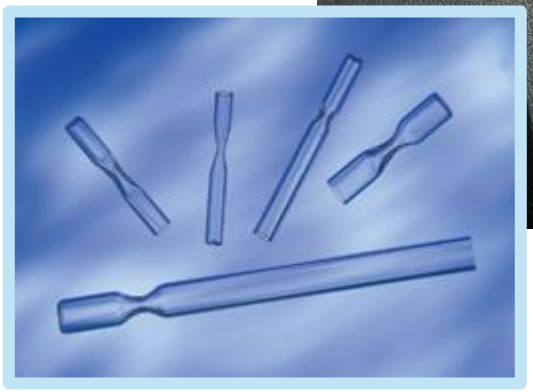

T. A. Carpenter, J. Klinowski, D. T. B. Tennakoon, C. J. Smith, D. C. Edward, J. Magn. Reson. 68 (1986) 561

First publication of in situ NMR: M. W. Anderson, J. Klinowsi, Nature 1989, 339, 200

Reaction Mechanisms

- **Beckmann rearrangement reaction**

- Depletion of NOx emissions

The Beckmann rearrangement (BR)of cyclohexanone oxime

ε-Caprolactam

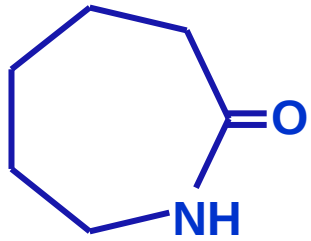

Nylon-6

World production:3.8 million tons per year

H. Ichihashi et al. Cata. Surv. Asia 7 (2003) 261; Y. Izumi et al. Bull. Chem. Soc. Jpn. 80 (2007) 1280

The Beckmann rearrangement
*BR of cyclohexanone oxime

Cyclohexanone Oxime

ε-Caprolactam

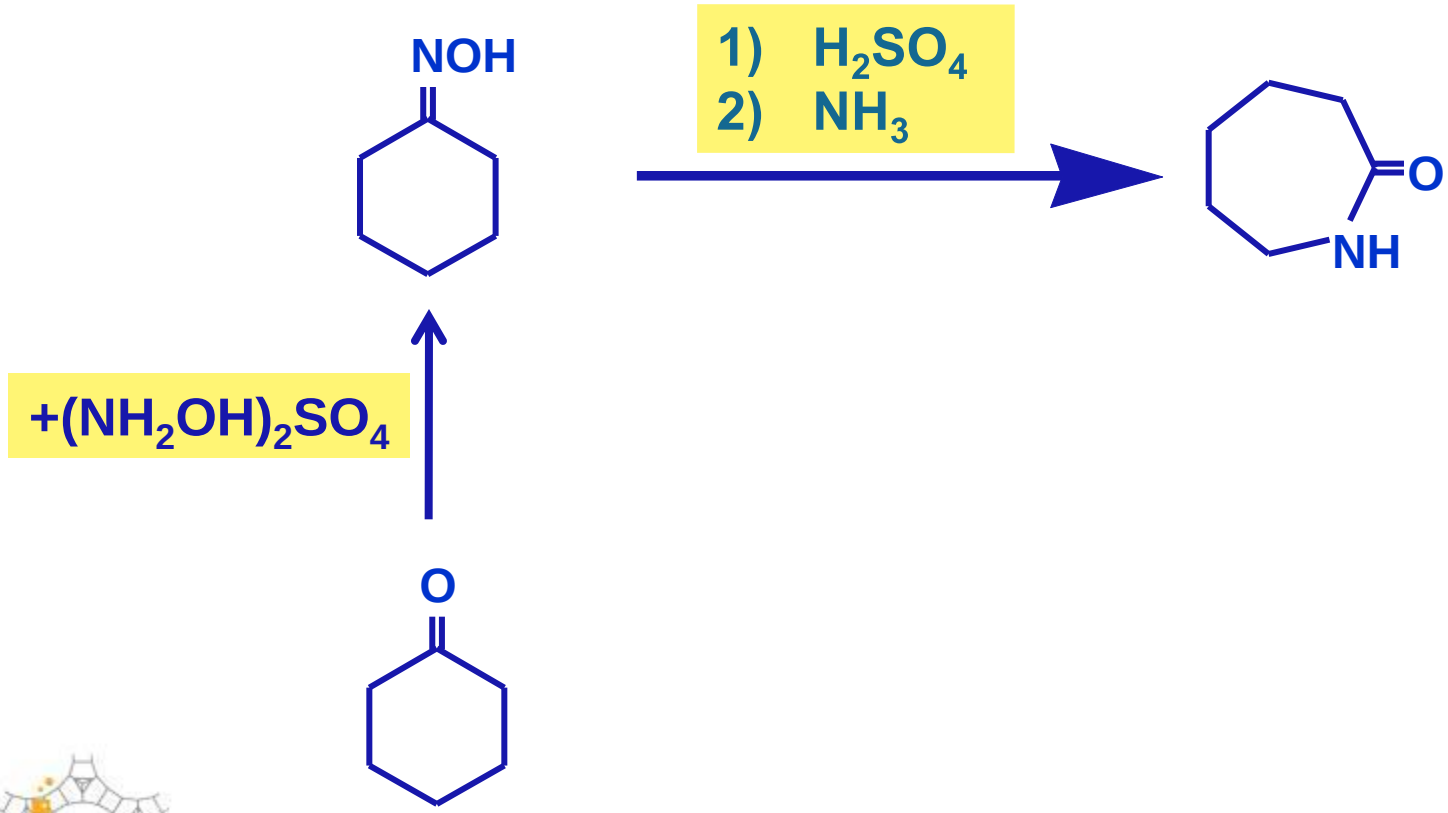

H. Ichihashi et al. Cata. Surv. Asia 7 (2003) 261; Y. Izumi et al. Bull. Chem. Soc. Jpn. 80 (2007) 1280

The Beckmann rearrangement *BR of cyclohexanone oxime

Cyclohexanone Oxime ε-Caprolactam

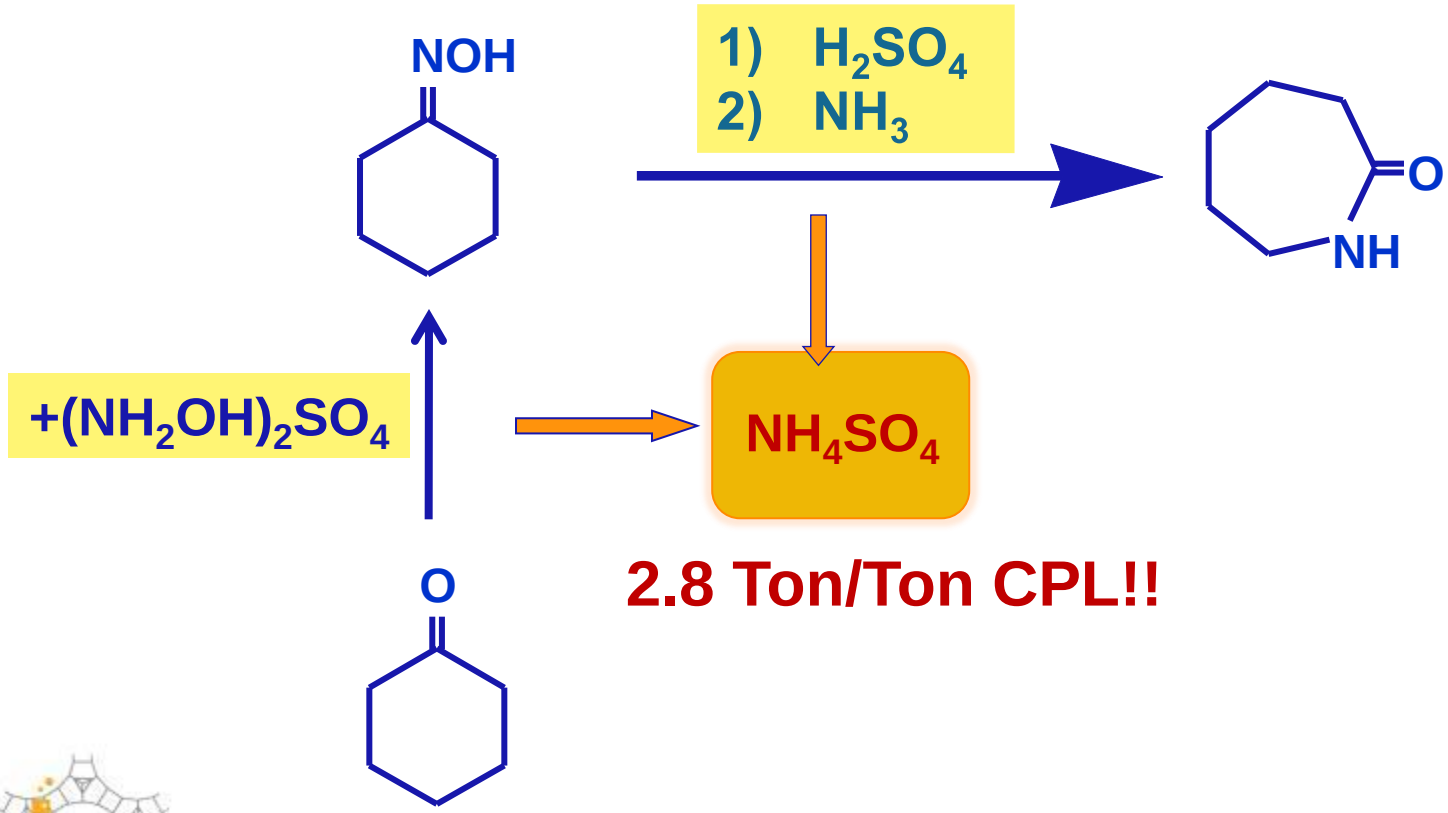

2.8 Ton/Ton CPL!!

H. Ichihashi et al. Cata. Surv. Asia 7 (2003) 261; Y. Izumi et al. Bull. Chem. Soc. Jpn. 80 (2007) 1280

The Beckmann rearrangement *BR of cyclohexanone oxime

Cyclohexanone Oxime

ε-Caprolactam

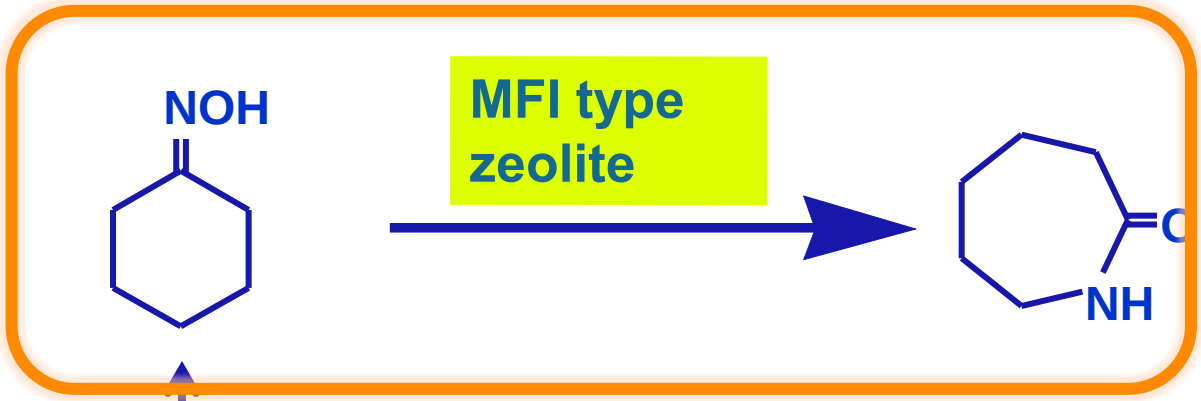

H_2O_2, NH_3, TS-1

Developped by Eni Chem

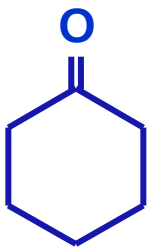

Fundamental catalyst was discovered by 1986 by Sumitomo Chemical Co.

H. Ichihashi et al. Cata. Surv. Asia 7 (2003) 261; Y. Izumi et al. Bull. Chem. Soc. Jpn. 80 (2007) 1280

The Beckmann rearrangement *BR of cyclohexanone oxime

Cyclohexanone Oxime

ε-Caprolactam

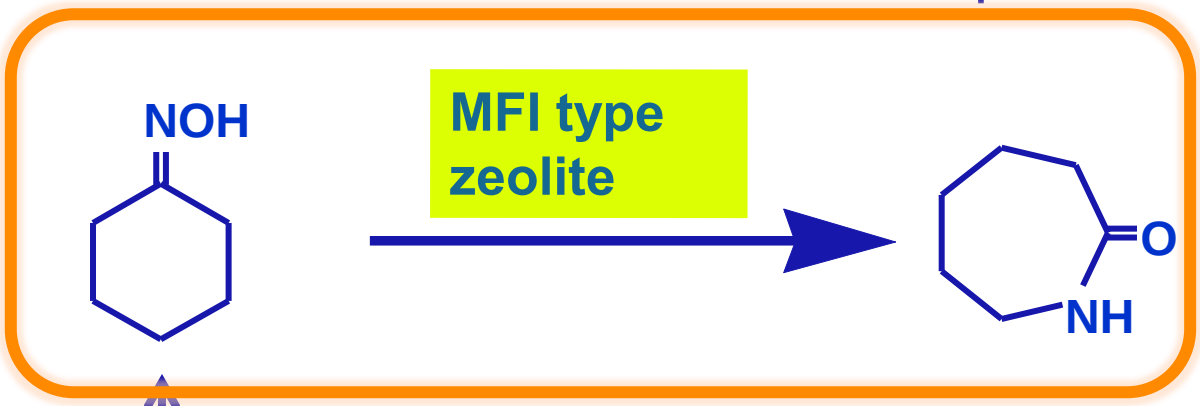

H_2O_2, NH_3, TS-1

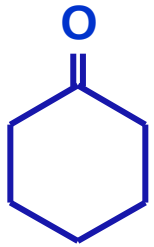

This new process was industrialized in April 2003

Production: 60.000 Ton per year

Sumitomo Chemical Co.

H. Ichihashi et al. Cata. Surv. Asia 7 (2003) 261; Y. Izumi et al. Bull. Chem. Soc. Jpn. 80 (2007) 1280

Reaction mechanism of the Beckmann rearrangement

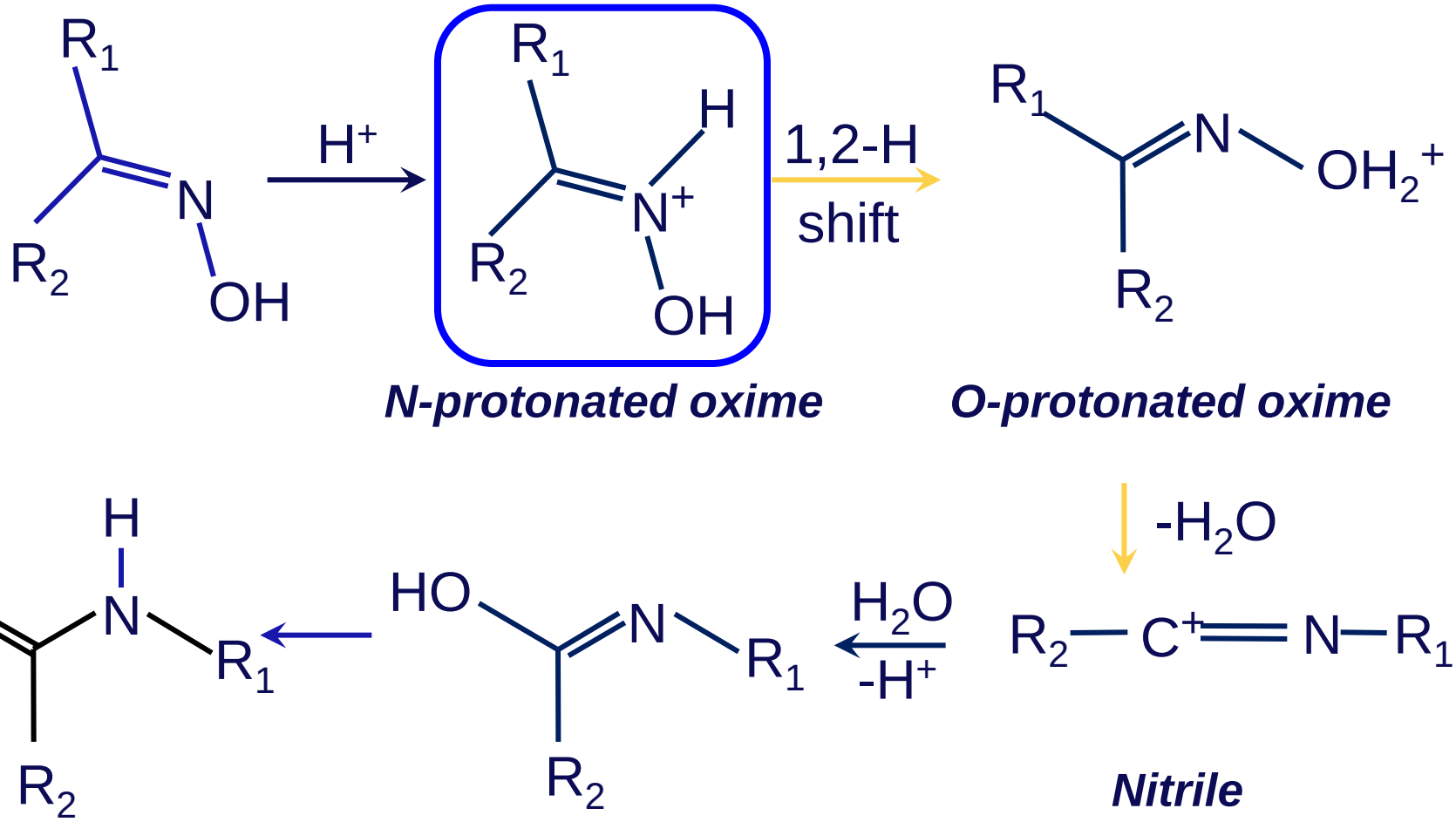

N-protonated oxime

O-protonated oxime

P. S. Landis, P. B. Venuto, J. Catal. 1966, 6, 245 – 252.
A. B. Fernandez-Sanchez et al. Angew. Chem. Int. Ed. 44 (2005) 2370

QUESTIONS

- Reaction mechanism, formation of the N protonated oxime?
- Does the rearrangement of CHOX occur inside the pores of MFI type zeolites?

Oxime adsorption

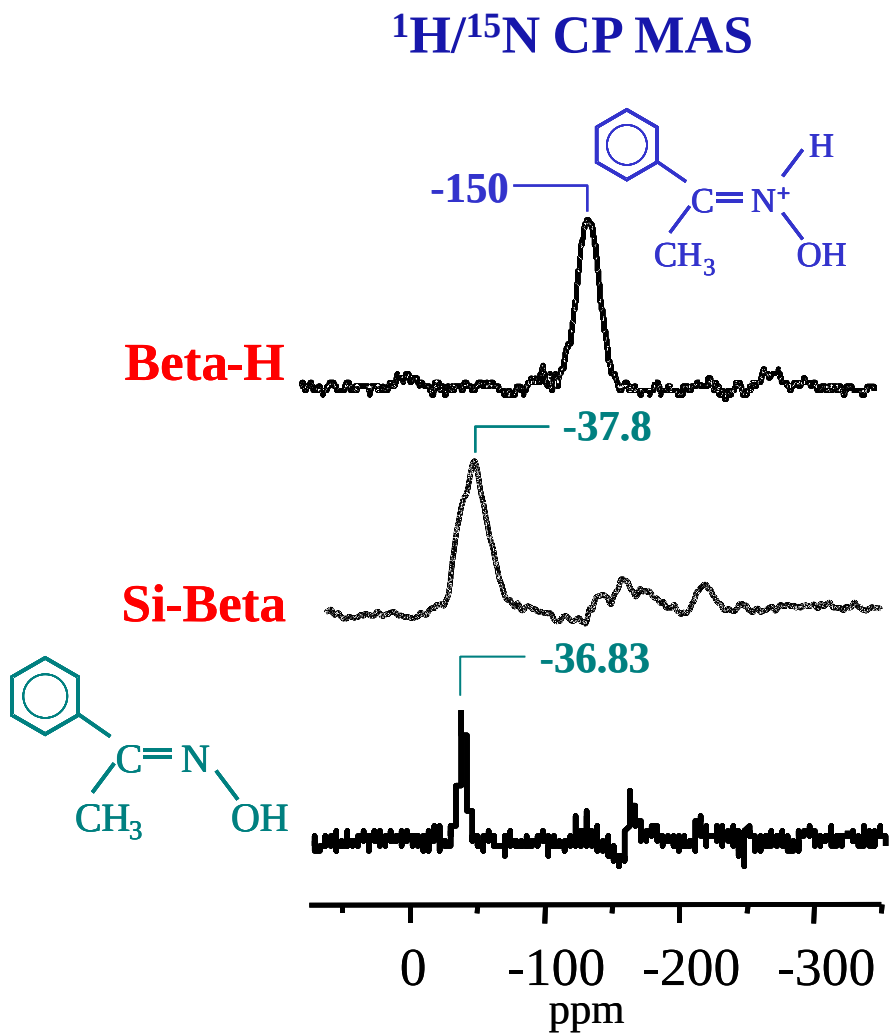

- *Angew. Chem., Int. Ed. (2005), 44(16), 2370-2373.*

The Beckmann rearrangement reaction

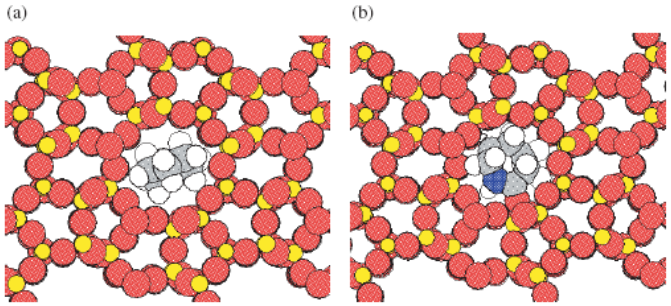

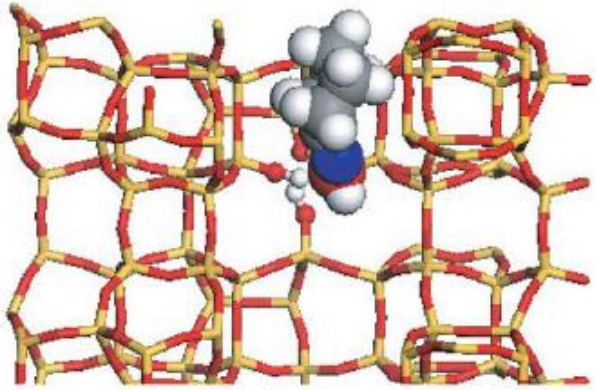

Does the reaction take place inside the pores or at the pore aperture of MFI zeolite?

H. Ichihashi et al. Catal. Survey Asia, 2003, 7, 261

The Beckmann rearrangement reaction

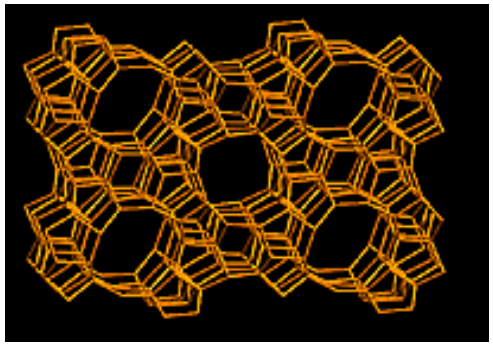

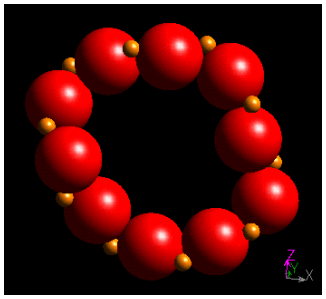

5.6 Å X 5.3 Å

MFI TYPE ZEOLITE

HZSM-5 (Si/Al=15): Bronsted acid site

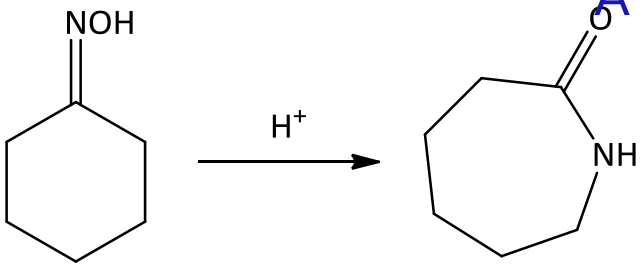

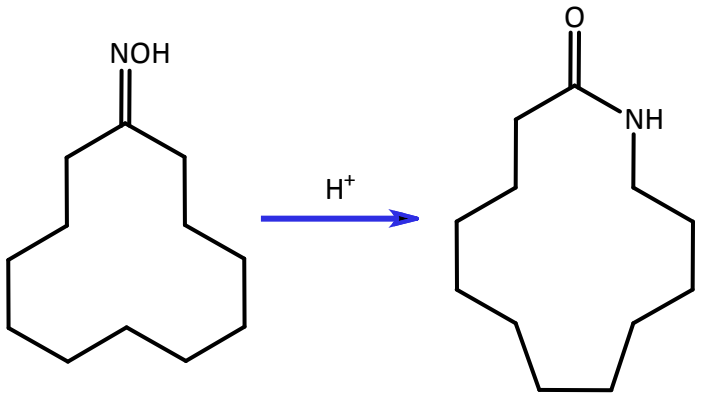

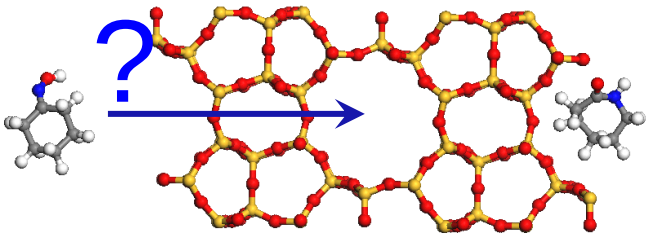

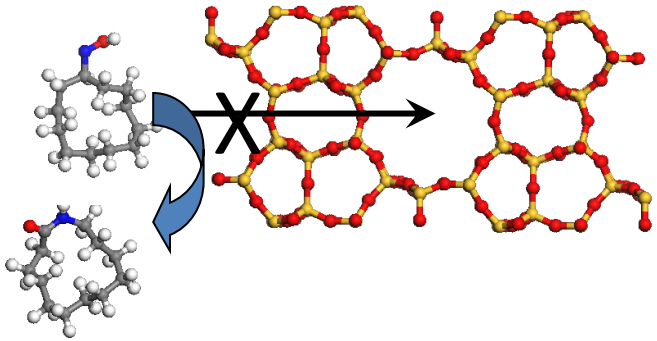

A.B. Fernández, I. Lezcano-Gonzalez, M. Boronat, T. Blasco , A. Corma, J. Catal. 249 (2007) 116

The BR reaction on zeolite H-ZSM-5

CPL-O/H

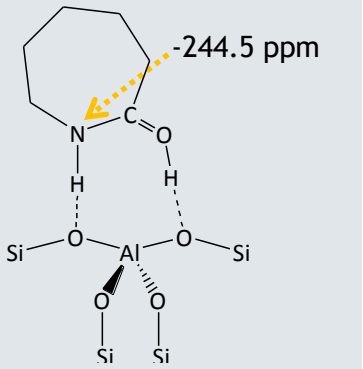

CHox-N/H

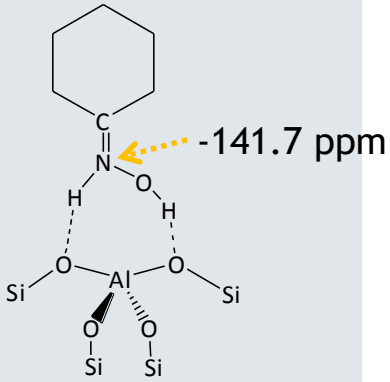

CHox (s)

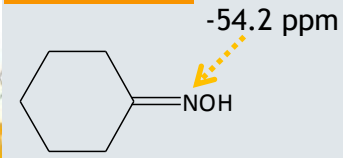

Zeolite H-ZSM-5

$^{1}H/^{15}N$ CP MAS RMN

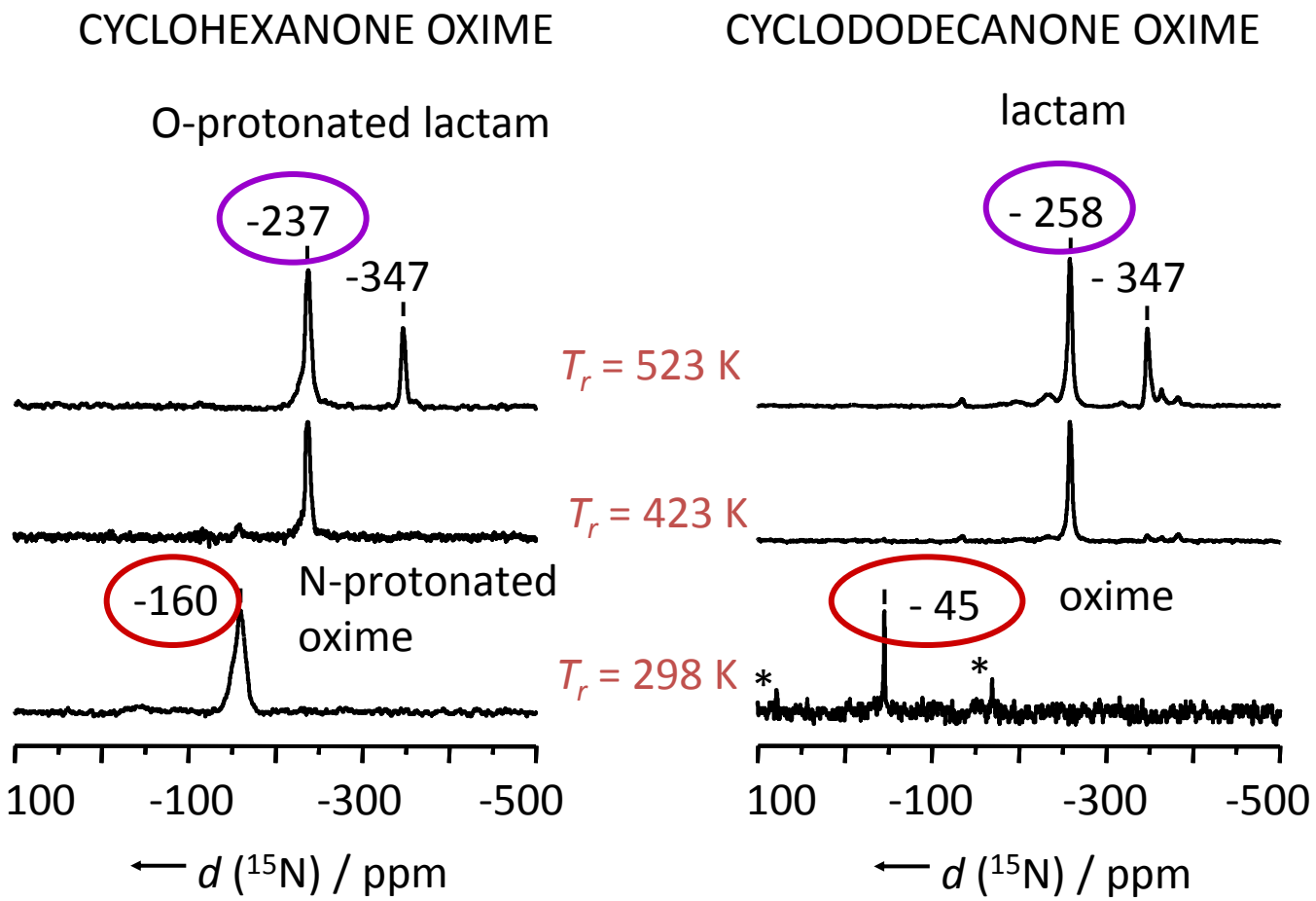

A.B. Fernández, I. Lezcano-Gonzalez, M. Boronat, T. Blasco , A. Corma, J. Catal. 249 (2007) 116

CONCLUSIONS

- Formation of the N-protonated oxime and the O-protonated lactam over the Bronsted acid sites in porous solids.

- The BR of CHOX occurs in the interior of the pores of the MFI type zeolite

A. B. Fernández et al., Angew. Chem. Int . Ed. 44 (2005) 2370; J. Catal 243 (2006) 270; J. Catal. 249 (2007) 116.

Reaction Mechanisms

- Beckmann rearrangement reaction

- **Depletion of NOx emissions**

Main atmospheric pollutants

- **NO_x**
- Sulfur oxides
- Volatile organic compounds
- NH_3

- Climate changes
- Human Health

Stable nitrogen oxides

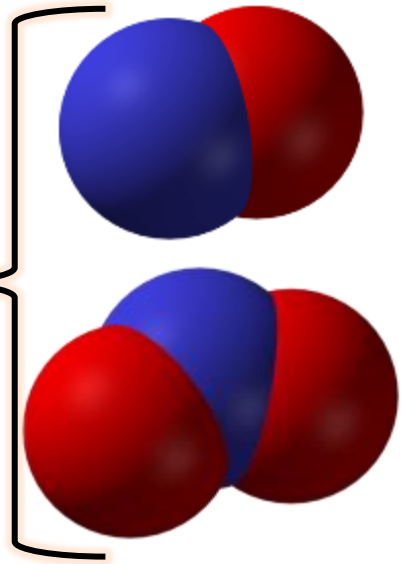

NO, NO_2: **Irritant gas** that causes pulmonary edema and exudative inflamations. *Chronic exposures:* coughing, headache and gastrointestinal disorder

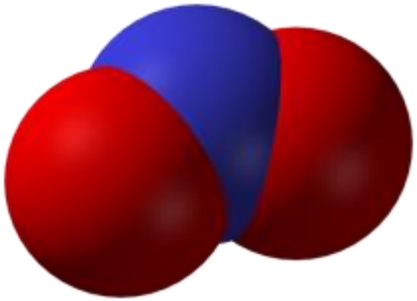

N_2O: From microbial action and other processes. Powerfull analgesic. Laughting gas

Contributes to ozone depletion and greenhouse effect.

***Chronic exposures*: polyneuropathy and myelopathy**

No_x polluntants: origin

- **NO is the predominant form of NO_x**

Thermal emissions:

$N_2 + O_2 \rightarrow 2\ NO$ at high temperature

$NO + O_2 \rightarrow NO_2$

Mobile sources

Exhaust of motor vehicles

Stationary sources

Burning of fuels, oil or natural gas

Manufacturing processes

NOx emissions in 2012

U.S.A. NOx emissions

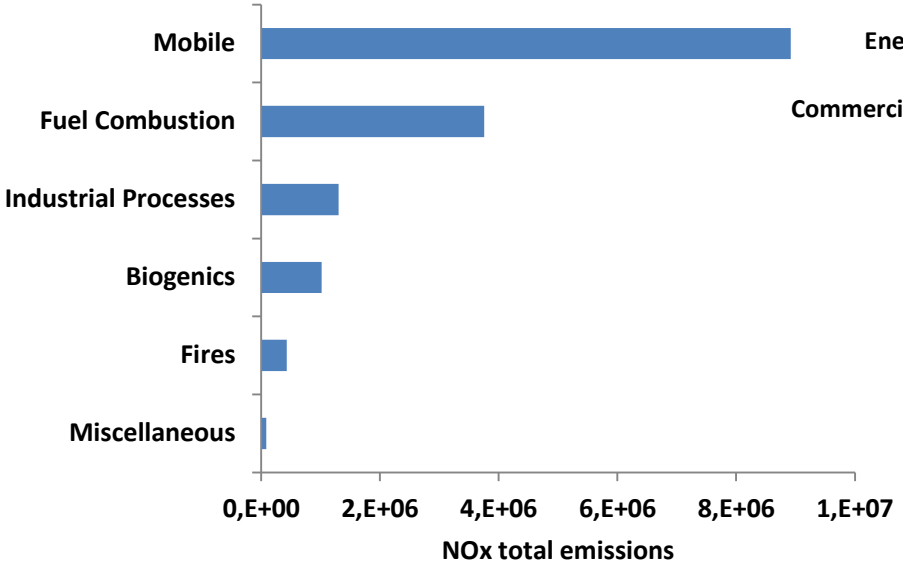

United States Environmental Protection Agency (EPA)

http://www.epa.gov/cgibin/broker?_service=data&_debug=0&_program=dataprog.national_1.sas&polchoice=NOX

Europe NOx emissions

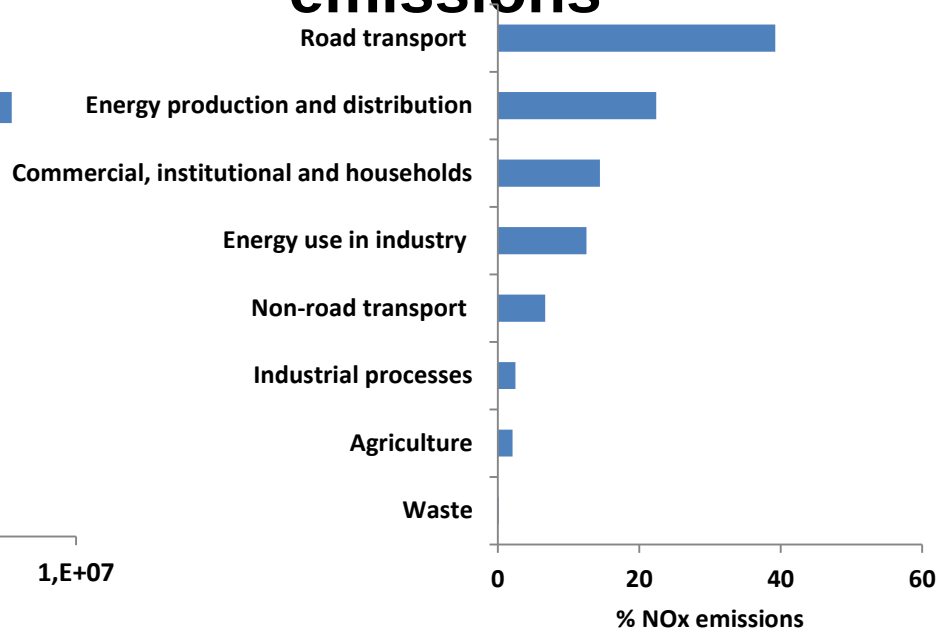

European Environment Agency (EEA)

http://www.eea.europa.eu/data-and-maps/figures/emission-trends-of-nitrogen-oxides-eea-member-countries-eu-27-member-states-3

NOx emissions from mobile sources

- 40 % of total NOx in Europe comes from road transport; 75 % of which is produced in diesel engines

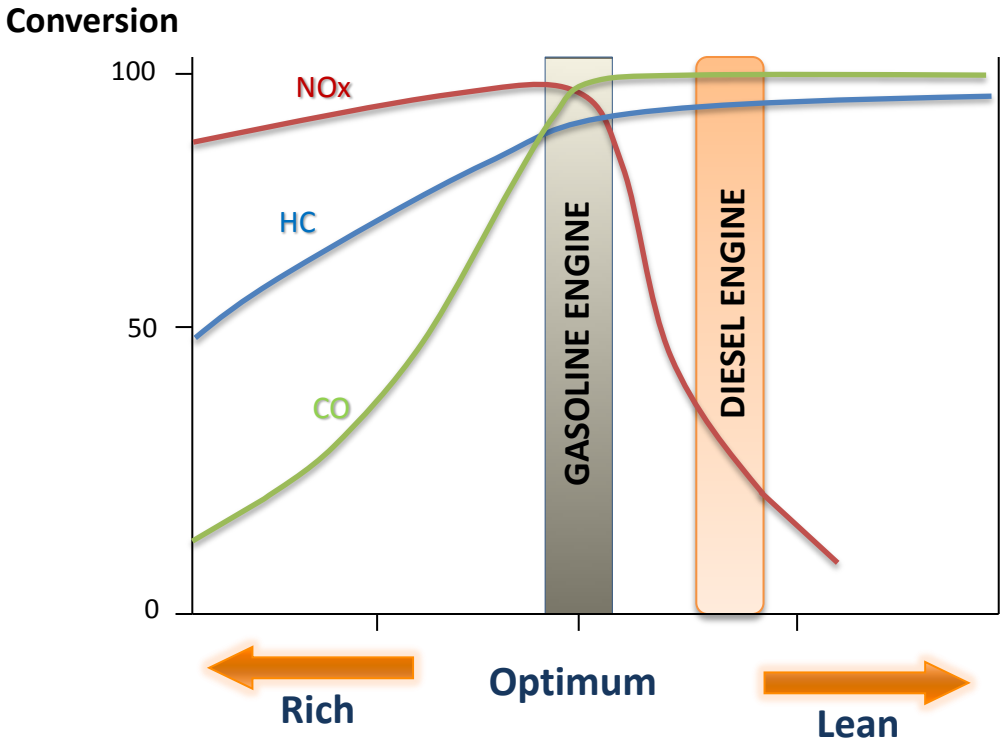

- Conversion of the three main pollutants with a three ways catalyst with air/fuel variations: NOT EFFICIENT FOR DIESEL ENGINES

http://www.jmsec.com/cm/Products/3-Way-NSCR-Catalysts.html

Effects of NO_x: Acid rain

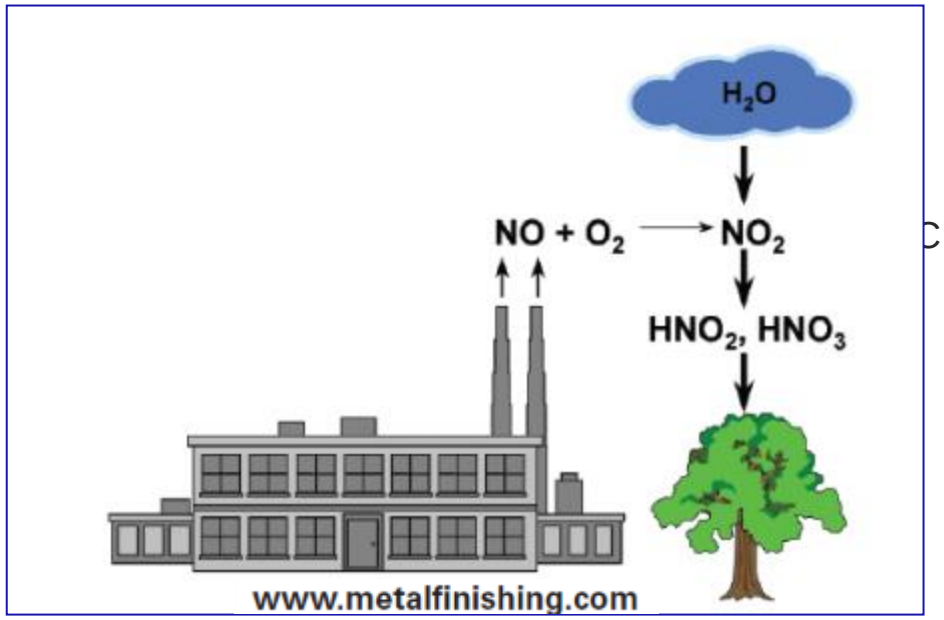

C, Tuls

David Woodfall y Getty Images
http://www.nationalgeographic.es/medio-ambiente/calentamiento-global/acid-rain-overview

Effects of NO_x: Photochemical smog

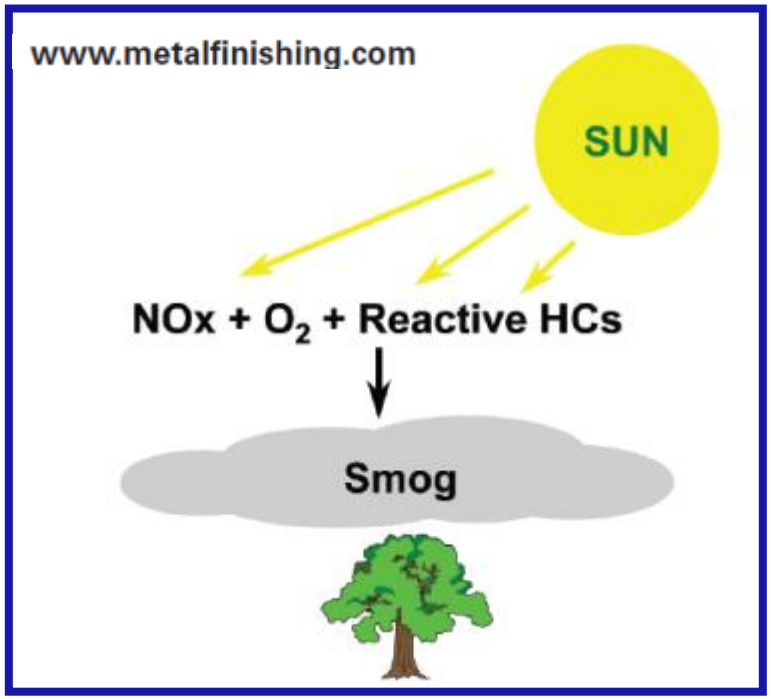

Everything You Need to Know About NOx
By Charles Baukal, Director of R&D, John Zinc Co. LLC, Tulsa, Okla.

$$NO_x + O_2 + h\nu + HC \rightarrow O_3$$
$$\rightarrow\rightarrow\rightarrow R^*+H_2O_2+R\text{-}CHO+\ldots P.A.N \text{ (Peroxoacyle nitrate)}$$

Legislations for NOx and PM emission for diesel vehicles

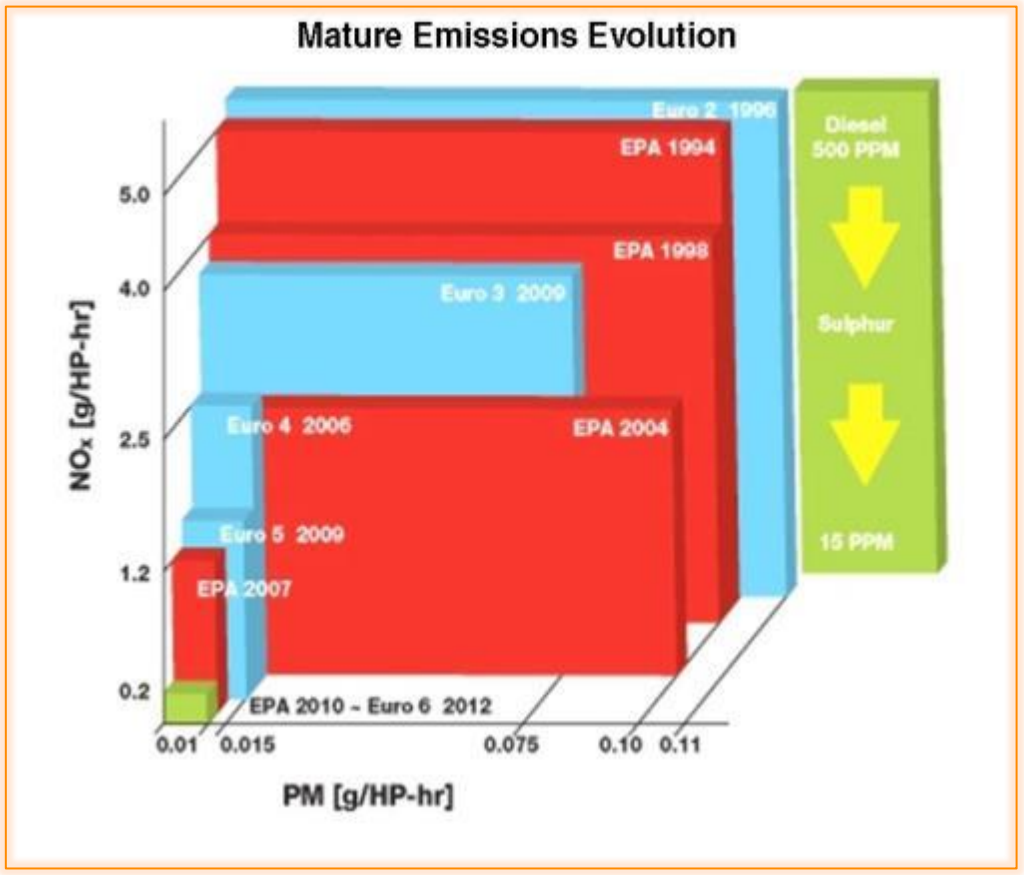

http://cumminsemissionsolutions.com/ces/navigationAction.do?url=SiteContent+en+HTML+EmissionsTechnology+Worldwide_Emissions_Regualtions

NH3 SCR catalyst

- **Vanadia catalysts** (for stationary sources)used in Europe since 2005 for heavy duty diesel vehicles using urea as a reductant
  - Low activity and selectivity (T < 650 °C)
  - Toxicity of vanadia species which volatilized at high temperatures

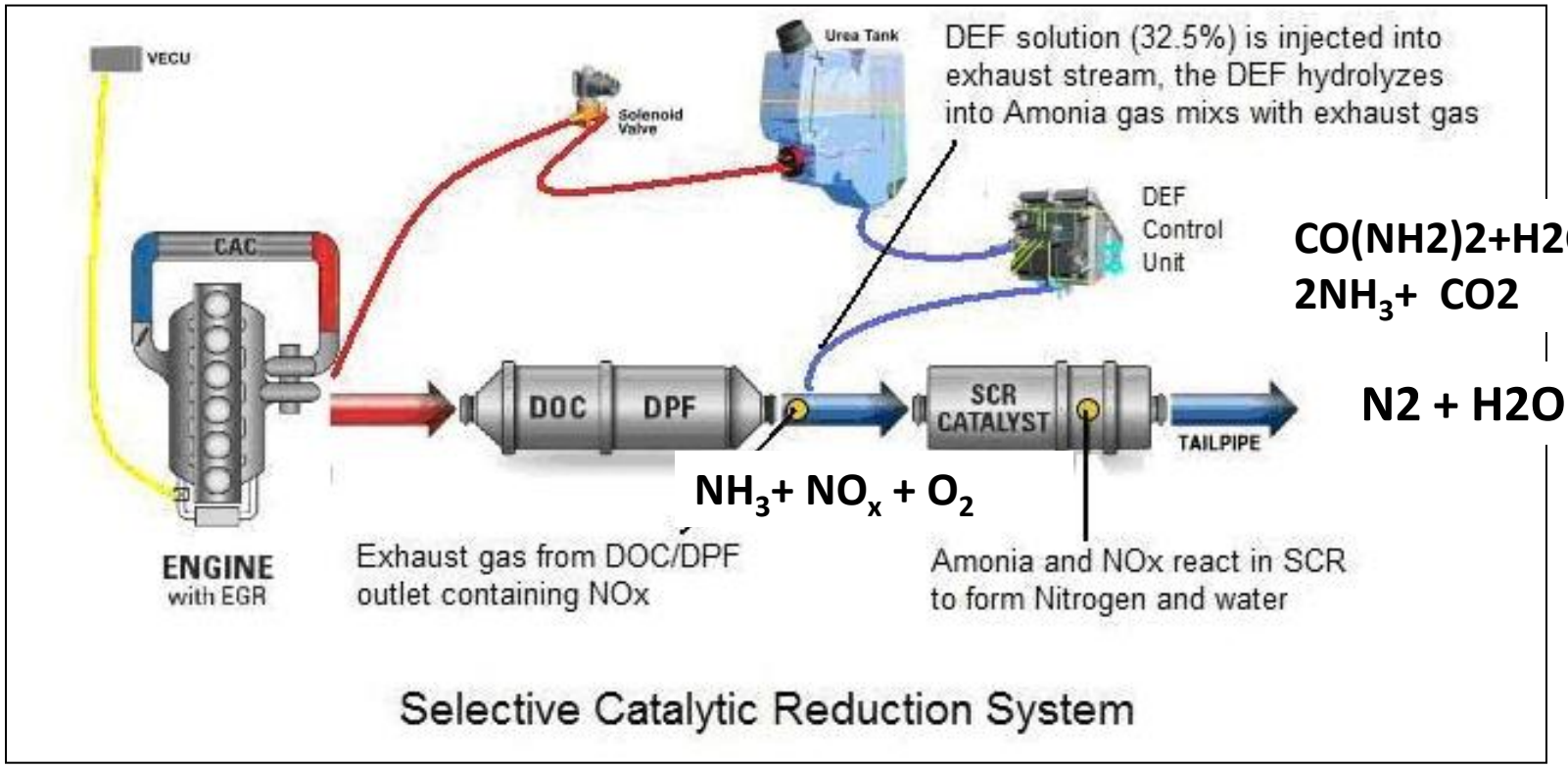

Development of new efficient SCR catalysts

- Standard NO > 90 %

  $4\ NH_3 + 4\ NO + O_2 \rightarrow 4\ N_2 + 6\ H_2O$

- Operating temperature window: 150 °C- 350 °C

- Hydrothermal stability (above 800 °C) (during regeneration of the diesel particulate filter (DPF)

TMI-ZEOLITES: Cu-Zeolites

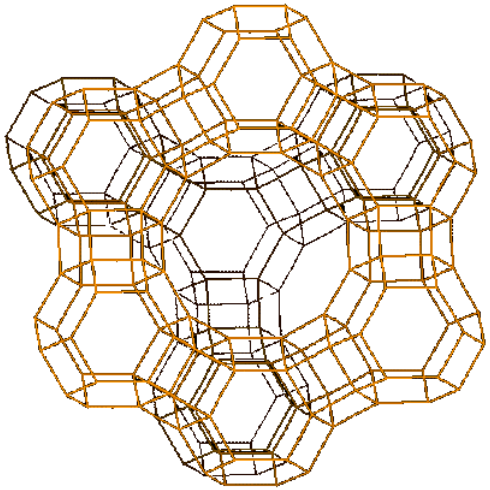

Faujasite
12 TO_2
7.4 x 7.4 Å

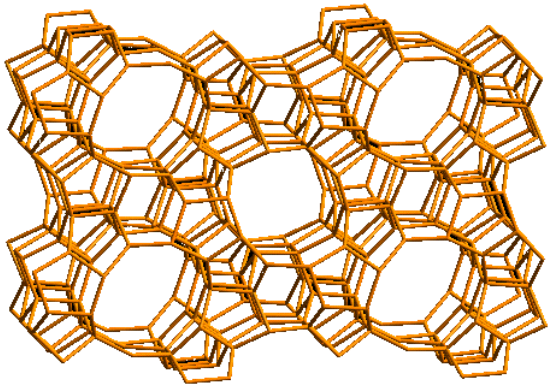

ZSM-5
10 TO_2
5.5 x 5.1 Å

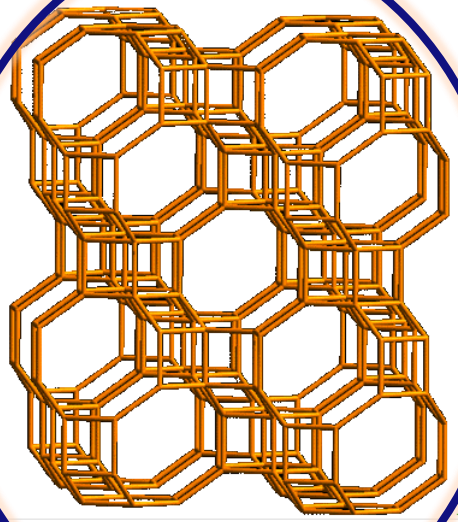

Chabazite
8 TO_2
3.8 x 3.8 Å

NH_3-SCR-NOx

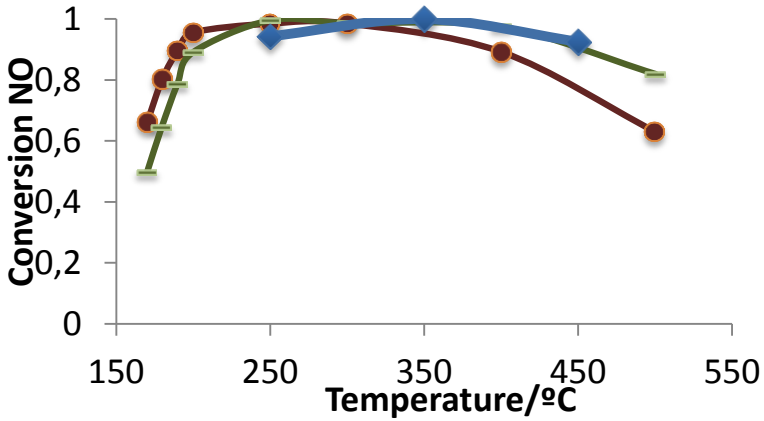

Kwak et al. J, Catal. 275, 187 (2010)

Development of new efficient SCR catalysts: CuZeolites Hydrothermal aging

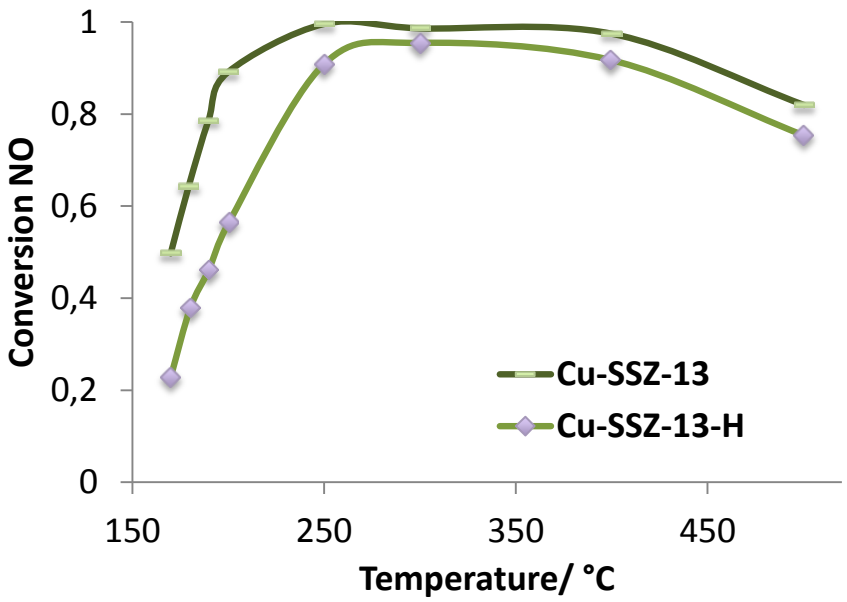

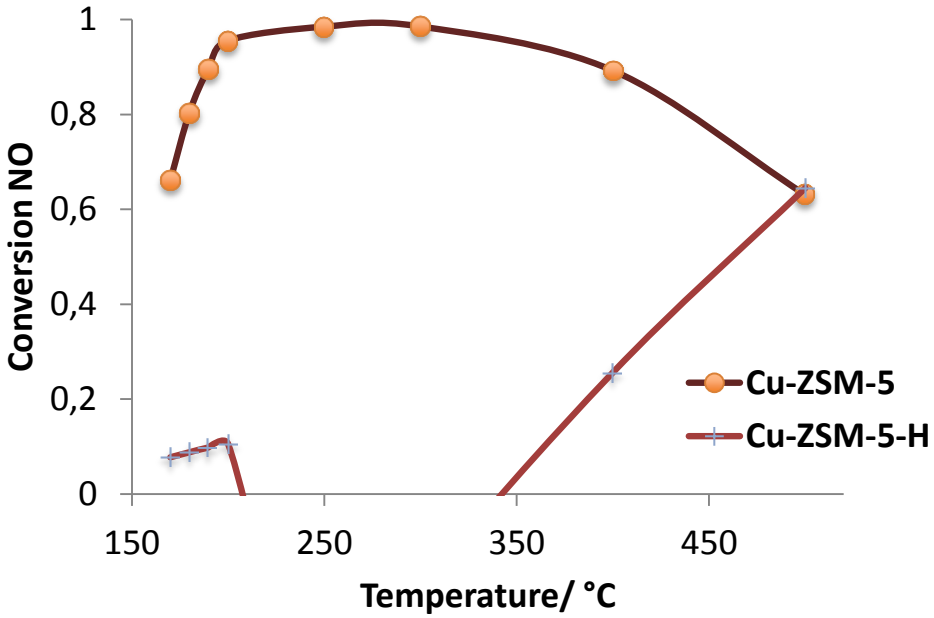

Active sites for NH_3-SCR: Isolated Cu^{2+}

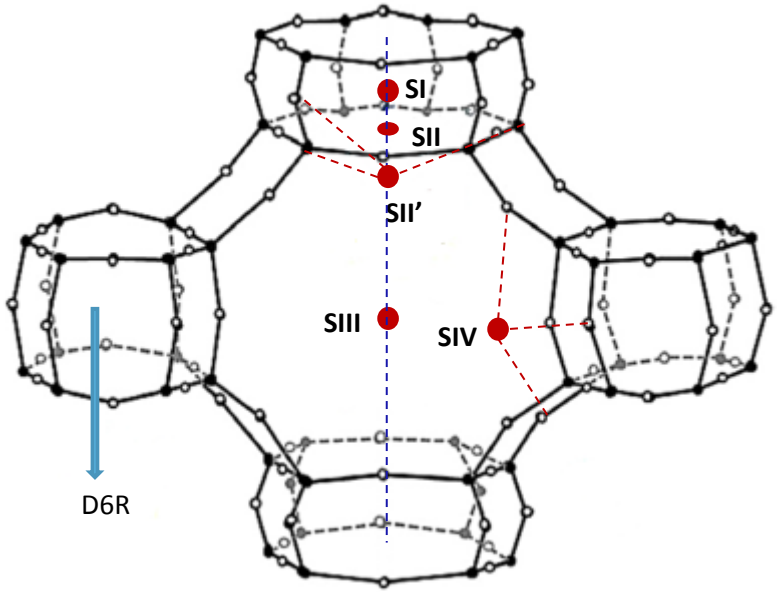

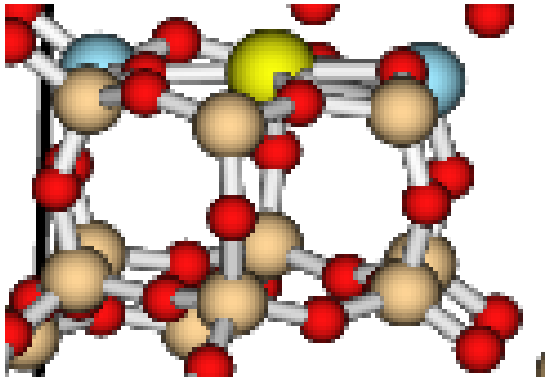

E. L. Uzunova, H. Mikosch, J. Hafner, J. Molec. Structure: THEOCHEM 912 (2009), 88; Deka, U. et al, ACS Catalysis, 2013, 4, 413; F. Gao et al. Top. Catal., 2013, 56, 1441; Fickel et al. J. Phys. Chem. C 2009, 114, 1663.

3. Low temperture reaction mechanism on Cu-CHA: Direct NO activation without formation of NO_2

A Common Intermediate for N2 Formation in Enzymes and Zeolites: Side-On Cu–Nitrosyl Complexes

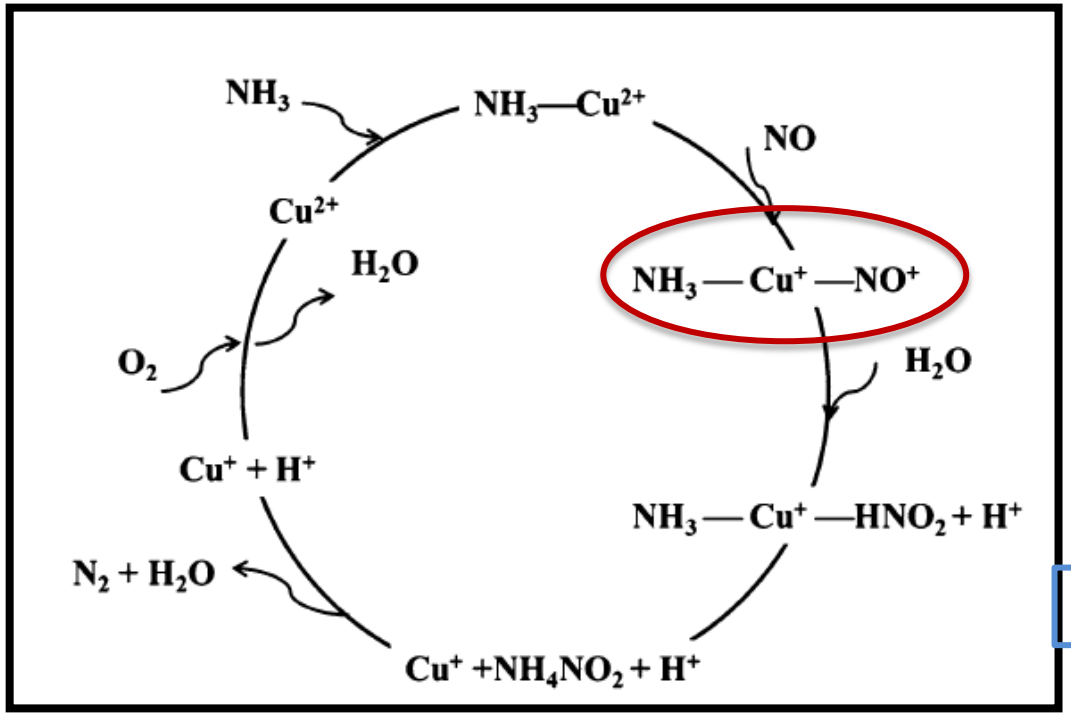

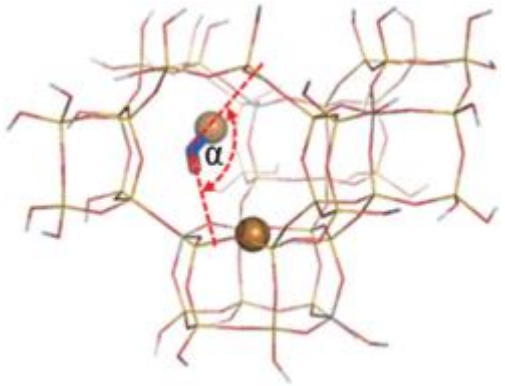

^{15}N NMR signal at 400 ppm

Kwak et al. Angew. Chem. Int. Ed. 2013, 52, 1 – 6;
Gao et a.. Topics in Catalysis, 2013. ***56****(15-17): p. 1441-1459.*

REACTION MECHANISM

- **The role of copper**
  - Active for NO oxidation to NO_2
  - Lewis acid site: Formation of Cu-NH_3 complexes
  - Redox behaviour Cu^{2+} /Cu^{+} pair
- **The role of Brønstes acid sites**
  - Ammonia reservoir
  - $NH_4^+ + NO \rightarrow N_2 + H_2O$
- **Reaction intermediates**
- **The involvement of NH_3 in the reaction**

1: NH_3-SCR-NOx requires that Cu is not bonded to NH_3

Dehydrated Cu-SSZ-13

SCR conditions (Interacting with NH_3) T ≈ 125 °C

SCR conditions T > 250 °C

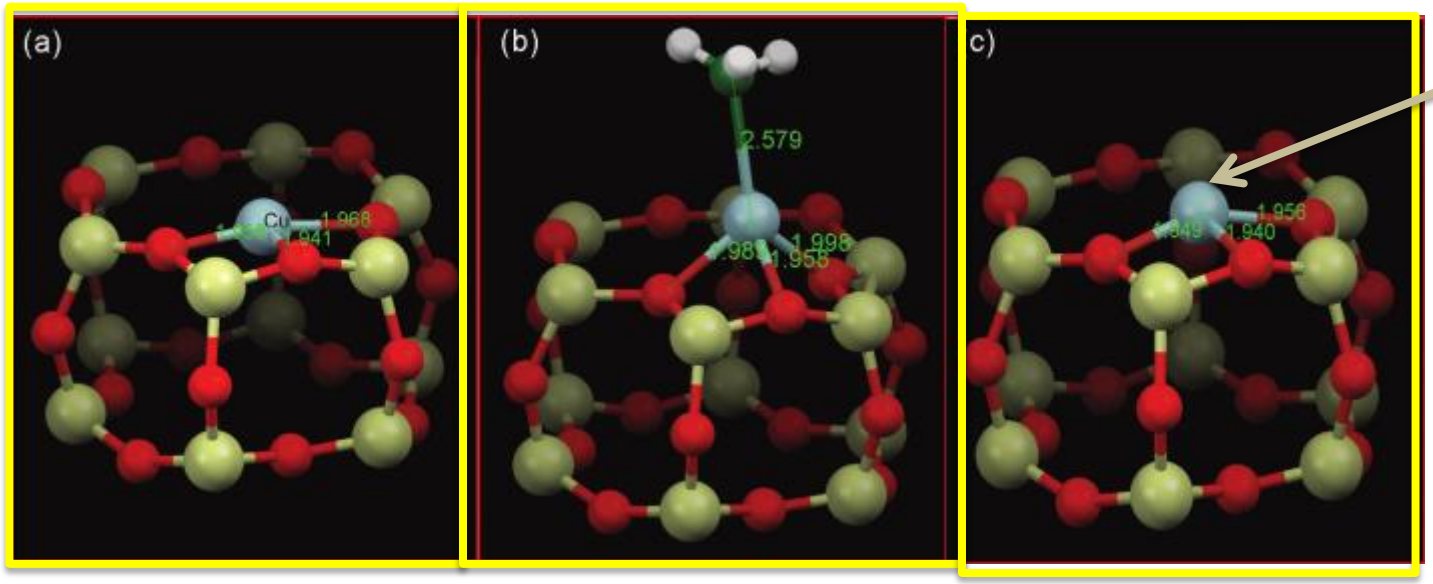

Cu^{2+}

- **Lower catalytic activity**
- **NH_3 blocking**

- **The formation of NO_3 and NO^+ requires the NH_3 desorption from Copper**
- **No evidence of copper reduction under reaction conditions**

Figure from U. Deka et al., J. Phys. Chem. C, 116, 2012, 4809-4818

XAFS/XRD under NH_3-SCR conditions

Cu-NH_3 complexes observed experimentally

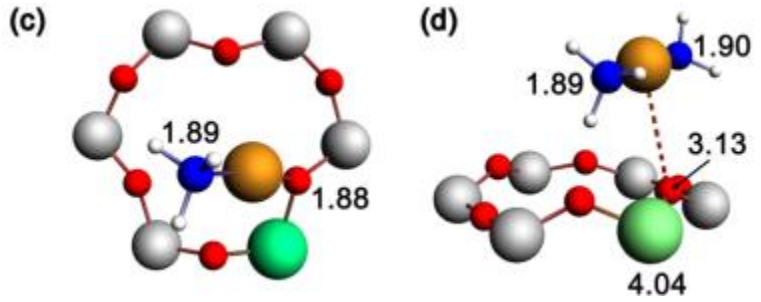

XANES, XES

Presence of **Cu^{2+} / Cu^{+}**

DFT: linear Cu^{+} species

PCCP 2014, 16, 1639

Cu-NH3 complexes

1) 1000 ppm NH3, 250 ºC ; 2) He 250 ºC , 3) 1000 ppm NO + 5% O2 250 ºC

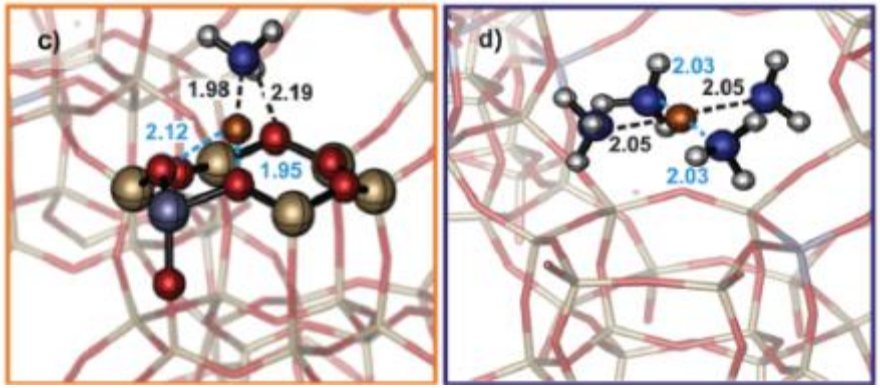

$[Cu(NH_3)_4]^{2+}$: NH_3 desorbs at 320 °C (TPD)

I. Lezcano-González et al. PCCP 2014, 16, 163

OBJECTIVES

IDENTIFICATION OF Cu-NH_3 SPECIES

- In situ RESONANCE TECNIQUES
  - EPR: Observation of isolated Cu^{2+} species $3d^9$)
  - ^{15}N, ^{1}H solid state NMR spectroscopy
- Peridodic DFT calculations with VASP codes

Materials

Cu-SSZ-13

- CHA
- 3D intercon.
- Small pore: 8MR (3,8 Å)

Si/Al = 13
Cu/Al = 0,3
Direct synthesis

Cu-ZSM-5

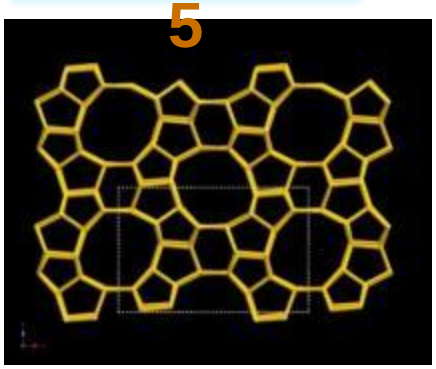

- MFI
- 3D intercon.
- Medium pore: 10MR (5,5 Å)

Commercial
Si/Al = 10,5
Cu/Al = 0,48

Martínez-Franco, R., et al., ChemCatChem, 2013. 5(11): p. 3316-3323.

Pretreatment: evacuation at 450 °C, adsorption of 6 NH_3/Cu dgassing at increasing temperatures

^{15}N NMR spectroscopy Cu-SSZ-13

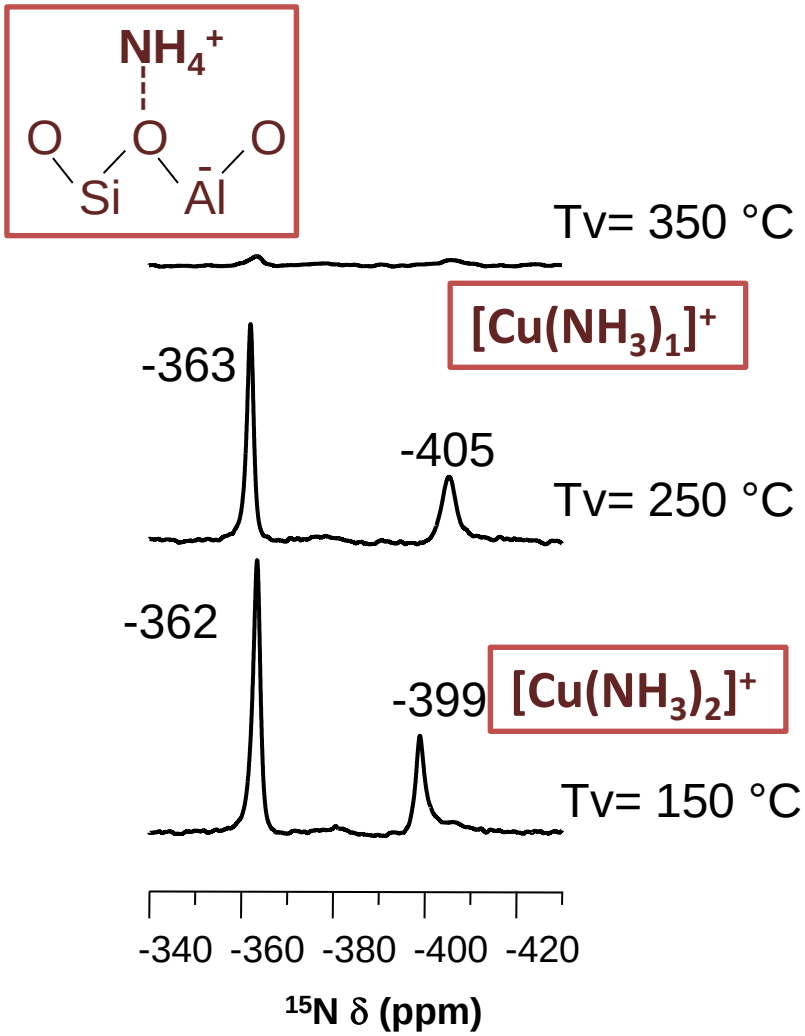

Conclussions

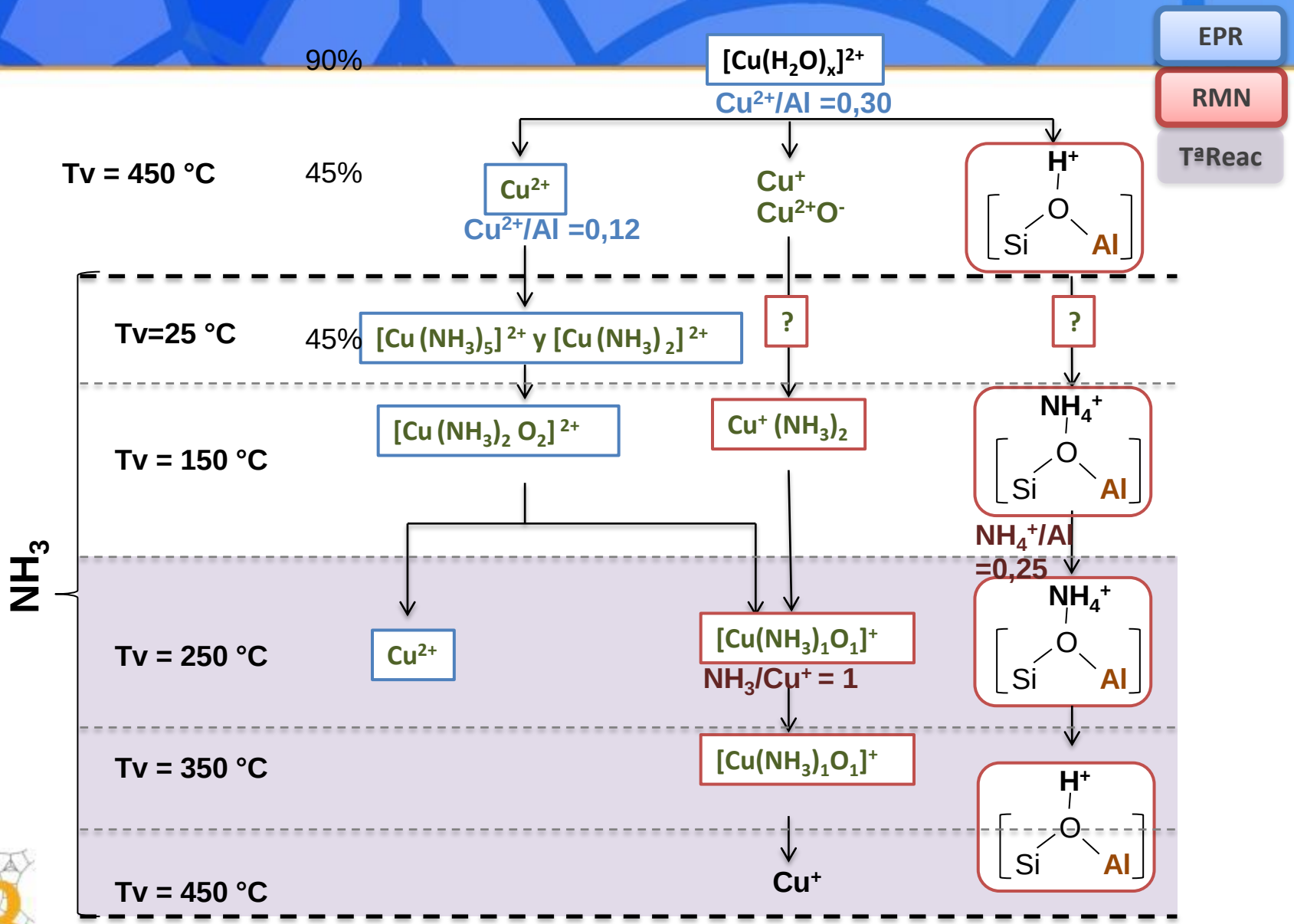

NMR

Manuel Sánchez-Sánchez

Alejandro Vidal-Moya

Ana Belén Fernández Sánchez

Inés Lezcano

NMR/EPR

Marta Moreno

Zeolite Synthesis

Fernando Rey

Susana Valencia

M. J. Díaz-Cabañas

Theoretical calculations

Mercedes Boronat

Avelino Corma

ACKNOWLEGEMENTS

MINISTERIO
DE ECONOMÍA
Y COMPETITIVIDAD

- **Severo Ochoa program (SEV-2012-0267)**
- Consolider Ingenio Multicat (CSD-2009-00050)
- MAT-2012-3856-C02-01

INSTITUTO DE TECNOLOGÍA QUÍMICA

CSIC

UNIVERSITAT POLITÈCNICA DE VALÈNCIA

PERSONAL

- Investigadores	31
- Ayudantes de Laboratorio	8
- Servicios analíticos y mantenimiento	25
- Administración	13
- Químicos/Ingenieros contratados	50
- Estudiantes de doctorado	41
- Post-doc	22

Prof. Avelino Corma.
Premio Príncipe de Asturias 2014

Oviedo, 24/10/2014. Teatro Campoamor. Ceremonia de entrega de los Premios Príncipe de Asturias 2014. Foto: © FPA/Iván Martínez.

El ITQ ha colaborado y colabora con empresas nacionales e internacionales así como con centros de investigación de alto prestigio. Algunos ejemplos son:

- BP
- ExxonMobil
- Huntsman
- Repsol YPF
- BIOeCON
- CEPSA
- UBE
- Eni Technology
- Sumitomo
- IFF
- IFP
- Shell
- Süd-Chemie
- Johnson Matthey
- Abengoa
  - Inabensa
  - Hynergreen
  - Ecocar. Esp.
  - Abengoa Solar
- Rhodia
- BASF
- Cargill
- FMC Foret
- CEMEX
- Ceracasa
- Isdin
- Pemex
- Total France
- Industrial Nalón
- Chemtura
- Petrobras
- Sasol
- UOP
- ……

Q.


VALENCIA
España
Spain
Portugal
Madrid
Barcelona
Zaragoza
Lleida
Valladolid
Salamanca
Burgos
Logroño
Pamplona
Vitoria-Gasteiz
Donostia
Bilbao
Santander
Gijón
Oviedo
León
A Coruña
Lugo
Vigo
Ourense
Ponferrada
Viveiro
Carballo
Santiago de Compostela
Viana do Castelo
Porto
Aveiro
Viseu
Coimbra
Santarém
Lisboa
Setúbal
Évora
Portimão
Faro
Cáceres
Badajoz
Talavera de la Reina
Ciudad Real
Albacete
Alacant
Murcia
Lorca
Cartagena
Córdoba
Jaén
Sevilla
Huelva
Jerez de la Frontera
Granada
Almería
Málaga
Estepona
Gibraltar
Alboran Sea
Balearic Sea
Palma
Manacor
Mao
Ibiza
Reus
Vilanova i la Geltrú
Girona
Andorra
Perpignan
Toulouse
Montauban
Mont-de-Marsan
Pau
Carcassonne
Narbonne
Montpellier
Nîmes
Avignon
Marseille
Toulon
Cannes
Monaco
Corte
Ajaccio
Sassari
Alghero
Oristano
Carbonia
Algiers
Oran
Chlef
Constantine
Annaba
Bejaia
Setif
Souk Ahras
Tangier

MINISTERIO
DE ECONOMÍA
Y COMPETITIVIDAD

CSIC
CONSEJO SUPERIOR DE INVESTIGACIONES CIENTÍFICAS

UNIVERSITAT
POLITÈCNICA
DE VALÈNCIA

INSTITUTO DE
TECNOLOGÍA
QUÍMICA